Tu-AM-SymII-3

DESIGN OF NOVEL THYMIDYLATE SYNTHASE INHIBITORS USING ITERATIVE CRYSTALLOGRAPHIC ANALYSIS. ((D.A. Matthews, R.J. Bacquet, C.A. Janson, S.H. Reich, M.D. Varney, S.E. Webber, and W.W. Smith)) Agouron Pharmaceuticals, San Diego, CA 92121

We report successful applications of an iterative cycle of ligand design, synthesis, biochemical evaluation and crystallographic analysis of the protein-ligand complex in the development of enzyme inhibitors. Several series of structurally distinct compounds have been designed as inhibitors of thymidylate synthase. The ability to study in detail the binding mode of each successive molecule in a series greatly facilitates the analysis of those forces which dominate receptor-ligand interactions. The methodology described may speed the discovery of lead compounds and assist their development into drugs.

Tu-AM-SymII-4

SOLVENT EFFECTS ON RECOGNITION AND BINDING ((Kim A. Sharp)) Dept. of Biochemistry and Biophysics, University of Pennsylvania, Philadelphia, PA 19104-6059

Specific binding and recognition implies a substantial negative free energy of interaction of the right ligand in the right conformation, compared to both the unbound state and other ligands and or conformations. This results from a balance between intermolecular interactions and molecule solvent interactions. The latter predominantly consists of electrostatic and hydrophobic interactions. The electrostatic contribution to solvation depends on the molecular charge distribution, the shape of the molecule and the distribution of ions around it. The hydrophobic solvation term depends on the solvent accessible area buried upon binding and also upon the shape of the molecule through the curvature of the buried area. Ways to treat these effects and applications to protein-protein and protein-nucleic acid binding will be discussed.

POTASSIUM CHANNELS II

Tu-PM-A1

FAST INACTIVATION BY THE BALL PEPTIDE IN *Shaker* B K CHANNELS IS HIGHLY TEMPERATURE DEPENDENT. ((M. Nobile, R. Olcese, Y.C. Chen, L. Toro, and E. Stefani)) Dept. Molecular Physiology & Biophysics. Baylor College of Medicine. Houston, TX 77030

The energy profile of the interaction between the ball peptide (BP) and the internal mouth of *Shaker* B K channels was investigated. Lowering the temperature had a major effect on the fast inactivation process. Macroscopic currents in the cut-open oocyte showed the following changes after lowering the temperature (20 to 10 ^{o}C): 1) Peak amplitude decreased with a Q_{10} of 1.5; 2) the activation time constant decreased with a Q_{10} of 3.14; 3) the decay time constant decreased with a Q_{10} of 7.2, and 4) the recovery from inactivation was less temperature dependent (Q_{10} = 1.57) than the installation of inactivation. At 0 mV the ratio between the peak amplitude and the steady-state level of the current was 4.0 at 20 ^{o}C and 1.44 at 5 ^{o}C. These findings indicate that the fast inactivation process has a high temperature dependence. To further investigate whether the high energy step was due to the interaction between the BP and the internal mouth of the channel we investigated in excised inside-out macropatches the temperature dependence of the inactivation induced by the synthetic peptide. The BP (93 μM) added to the internal side of Shaker-B IR (inactivation removed, delta 6-46) induced rapid inactivation (decay time constant of 20 ms at 40 mV). Lowering the temperature from 20 to 15 ^{o}C greatly slowed down the current decay, practically removing fast inactivation. These results suggest that the energy step resides mainly in the interaction between the inactivating peptide and the channel and not in the hypothetical bending of the chain. Supported by grants HL47382, HL37044 and AHA-Natl. Center 900963.

Tu-PM-A2

Model for Channel Activation Based on the Kinetics of Wild-Type and V2 Mutant *Shaker* 29-4 Potassium Channels. ((N.E. Schoppa, K. McCormack, and F.J. Sigworth)) Dept. of Cell. and Mol. Physiology, Yale Univ., New Haven, CT.

Mutating the second leucine in the conserved heptad repeat region of *Shaker* 29-4 potassium channels to valine (V2) causes a ~60 mV depolarizing shift and reduction in voltage sensitivity of channel activation without altering the total amount of charge moved in the activation process (Schoppa et al., *Science* 255: 1712, 1992). An explanation for this surprising result based on the steady state properties of V2 and the wild-type channel (WT) is that the V2 mutation has only a small effect on "early" steps but shifts the equilibrium of a "late" step in the channel opening process by ~60 mV. Several lines of kinetic evidence from ionic and gating currents at least qualitatively support this hypothesis. First, ionic tail currents at all membrane potentials decay much more quickly in V2 than in WT, and at very negative membrane potentials, where tail currents should reflect the rate constants of the final transition in the opening process, the V2 mutation shifts the voltage dependence of the decay time constants by about +80 mV. Secondly, while the gating currents of WT show a prominent second exponential component at potentials where the opening of these channels is the most voltage sensitive, V2 gating currents decay monoexponentially. Finally, while single channel closed times of WT exhibit many exponential components, V2 exhibits only 2 or 3 closed time components, consistent with the notion that the V2 mutation has separated activation transitions in their voltage dependence. We are exploiting this fact in a more thorough kinetic analysis of V2 and WT ionic and gating currents.

Tu-PM-A3

CONSERVED CYSTEINE RESIDUES IN S2 AND S6 ARE NOT ESSENTIAL FOR EXPRESSION OF Kv2.1 (DRK1) IN *XENOPUS* OOCYTES.
((Roger D. Zühlke, Hui-juan Zhang and Rolf H. Joho)) Department of Cell Biology and Neuroscience, The University of Texas Southwestern Medical Center at Dallas, Dallas, Texas 75235-9039.

The wealth of data derived from functional expression of cloned voltage-gated potassium (K^+) channels contrasts markedly with the virtual absence of structural information about the channel protein. Recombinant DNA techniques have been used to correlate biophysical properties with putative channel domains. However, there is still a considerable lack of structurally meaningful data. Comparative sequence alignments of known voltage-gated K^+ channels revealed two conserved cysteine residues in the putative transmembrane segments S2 and S6 (C232 and C393 in Kv2.1). If these residues were connected by a disulfide bridge, it would put a structural constraint on possible channel models by placing S2 next to S6, and it would also imply an essential role in the folding process and/or in the maintenance of functional integrity of the channel. We used site-directed mutagenesis to investigate this possibility. Replacement in Kv2.1 of C232 with serine, phenylalanine or tyrosine did not affect expression levels when measured in *Xenopus* oocytes with a two-electrode voltage-clamp technique. Substitutions of C393 with serine or glycine were well tolerated, however, the bulky residue phenylalanine or the charged residue arginine in position 393 led to loss of function. We suggest that a disulfide bridge between C232 and C393, although possible, is not essential for functional expression of Kv2.1 in *Xenopus* oocytes. Whether disulfide bridges within or across channel subunits, linking S2 to S6, are indeed present, and how other mutations of these cysteine residues affect channel function is currently under investigation.
(Supported by NS28407 to R.H.J.).

Tu-PM-A4

MUTATIONS IN THE S6 DOMAIN AFFECTING CONDUCTANCE, TEA AND BARIUM BLOCKADE IN THE PERMEATION PATHWAY OF THE *SHAKER* POTASSIUM CHANNEL. ((G.A. Lopez, Y.N. Jan and L.Y. Jan)) Howard Hughes Medical Institute and Departments of Physiology and Biochemistry, University of California San Francisco, San Francisco, CA 94143-0724.

In order to identify regions of the potassium channel protein which may contribute to the internal mouth and pore lining structure, we have made use of a chimeric channel. The chimeric channel contained part of the sixth transmembrane domain (S6) and several adjacent residues from NGK2, transplanted into the N-terminal deletion mutant of *Shaker B*. These two channels differ in several pore properties including single-channel conductance, blocking by internal and external TEA, and block by internal Ba^{++}. NGK2 has a high sensitivity for external TEA and a low affinity for internal TEA, whereas *Shaker* has the opposite sensitivities. In addition, the single-channel conductance of NGK2 is approximately three times of that of *Shaker*. The chimeric channel showed an internal TEA sensitivity and single-channel conductance similar to NGK2. We have also found that the NGK2 channel, like the chimera, is extremely sensitive to block by internally applied Ba^{++} whereas *Shaker* is less sensitive to block. The block by Ba^{++} is extremely voltage dependent in the NGK2 and chimeric channel. Because the S6 domain from NGK2 transferred several pore properties typical of NGK2 to the *Shaker* channel, we propose that the S6 domain is a structural component of the ion conducting pore.

Tu-PM-A5

MOLECULAR MECHANISMS OF Shaker K+ CHANNEL SUBUNIT ASSEMBLY

((Min Li, Yuh Nung Jan, and Lily Y. Jan)) Howard Hughes Medical Institute, University of California, San Francisco, CA 94143

The voltage-gated K^+ channel polypeptides contain a hydrophobic core region which includes six putative membrane spanning segments and is flanked by two hydrophilic cytoplasmic domains. They resemble one of the four internal repeats of the sodium or calcium channel polypeptide and are likely to form tetramers. The functional heterogeneity of potassium channels in eukaryotic cells is likely to arise not only from the multiple K^+ channel genes and splice variants but also from the combinatorial use of different K^+ channel polypeptides in the formation of heteromultimeric channels with novel properties. The results from our biochemical and electrophysiological experiments have shown: (1) One structural element which determines the compatibility of different K^+ channel polypeptides in subunit assembly is localized within their hydrophilic N-terminal domains. The minimal requirement for the homophilic interaction has been localized to a fragment of 114 amino acids. (2) A truncated Shaker B (ShB) K^+ channel polypeptide that contains only the hydrophilic N-terminal domain can form a homomultimer. (3) Substitution of the N-terminal domain of a distantly related mammalian K^+ channel polypeptide (DRK1) with that of ShB confers the ability to coassemble with ShB.

Tu-PM-A6

THE S4-S5 CYTOPLASMIC LOOP FORMS PART OF THE INNER MOUTH OF THE *SHAKER* POTASSIUM CHANNEL PORE.

((P.A. Slesinger, Y.N. Jan and L.Y. Jan)). Depts. of Physiol. and Biochem., Univ. of Calif. Medical School & H.H.M.I., San Francisco, CA 94143.

Recent mutagenesis experiments on voltage-gated potassium channels have provided evidence that the H5 (SS1-SS2) region connecting S5 & S6 transmembrane segments lines the ion conducting pore, probably by forming a β pleated sheet and inserting into the membrane. We have identified another segment of the *Shaker* potassium channel which appears to form the part of the cytoplasmic mouth of the pore. Mutations in the cytoplasmic loop connecting the S4 & S5 segments decrease the single-channel conductance measured in symmetrical Rb or K solutions and alters the permeability ratio for Rb relative to internal K. We have used ions which block current through potassium channels (Ba^{2+} and TEA^+) as probes for the internal mouth of the pore. Mutations at L385 and E395 in the S4-S5 loop make the channel less sensitive to block by internally applied Ba^{2+} or TEA^+. We have also found that strong depolarizations (>+150 mV) produce a novel form of inactivation that is altered by mutations in the S4-S5 loop. All mutations were made in the non-inactivating *Shaker* B channel (Δ6-46). Our results indicate that the inner mouth of the potassium channel is comprised of structural elements from the S4-S5 loop (and S6, Lopez *et al.*) in addition to H5.

Tu-PM-A7

GATING CURRENTS OF *Shaker* K CHANNEL S4 MUTANTS

((E. Perozo, D.M. Papazian, R.E. Weiss, L. Toro, E. Stefani and F. Bezanilla)) Dept. of Physiology UCLA and Dept of Mol. Biophysics Baylor College of Medicine.

The S4 sequence has been proposed to function as the voltage sensor in K, Na, and Ca channels. Mutation studies have implicated this region in the activation of Shaker K channels (Papazian et al, Nature 349:305, 1991). Using the cut-open oocyte technique, we have measured gating currents in three S4 mutants, R368Q, R377K, and R371Q, in constructs lacking inactivation and ionic conductance. R368Q, and to a lesser degree R377K, decrease the slopes of the conductance-voltage curve (G-V). R371Q, which neutralizes the next S4 basic amino acid after R368, slightly shifts the channel's G-V curve without changing its slope. Of the three mutants, R368Q has the most dramatic effect on the gating current. It splits the gating charge movement into two components. One component is shifted by about -40 mV, with a slope similar to that of the gating current of the wild-type channel. The second component of charge movement is shifted 90 mV and is much shallower than that of the wild-type channel, similar to the effect on the conductance vs. voltage curve. In contrast, the gating current of R377K resembles that of the wild-type channel, even though R377K and R368Q have similar effects at the whole cell and single channel levels (Shao & Papazian, Biophys J. 61:a367, 1992). Thus, these two mutations differentially affect the voltage-dependent transitions in the pathway to the open state, but have similar effects on the relatively voltage-independent transitions connecting the open state to nearby closed states. Interestingly, the neutralizing mutation R371Q has little effect on the gating current of the channel. The present data do not support models in which the S4 basic residues have an equivalent role in channel gating.

Supported by USPHS GM30376, GM43459, HL37044 and the PEW Charitable Trust

Tu-PM-A8

CAPACITANCE INDUCED BY SHAKER K CHANNEL.

((F. Bezanilla and E. Stefani)) Dept. of Physiology, UCLA. Los Angeles CA and Dept. Molec. Physiol. and Biophysics, Baylor College of Medicine, Houston TX.

Gating currents are the electric expression of the dielectric properties of the channel molecule observed as time relaxations for step changes in membrane potential. We report here the frequency (f) characteristics of the dielectric after K channels have been inserted in the membrane. The cut-open oocyte technique was used and a synthesized noise signal of 3 mV peak amplitude was superimposed on the command potential (V) of the voltage clamp at least 100 ms after it settled. The admittance was calculated as the ratio of the Fourier transforms of the measured current and the imposed signal. Complex capacitance (C) was calculated as the ratio of the admittance divided by $2\pi f$ after correction for series resistance and zero frequency conductance. Uninjected oocytes, treated with ouabain, showed no detectable voltage dependent C. Injected oocytes with the non-inactivating non-conducting cRNA of the Shaker K channel (Mutant H4-IR, W434F) induced a large voltage dependent C that was proportional to the induced gating current and in some cases it was as large as 90% of the background membrane capacitance. The C was frequency dependent in the range of -130 to -20 mV, peaked at around -60 mV, consistent with the shift produced by slow inactivation, and its f-dependence became that of the background C outside this V range. The induced C(f) showed two distinct components that were fitted with two single Debye relaxations. These results show that the channel protein adds at least two lossy dielectric processes: the main dispersion has a maximum around -60 mV, decreases sharply at more positive potentials and it can be associated to channel opening; the second dispersion is about 8 times smaller and peaks at more negative V indicating that there is a V-dependent capacitance in the potential region where no channel openings occur. Supported by USPHS GM30376 and HL37044.

Tu-PM-A9

I2 MUTATION UNCOUPLES ACTIVATION / INACTIVATION IN *SHAKER* K CHANNELS.

((R.K.Ayer, Jr., K.McCormack, L.Lin, and F.J.Sigworth)) Dept. Cell and Molec. Physiol., Yale U. Sch. of Med., New Haven CT 06510.

We have analyzed a mutant of *Shaker* 29-4 with a conservative (isoleucine) substitution of the leucine residue positioned at the end of the S4 domain. Substitution of this leucine (L370 or L2 of the putative leucine zipper motif) with uncharged residues (M, F, I, V, C, or A) produced channels with positive shifts in the voltage dependence of current activation. The magnitude of the shift in the midpoint of the activation curve was dependent on the substitution (M2<F2<I2<V2<C2<A2); with respect to L2, shifts ranged from +15mV for M2 to +130mV for A2. With the exception of I2, each substitution produced a shift in the midpoint of the steady-state inactivation curve essentially equal to the shift in activation (McCormack et al., *PNAS* 88, 2931-35, 1991; McCormack et al. submitted). Equivalent shifts in these two parameters are predicted by gating schemes where inactivation is strongly coupled to channel opening. The isoleucine substitution (I2) differs in that while the midpoint of the activation curve shifts by +40mV that of inactivation shifts by only +20mV. I2 also shows significant steady-state inactivation at potentials where the channel does not open. For coupled gating schemes, the rate of macroscopic inactivation should be dependent on the number of open channels available to inactivate. I2 channels do not seem to fit this simple model; over the entire range of channel activation the macroscopic inactivation kinetics of I2 are relatively voltage independent. Taken together these data suggest that the I2 channel readily inactivates from closed states and therefore channel inactivation has become partially uncoupled from channel opening.

Tu-PM-B1

ACTIVATION OF QUANTAL TRANSMITTER RELEASE BY SINGLE CALCIUM DOMAINS AT A CHOLINERGIC PRESYNAPTIC NERVE TERMINAL. ((E.F. Stanley)) *Section on Synaptic Mechanisms NINDS NIH Bethesda MD 20892 USA.*

Neurotransmitter secretion at fast transmitting synapses is triggered by the influx of calcium ions through voltage-sensitive channels. Current theories propose that the activation of several adjacent channels and the overlap of their calcium domains at the release sites is required to activate the vesicle release mechanism (VRM). We have tested this hypothesis directly by simultaneously recording single calcium channel currents and quantal acetylcholine secretion from a nerve terminal transmitter release-face.

The patch clamp technique in the on-cell configuration was applied to the release-face of the chick ciliary ganglion calyx-type presynaptic nerve terminal to record single calcium channel activity, as described (Neuron,7:585). ACh secretion was detected by a luminescent assay included in the pipette solution. We find that evoked ACh release can be correlated with single, short duration openings of presynaptic calcium channels that admit only a few hundred calcium ions.

These findings support a model of transmitter secretion in which the presynaptic calcium channel is directly linked to the VRM as part of a multi-molecular complex.

Tu-PM-B2

KINETIC BEHAVIOR OF WT AND MUTANT MOUSE ACETYLCHOLINE RECEPTORS: AROMATIC RESIDUES IN EXTRACELLULAR DOMAINS. ((Yinong Zhang, Bruce Nicholson, and Anthony Auerbach)) Dept. Biophysical Sciences and Dept. Biology, SUNY, Buffalo, NY 14214.

We have been studying the properties of mouse BC_8H_1 acetylcholine receptors (AChR) expressed in *Xenopus* oocytes. The kinetic properties of clusters of single-channel currents were analysed at several ACh concentrations in cell-attached patches at 20 °C, -100 mV. In addition to wt AChR, our work has focused on aromatic residues in extracellular domains: αY198 (changed to F) and δW57 (changed to Y). In wt AChR the dose-reponse (DR) profile determined from burst Popen is half maximal at about 10 μM ACh, the maximal effective opening rate estimated from gap durations at very high ACh concentrations (1 mM) is about 20,000 s^{-1} (the time resolution limit), and the predominant (85%) open interval time constant is about 20 ms. The αY198F mutant DR curve is half maximal at about 65 μM, with much longer closed interval durations than wt channels. Neither the apparent limiting effective opening rate nor the open channel lifetime are altered in this mutant, suggesting that altered association and/or dissociation rates underly the shifted DR curve. The δW57Y DR curve is half maximal at about 15 μM. In this mutant closed interval duration distributions were similar to wt channels (e.g., 3 exponentials, main component at about 3 ms at 20 μM ACh) but open interval distributions were distinctly different, with two components apparent at about 4 (67%) and 1 ms. This suggests that altered gating rates in part underly the shifted DR profile of this mutant. Mutant and wt AChR have similar current-voltage properties. More detailed kinetic characterization is in progress.

Tu-PM-B3

PROBING THE NMDA RECEPTOR CHANNEL PORE WITH ORGANIC IONS

((A. Villarroel)) Max-Planck-Institut für medizinische Forschung Abteilung Zellphysiologie D-6900 Heidelberg, Germany.

The N-methyl-D-aspartate activated glutamate receptor channel (NMDA-R) has unique conduction properties that differ from other ligand-gated ion channels. It is permeable to Ca^{2+} and blocked by Mg^{2+}. To characterise the conduction pathway of the NMDA-R channel we studied the blockade by organic ions. NR1-N2A subunits receptor were expressed in *Xenopus* oocytes. Single channel currents were measured from insed-out patches in 100 mM Cs, 5 μM glycine and 5 μM glutamate. In these conditions the single-channel current has almost no substates. In the absence of divalent cations the current-voltage curve is inwardly rectifing (57.3±0.6 pS an -100 mV; 46.2±0.3 pS at +100 mV n=5) for inward current. The presence of 10 mM external Tris produces a voltage dependent block that can be described with an apparent dissociation constant (Kd) of 50 mM and an electrical distance (zδ) of 0.5. Blockade by internal Tris is weaker (Kd=200 mM) and more voltage dependent (zδ=0.8). In bi-ionic condition the channel has no measurable permeability for Tris. Tetramethylammonium produces a similar voltage dependent blockade. Trimethylamine and Dimetylamine does not produce voltage-dependent blockade suggesting that they are permeant. The present results suggest that the narrow part of the pore has a cross section smaller than 5.4X5.4 $Å^2$ and it is located near the extracellular side of the pore.

Tu-PM-B4

DIFFERENTIAL ZINC MODULATION BETWEEN GLUTAMATE RECEPTOR CLONES GLUR1 AND GLUR3.

((J.C. Dreixler and J.P. Leonard)) University of Illinois at Chicago, Chicago, IL 60680.

We compared the effects of zinc on the kainate responses of two similar homomeric glutamate receptors, GluR1 and GluR3, by using the *Xenopus* oocyte expression system and two-electrode voltage-clamp. We found that GluR3 but not GluR1 receptors were enhanced by coapplication of 5 μM Zn^{2+}. Surprisingly, this Zn^{2+} potentiation occurred over a narrow concentration range as both 2.5 μM and 10 μM were ineffective. The zinc-induced enhancement of GluR3 current was not mediated by a change in sensitivity to agonist as the EC_{50} for kainate was unaltered by 5 μM Zn^{2+}. The kainate current-voltage (I-V) relationship for inward current showed an increase without any apparent change in shape. We also noted no change in reversal potential, but outward rectification became more pronounced during Zn^{2+} exposure. Additionally, Ca^{2+} removal greatly reduced the outward rectification of the I-V, however, the zinc-induced enhancement of GluR3 current still occurred in Ca^{2+}-free saline. The above I-V relationship phenomena may help elucidate the modulatory mechanism(s) of Zn^{2+} action on the two receptors. As Zn^{2+} is co-released in this concentration range along with neurotransmitter, the differential modulation may be physiologically important. Mutant receptors are being constructed to localize the Zn^{2+}-sensitive domain(s).

Tu-PM-B5

MECHANISM OF MAGNESIUM BLOCK IDENTIFIED BY SINGLE-CHANNEL RECORDING FROM MUTATED NMDA-RECEPTOR CHANNELS.

((J.P. Ruppersberg*, N. Burnashev*, W. Günther*, T. Kuner, H. Monyer, B. Sakmann*, P.H. Seeburg and R. Schoepfer)) *MPI med. Forschung, Abteilung Zellphysiologie, Jahnstraße 29, 6900 Heidelberg, Germany. ZMBH, Abteilung Molekulare Endokrinologie, Im Neuenheimer Feld, 6900 Heidelberg, Germany.

Recombinant NMDA receptor channels are composed of NR1 and NR2 subunits in yet unknown stoichiometry. They show calcium (Ca^{2+}) permeability and magnesium (Mg^{2+}) block like native NMDA receptors in neurons. Mutations of the asparagine at the Q/R/N-site of the NR1 and NR2 subunits of cloned NMDA receptor channels have been found to change the sensitivity to Mg^{2+} and Ca^{2+} in a subunit specific manner. The underlying mechanism is investigated using single-channel measurements. Our results show that Mg^{2+} and Ca^{2+} are pore blockers and that there is fundamental similarity between the mechanisms underlying Mg^{2+} and Ca^{2+} evoked block. Whereas the wild-type channel is optimized for block by Mg^{2+} and for permeating Ca^{2+}, the NR2A(Q)-mutant lowers the energy barrier for Mg^{2+} permeation. As a result Mg^{2+} becomes permeant and produces block with a weaker voltage-dependence and lower potency than in wild-type receptors. On the other hand in the NR1(Q)-mutant the blocking site is less selective for Mg^{2+} and there is considerable block by Ca^{2+} associated with a reduction in the effective permeability for Ca^{2+} ions. Moreover, it was found that sensitivity to divalent block of NMDA receptors changes not only with voltage, but depends on electrochemical potential of all permeant ions.

Tu-PM-B6

STRUCTURAL DETERMINANTS OF THE SUBUNIT - SPECIFIC SPIDER TOXIN BLOCK OF AMPA/KAINATE RECEPTOR CHANNELS.

((B.U. Keller, M. Blaschke, R. Rivosecchi, M. Hollmann*, S. Heinemann* and A. Konnerth)) MPI für biophysikalische Chemie, Am Fassberg, 34 Göttingen, Germany and *MNL, The Salk Institute, La Jolla, Ca 92093.

Joro Spider Toxin (JSTX) is a potent antagonist of AMPA/KAINATE (AMPA/KA) receptor mediated synaptic transmission in central neurones. We have investigated the molecular basis of JSTX action by studying its blocking effect on recombinant AMPA/KA receptors GluR1 - GluR6 after expression in Xenopus oocytes. Agonist-induced currents through receptors GluR1, GluR3, GluR4 and the subunit combination GluR1,3 were blocked by submicromolar concentrations of JSTX. The block was reversible and did not interact with the agonist binding site. In contrast, receptors GluR1,2, GluR2,3 and GluR6 were not affected by micromolar toxin concentrations. By studying receptor mutants obtained by site directed mutagenesis, we could identify a single amino acid position (Arg/Gln in the putative transmembrane region MII) which was critical for Joro spider toxin block. These findings demonstrate that a single amino acid position determines both the current voltage relationship and the subunit - specific block of AMPA/KA receptor channels by Joro spider toxin.

Tu-PM-B7

PURIFICATION AND NICOTINIC RECEPTOR BINDING ACTIVITY OF A RECOMBINANT α-BUNGAROTOXIN. ((J.A. Usselman, S.H. Hsu, N.J. Messier, C.A. Vaslet, and E. Hawrot)) Section of Molecular and Biochemical Pharmacology, Division of Biology and Medicine, Brown University, Providence, RI 02912.

α-Bungarotoxin (BGTX) is a 74-amino acid protein derived from snake venom which contains five stereotypic disulfide bonds conserved in all the long α-neurotoxins. Four of the five disulfides are also conserved in the short α-neurotoxins (e.g., erabutoxin) and in the α-cardiotoxins. Although the molecular site of action of the α-cardiotoxins is unclear, BGTX and the other α-neurotoxins are well characterized binding site antagonists of nicotinic acetylcholine receptors (nAChR).

In order to facilitate a structure-function analysis of BGTX and to prepare labeled BGTX for 2-D NMR studies, a synthetic gene for BGTX was constructed by back-translating the primary amino acid sequence of BGTX. The BGTX-gene was fused to a gene encoding a T7 coat protein and a protease site was engineered to allow selective release of the recombinant BGTX. Transfectants containing the recombinant BGTX gene express BGTX activity as determined by competition binding assays utilizing ^{125}I-labelled authentic BGTX and nAChR-enriched membranes. The specific activity of the 55kD fusion protein, purified by Mono-Q FPLC, is reduced by approximately 100-fold compared to authentic BGTX. After Factor Xa cleavage, the major released product co-migrates with authentic BGTX on reverse phase HPLC. This result suggests that recombinantly expressed BGTX is capable of refolding correctly. A similar synthetic gene approach is being used to construct a recombinant form of a structurally related, snake venom-derived α-cardiotoxin.

Supported by NSF-IBN-9021227 and NIH-GM32629. S.H. Hsu is a Howard Hughes Medical Institute Medical Student Research Training Fellow.

CALCIUM CHANNELS II

Tu-PM-C1

A CYTOSKELETAL MECHANISM FOR CALCIUM CHANNEL RUNDOWN AND BLOCK BY INTRACELLULAR CALCIUM. ((B.D. Johnson and L. Byerly)) Dept. of Biological Sciences, University of Southern California, L.A., CA 90089-2520.

Using large inside-out patches taken from isolated *Lymnaea* neurons, we examined the mechanisms underlying both rundown (washout) and Ca^{2+}-dependent inactivation of Ca^{2+} channels. These large patches (5-10 μm diameter) provided a 20-100 pA macroscopic Ca^{2+} channel current (I_{Ba}) and rapid access to the cytoplasmic side of the channel. Despite a stable patch capacitance, I_{Ba} declined to 50% within 60 s (median t½) following patch excision into an ATP-free saline. Ca^{2+} channel activity was extended by excising patches into salines containing ATP, ATP-γ-S, or GTP (t½ of 400, 140, and 150 s, respectively), but not AMP-PNP, indicating that NTP hydrolysis was required. The ability of ATP to rescue "washed-out" I_{Ba} declined with time, ranging from complete recovery after a delay of under one minute, to the absence of recovery when ATP was applied later than three minutes. We found no evidence for the involvement of phosphorylation in the process of channel rundown using both kinase and phosphatase inhibitors, while there was strong evidence for a role of cytoskeleton in maintaining Ca^{2+} channel function. The cytoskeletal inhibitors colchicine and cytochalasin B blocked the effect of ATP, while the presence of the cytoskeletal stabilizers, taxol and phalloidin (without ATP), extended channel activity. In addition, Ca^{2+}-dependent inactivation (block) of Ca^{2+} channels by nanomolar Ca^{2+} was significantly reduced in the presence of taxol and phalloidin. The evidence thus far suggests that *Lymnaea* Ca^{2+} channels must be attached to an interconnected network of microtubules and microfilaments to function, and that the disruption of this cytoskeleton underlies both channel rundown and block by intracellular Ca^{2+}. This work was supported by NINDS grant NS28484.

Tu-PM-C2

CHARGE IN L-TYPE Ca^{2+} CHANNELS IS CONVERTED BY VOLTAGE- BUT NOT Ca^{2+}-DEPENDENT INACTIVATION. ((R.Shirokov, R.Levis, N.Shirokova & E.Ríos.)) Rush Univ., Chicago, IL 60612

Inactivation properties of Ca^{2+} currents as well as intramembrane charge movement from L-type Ca^{2+} channels were studied in guinea pig ventricular myocytes using the whole-cell patch-clamp. The very negative distribution ($V_{½} \approx -100$ mV) of charge 2 (Q2) allowed us to measure ionic currents and charge from inactivated channels in the same ionic conditions. The availability of Ca^{2+} current measured in a double pulse protocol had the U-shape characteristic of Ca^{2+}-dependent inactivation (filled circles). On the other hand, Q2 (open squares), measured after the same conditioning pulses, increased smoothly with conditioning voltage. Q2 did not depend on the ionic current during conditioning. The current left after conditioning to high voltages corresponded well with the part of charge 1 wich was not converted to Q2. We conclude that V-dependent inactivation (but not Ca^{2+}-dependent inactivation) is accompanied by appearance of Q2, and that the voltage sensing moieties of the channel molecule are, thus, not affected by Ca^{2+}-dependent inactivation.

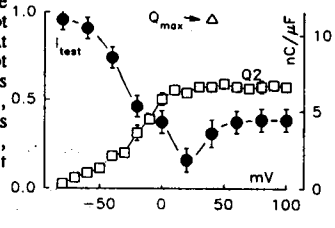

Supported by NIH and AHA-Chicago.

Tu-PM-C3

CALCIUM INDUCED FACILITATION OF CALCIUM CURRENT IN GUINEA PIG VENTRICULAR MYOCYTES IS NOT MEDIATED BY PHOSPHORYLATION ((Alison M. Gurney & Susan E. Bates)) Department of Pharmacology, U.M.D.S., St. Thomas's Hospital, London, U.K. SE1 7EH.

The L-type Ca^{2+} current of guinea pig ventricular myocytes is modulated by cytosolic Ca^{2+}. Following a sudden increase in $[Ca^{2+}]_i$, produced by photolysis of the caged Ca^{2+} molecule nitr-5, the amplitude of the Ca current (I_{Ca}) doubles over the next few min. Previous studies suggested that this facilitation was mediated by Ca^{2+}-dependent phosphorylation of the Ca^{2+} channels. Consistent with this, the facilitation depends on the intracellular [ATP], as studied by varying the [ATP] in the patch pipette used to record I_{Ca}; a facilitation of 98 ± 10 % was observed with 5mM ATP compared to 62 ± 3 % in the absence of ATP ($p<0.01$). However, several results are not consistent with this hypothesis. Firstly, the facilitation was not inhibited by intracellular Rp-cAMP-S (1 mM), although it blocked the isoprenaline-induced enhancement of I_{Ca} by inhibiting the cAMP-dependent (A) kinase. The facilitation was also unaffected by H-7 (100 μM), an inhibitor of both C and A kinases. Finally, when ATP in the pipette was replaced with the non-hydrolysable ATP analogue AMP-PNP, the Ca^{2+}-induced facilitation was not blocked but enhanced ($p<0.01$). In the presence of 5 mM AMP-PNP, photo-induced release of Ca^{2+} increased I_{Ca} by 220 ± 32 % following photolysis. The Ca^{2+}-dependent augmentation of I_{Ca} is thus mediated through a nucleotide-dependent mechanism that does not involve phosphorylation.

Tu-PM-C4

DUAL EFFECT OF CALCIUM ENTRY THROUGH VOLTAGE-GATED Ca CHANNELS ON THE SECRETION OF ALDOSTERONE. ((P.Q. Barrett, E.A. Ertel*, M.M. Smith*, J.J. Nee & C.J. Cohen*)) Dept of Pharmacol, U.Virginia, Charlottesville, VA & *Merck Res Labs, Rahway, NJ.

We have examined the involvement of voltage-gated Ca channels in high K-stimulated aldosterone (Aldo) secretion by calf adrenal glomerulosa cells. We used the whole-cell patch-clamp technique to record slowly-deactivating (T-type) and rapidly-deactivating (L-type) Ca channel currents. The peptide spider toxin ω-Aga-IIIA (30-150 nM) completely blocks L-type currents, even when elicited from negative holding potentials, but has no effect on T-type currents. In contrast, Nickel ions and the 1,4-dihydropyridines (DHP) felodipine and nitrendipine block both channel types, so that L-type current is not selectively eliminated. When freshly dispersed cells are stimulated by raising external K^+ from 3.5 to 7 mM, Aldo secretion increases 248±24%. Secretion in 7 mM K^+ is blocked by the addition of Ni or nitrendipine whereas ω-Aga-IIIA affects it only slightly (table). When external K^+ is raised from 3.5 to 60 mM, Aldo secretion increases 300±25%. Remarkably, secretion is further *enhanced* by ω-Aga-IIIA, 1 nM nitrendipine, or Ni. Yet it is blocked by 1 μM nitrendipine and by BAY K 8644 (>80% at 100 nM). These results suggest that 1) 7 mM K^+ stimulates Aldo secretion primarily by enhancing Ca entry through T-type Ca channels, 2) in 60 mM K^+, Ca entering the cell through L-type Ca channels *reduces* Aldo secretion, and 3) unlike ω-Aga-IIIA, DHPs modify secretion by multiple mechanisms.

	7 mM K^+	60 mM K^+
	(% change in secretion ±SEM)	
ω-Aga-IIIA (30 nM)	-12 ± 4	+22 ± 9
nitrendipine (1 nM)	+17 ± 13	+65 ± 12
nitrendipine (1 μM)	-82 ± 3	-74 ± 4
Ni (250 μM)	-66 ± 10	+52 ± 9

Tu-PM-C5

ω-Aga-IVA SPIDER TOXIN INHIBITS ONLY THE INACTIVATING Ca^{2+} CURRENT OF ISOLATED NEUROHYPOPHYSIAL TERMINALS.

((Gang Wang and José R. Lemos)) Worcester Found. Experimental Biology, 222 Maple Avenue, Shrewsbury, MA 01545

The funnel-web spider polypeptide toxin, ω-Aga-IVA, potently and specifically blocks P-type Ca^{2+} channels in neuronal cell bodies (Mintz et al, 1992, *Nature* 355: 827). 'Whole-cell' patch-clamp measurements of Ca^{2+} currents in isolated neurohypophysial nerve terminals of the rat were performed in order to examine the sensitivity of their Ca^{2+} channels to ω-Aga-IVA (a generous gift from Michael E. Adams, Univ. of California at Riverside). In the presence of 10 mM Ca^{2+}, stepping from a holding potential -90 mV, elicits an inactivating and non-inactivating high-voltage-threshold Ca^{2+} current. The inactivating Ca^{2+} current was strongly inhibited by externally applied ω-Aga-IVA with a K_d of approximately 15 nM. In contrast, the non-inactivating Ca^{2+} current was not significantly affected by the same concentration of ω-Aga-IVA. The inhibition of the inactivating Ca^{2+} current by ω-Aga-toxin appears identical to that previously observed (Lemos & Wang, 1991, *Soc. Neurosci Abstr.* 17:342) using FTX, another funnel-web spider toxin. These data suggest that at least one of the channels underlying the inactivating Ca^{2+} current of the rat neurohypophysial nerve terminals is a P-type Ca^{2+} channel. (Supported by NIH & NSF grants to JRL and NS24472 to MEA)

Tu-PM-C6

ω-Aga-IIB: A HIGH AFFINITY PEPTIDE BLOCKER OF MULTIPLE TYPES OF VOLTAGE-GATED Ca CHANNELS.

((E.A. Ertel, C.J. Cohen, M.D. Leibowitz, V.A. Warren & M.M. Smith)) Merck Research Labs, PO Box 2000, R80N-31C, Rahway, NJ. 07065.

We have isolated the peptide ω-agatoxin-IIB (ω-Aga-IIB) from the venom of the funnel web spider *Agelenopsis aperta*. The primary structure of the N-terminal 75 residues has been determined by peptide mapping and Edman sequencing; it is identical to that of ω-Aga-IIA in 26 of the first 28 positions. ω-Aga-IIB blocks at least one type of Ca current in locust metathoracic ganglion neurons. Like the Type III ω-agatoxins (ω-Aga-IIIA, B & D), ω-Aga-IIB inhibits the binding of ^{125}I-ω-conotoxin GVIA to rat brain synaptosomal membranes (IC_{50} ≈ 20 pM, Type III's ≈ 10-20 pM) and blocks L-type Ca channels in guinea pig atrial myocytes (IC_{50} ≈ 25 nM, Type III's ≈ 0.3-130 nM). Unlike the Type III ω-agatoxins, ω-Aga-IIB blocks T-type Ca channels in atrial myocytes (fig). The toxin blocks all L-type current, but a variable fraction of the slowly-deactivating T-type current is sensitive (15-60%, n=16).

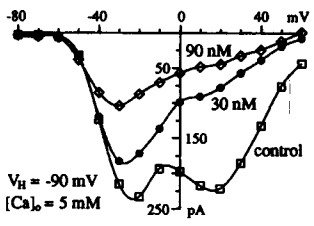

Additionally, ω-Aga-IIB blocks T-type Ca currents in rat somatotrophs, pancreatic ß-cells, and the A10 aortic muscle cell line, but not in calf adrenal glomerulosa cells. These results suggest that ω-Aga-IIB recognizes a high affinity binding site(s) on electrophysiologically distinct Ca channel types and that it may distinguish between multiple subclasses of T-type Ca channels.

Tu-PM-C7

FUNCTIONAL DIVERSITY OF L-TYPE CALCIUM CHANNELS IN RAT CEREBELLAR NEURONS.

((L. Forti and D. Pietrobon)) C.N.R. Center Biomembranes, Univ. of Padova, 35121 Padova, Italy.

Single channel recordings show that functionally different L-type calcium channels coexist in rat cerebellar granule cells. Besides two different dihydropyridine(DHP)-sensitive gating patterns with properties similar to those of cardiac L-type channels, cerebellar granules contain a third DHP-sensitive gating pattern with novel and unusual voltage-dependent properties and slightly different conductance. This "anomalous gating" is characterized, on one hand, by rare short openings with very low open probability even at high positive voltages (because open times shorten with increasing voltage and closed times decrease to a minimum and then increase with voltage). On the other hand it displays remarkably long openings with high open probability at negative voltages after a positive prepulse, often with some delay after the predepolarization. We show that these long openings are not reopenings during recovery from inactivation. The anomalous gating can be explained by a model in which voltage controls the equilibrium between two gating modes analogous to mode 1 and mode 2 of cardiac L-type channels, but with a distinctive feature. In the set of states constituting each mode there is a special closed state connected to the open state by a voltage-dependent transition, such that mode 2 has long openings with high open probability at negative voltages but short openings with low open probability at positive voltages.

Tu-PM-C8

VERY LONG OPENINGS OF CARDIAC CALCIUM CHANNELS EXPOSED TO FPL 64176.

((A.E. Lacerda[1], W.J. Crumb[1], D. Rampe[2], M.B. Ladner[3], M. Coyne[3], X. Wei[4], E. Perez-Reyes[1], L. Birnbaumer[1,4,5] and A.M. Brown[1])) [1]Dept. of Molecular Physiology & Biophysics, [3]Cell Biology and [4]Div. of Neuroscience, Baylor College of Medicine, Houston, TX 77030 and [2]Chiron Corporation, Emeryville, CA 94608 and [5]Dept. of Pharmacology, Marion Merrel Dow Research Institute, Cincinnati, OH 45215.

Single channels from the α_1 subunit of the rabbit cardiac dihydropyridine (DHP) sensitive calcium channel expressed in either *Xenopus* oocytes or Sf9 insect cells and single channels from native cardiac calcium channels respond to DHP agonists with prolonged openings. Openings in the presence of the DHP agonist Bay K 8644 are similar in native and expressed channels. Open time histograms show the presence of three open time taus with the slowest tau less than 50 ms. FPL 64176 binds to a site distinct from the DHP binding site. Openings of expressed channels exposed to FPL 64176 are similar to those seen with Bay K 8644. However, in native channels, the openings are very prolonged with average values for the slowest tau from 70 to 300 ms. Modulation of calcium channel gating by FPL 64176 appears to be sensitive to factors including associated subunits which do not affect DHP gating. The FPL site may be useful in probing calcium channel function and in the design of calcium channel subtype selective compounds.

Unlike DHP agonists, FPL 64176 does not increase current decay during a step depolarization. Comparison of first latency distributions with averaged single channel currents shows that the average current is still increasing after most channels have opened for the first time, suggesting that later openings of the channels are modified in the presence of FPL 64176 through a unique interaction with the open state of the channel. *(Supported by HL37044)*

Tu-PM-C9

HIDDEN MARKOV ANALYSIS OF SINGLE CHANNEL EVENTS.

((F. J. Sigworth and Y. Yang)) Department of Cellular and Molecular Physiology, Yale School of Medicine, New Haven CT 06510.

Digital signal processing for the extraction of information from 'hidden' Markov processes has recently been applied to single-ion-channel events (Chung et al, Phil Trans. R. Soc. B 329: 265, 1990 and 334:357, 1991; Walsh and Sigworth, Biophys. Soc. Abstr. 1992). We report the application of these processing techniques to simulated and actual channel recordings that include nonwhite background noise, baseline drifts and very rapid channel kinetics. We pass the digitized signal through an n-tap FIR filter to prewhiten the background noise, and then analyze it with an n^{th}-order hidden Markov model to account for both channel kinetics and filtering. We find that estimates of the amplitude and some kinetic information about channel events can be obtained at signal to noise ratios (SNR = channel amplitude / rms noise) as low as ~1.0 in cases where channel open or closed dwell times have components as short as one sample interval. Of more practical interest is the analysis of data having higher SNR values but which are still too noisy for conventional threshold detection techniques.

Tu-PM-D1

HOLOGRAPHIC OBSERVATION OF CORRELATION IN CROSSBRIDGE MOTIONS DURING ACTIVE CONTRACTION. ((Mark Sharnoff and Hungyi Lin)) Dept. of Physics, Univ. of Delaware, Newark, DE 19716-2570

By recording fluctuations in the phase of light scattered primarily from crossbridges, we are studying ultrastructural motion in activated intact skeletal fibers. Light scattered near 90° from the doubly flashed laser beam (514.7 nm) is collected by a microscope objective of N. A.=0.8, passed to a holographic plate, and there recorded, simultaneously, in a pair of phase-conjugate differential holograms. The conjugate differential images reconstructed from the holograms were scanned by a CCD camera at a resolution of 1 pixel per optical resolution cell of diameter ca. 330 nm. A typical pixel therefore received light scattered by ca. 7,000 crossbridges. Motion of the aggregate center of mass of the crossbridges is reflected in the resultant phase of the light which they scatter. Since phase-conjugate differential recording converts the inter-flash (ca. 2 - 30 msec) change in phase of the light scattered from any optical resolution cell into a shift in reconstructed intensity, the pixel intensities map the migration of crossbridge aggregate centers of mass. Sums and differences of the images were interrogated digitally and analyzed statistically. The interflash redistribution of centers of mass proved grossly inconsistent with the view that crossbridges cycle independently of each other during contraction. A simple model of their behavior suggests that crossbridge motions are coordinated within groupings of ca. 500 individuals. Supported by NSF under DCB 8821065.

Tu-PM-D2

CROSSBRIDGE STRUCTURE IN RIGOR INSECT FLIGHT MUSCLE IMAGED BY 3-D RECONSTRUCTION FROM OBLIQUE SECTIONS. ((K. A. Taylor[1], M. C. Reedy[1], M. K. Reedy[1] and R. A. Crowther[2])) [1]Dept. of Cell Biology, Duke Univ. Med. Center, Durham, NC 27710; [2]MRC Lab. of Molecular Biology, Hills Road, Cambridge CB2 2QH, England.

3-D reconstructions from single images of oblique cross sections through rigor insect flight muscle permit simultaneous examination of all myosin crossbridges within the unit cell. These reconstructions reveal variations in the rigor double chevrons within the 116 nm long axial repeat and establish that, in rigor, the 116 nm period contains nine 12.9 nm repeats of attached crossbridges rather than the eight 14.5 nm repeats of myosin head origins observed in the relaxed state. This observation indicates that the actin repeat dominates and enforces axial and azimuthal changes on the myosin crossbridge origins on the thick filament. The reconstructions confirm in greater detail the presence of both two-headed and single-headed crossbridges, implying heads with differing angles and conformation, and suggest twist variation in the thin filament coincident with the lead crossbridge. In addition, these 3-D maps show a feature on the thin filament, just Z-ward of the attachment site of the rear crossbridge, which antibody labelling evidence identifies as part of the large insect troponin complex. Supported by NIH grants GM-30598 and AR-14317.

Tu-PM-D3

FORMATION OF 2-D CRYSTALS OF SMOOTH MUSCLE α-ACTININ ON POSITIVELY CHARGED LIPID LAYERS. ((Kenneth A. Taylor and Dianne W. Taylor)) Dept. of Cell Biology, Duke Univ. Med. Center, Durham, NC 27710 (Spon. by M. Titus).

Chicken gizzard α-actinin crystallizes in 2-D on positively charged lipid monolayers. The crystals have space group symmetry P2 with cell dimensions of a=248Å, b=194Å, γ=106°. There are two α-actinin molecules each 340 Å in length within the unit cell. Projection images calculated to a resolution of 25Å reveal a complex substructure consisting of twelve density peaks that probably correspond to protein domains. Two of these are found at each end of the molecule and probably correspond to the actin binding region. Eight additional peaks are observed in the central, rod-shaped region that may correspond to the spectrin-like repeats predicted from the amino acid sequence. These eight central peaks are arranged in three central pairs flanked at either end by a single peak that appears larger and denser in projection than the three central pairs. The extra density may indicate proximity with the C-terminal peptide. The ends of the molecule have different appearance in projection suggesting that the molecule is twisted about the long axis. An hypothesis is proposed to explain the variations in molecular length and Ca^{2+} sensitivity between α-actinin isoforms. Supported by a grant-in-aid from the American Heart Association and NIH grant GM-30598.

Tu-PM-D4

MOLECULAR PHYSIOLOGY OF THE LENGTH-DEPENDENCE OF Ca^{2+}-SENSITIVITY OF SKINNED FIBERS, WITH A LOW AND A HIGH AFFINITY TNC- MUTANT

((J. Gulati, A. Babu, and Hong Su)) Albert Einstein College of Medicine, Bronx, NY 10461

To investigate the role of TnC as a length-sensor modulating the Ca^{2+}-sensitivity, we generated a unique low sensitivity mutant (*ΔNtΔKGK*) and a high sensitivity mutant (*GS9092LL*), using genetic engineering. The overall Ca^{2+}-sensitivity was 2.5-fold higher and 5 fold lower, respectively, by force development in rabbit psoas muscle. The effects of the mutants on length-dependence are reported. The TnC from only half of each thin filament of skinned fibers was deleted around the Z-line (Asymmetric-extraction). Subsequently, the fibers were reconstituted with the individual mutants. The pCa-force were measured at 2.4μm and 1.9μm. The length-dependent shifts in pCa_{50} were close to 0.17 pCa unit in both the normal and symmetrically loaded fibers, irrespective of the mutant. But in asymmetric fibers, the length-dependence was *diminished* with *GS9092LL*-loading (ΔpCa_{50}=0.04±0.01, n=4) and *enhanced* with *ΔNtΔKGK*-loading (ΔpCa=0.40±0.08, n=3). The results show that (1) TnC molecules only within the overlap domain of thin-thick filaments interact to determine the mean sensitivity. (2) The Ca^{2+}-affinity of each TnC unit varies with its disposition on thin filament – the Ca^{2+}-affinity progressively increases from the Z-line towards the sarcomere center. This novel polarity of the thin filament is suggested as the molecular mechanism of length transduction in the modulation of Ca^{2+}-sensitivity within the sarcomere. [NIH & NYH funded]

Tu-PM-D5

DISTORTION-DEPENDENCE OF PHOSPHATE RELEASE MONITORED BY WATER-PHOSPHATE OXYGEN EXCHANGE.

((D.C.S. White[1], J. Lund[1], J.E. Molloy[1] & M.R. Webb[2])) [1]Department of Biology, University of York, YO1 5DD, UK & [2]NIMR, Mill Hill, NW1 1AA, UK

Oxygen exchange between phosphate and [^{18}O]water during ATP hydrolysis was monitored during a series of incubations of dorsal longitudinal flight muscle fibres from the giant waterbug *Lethocerus indicus*, in which the length was oscillated between 2 and 4% strain at 2Hz, but with a different duration t1 at 4% strain in the separate incubations. There was a marked increase in the proportion of phosphate with fully-exchanged oxygen at intermediate values of t1, maximal at about 50ms. Two factors can contribute to this effect: (a) cross-bridges with no available actin sites at the lower strain (and thus with fully-exchanged phosphate) being brought into alignment with actin sites by strain, and (b) attached cross-bridges distorted by the length change being less able to proceed with their working stroke and thus acquiring more fully-exchanged phosphate. Supported by MRC and SERC.

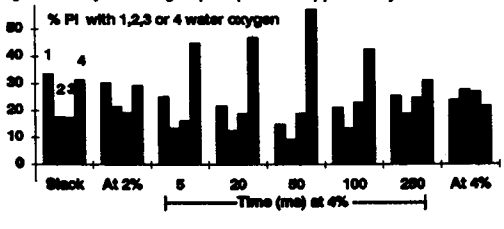

Tu-PM-D6

BDM AFFECTS NUCLEOTIDE BINDING STEPS OF THE CROSS-BRIDGE CYCLE IN RABBIT PSOAS FIBERS. ((Yan Zhao and Masataka Kawai)) Dept. of Anatomy, University of Iowa, Iowa City, IA 52242.

It has been known that BDM (2,3-butanedione monoxime) reversibly suppresses tension development in skinned fibers, but the molecular mechanism of BDM in contraction is still unknown. We are intrested in studying the effect of BDM on elementary steps of the cross-bridge cycle with sinosioidal analysis in skinned fibers. Our earlier reports showed that the exponential process (C) characterizes the cross-bridge detachement step (step 2), and process (B) characterizes the power stroke step (step 4).

$$\mathrm{AMD} \overset{D}{\underset{K_0}{\rightleftharpoons}} \mathrm{AM} \overset{K_1}{\underset{S}{\rightleftharpoons}} \mathrm{AMS} \overset{k_2}{\underset{k_{-2}}{\rightleftharpoons}} \mathrm{Det} \overset{k_4}{\underset{k_{-4}}{\rightleftharpoons}} \mathrm{AM^*DP} \overset{P}{\underset{K_5}{\rightleftharpoons}} \mathrm{AM^*D} \overset{k_5}{\rightarrow}$$

Where D=MgADP, S=MgATP, Det=detached state, P=phosphate. We studied the effect of MgATP and MgADP on exponential process (C), and the effect of Pi on process (B) in the presence/absence of BDM (18mM) at maximal Ca activation and at 20°C. Our results demonstrate that ADP and ATP binding constants (K_0 and K_1) respectively increase 7 and 31 times with BDM, but phosphate binding constant (K_5) does not change at all; The equilibrium constant of detachement step (K_2) increases almost two times, whereas the equilibrium constant of attachement (power stroke) step (K_4) decreases about two times with BDM. Thus, in the presence of BDM, more cross-bridges accumulate in the detached state, causing isometric tension to decline. We conclude that BDM is an allosteric effector that affects many steps in the cross-bridge cycle, in particular, enhances the nucleotide binding to cross-bridges.

Tu-PM-D7

MULTIPLE STEP ATP HYDROLYSIS GATED BY PHOSPHATE RELEASE AND RE-BINDING TO THE CROSSBRIDGES OF MUSCLE

((C.Y. Seow and L.E. Ford)) University of Chicago, Chicago, IL 60637

Skinned rabbit psoas fibers were studied at 1-2°C. 40 mM phosphate decreased isometric force by 29% and 38%, respectively at pH 6.35 and 7.35. Its effect on maximum velocity depended on pH, increasing it by 29% at pH 7.35 and decreasing it by 11% at pH 6.35. Sarcomere stiffness measured in tension transients at both pH's was depressed to a lesser extent than force, suggesting a decreased force/stiffness ratio and less average force per crossbridge. In addition, the early rapid (Phase 2) force recovery following a step was slowed, suggesting that the lower force was caused by the detention of crossbridges in low force states that precede the power stroke. At high pH but not low pH, the later force recovery was both more rapid and more extensive, suggesting that phosphate might increase shortening velocity at high pH by altering a transition that occurs after a delay, as would be imposed by the power stroke. At pH 7.35, 5 mM ADP increased isometric force by 28% and decreased maximum velocity by 42%. The increased force was entirely reversed by 2.5 mM phosphate. 40 mM phoshate further depressed force by 42% and reversed about half of the decrease in velocity. These results suggest that phosphate has a dual role; its release is required to allow attached bridges to undergo their power stroke, and its rebinding to high force bridges with bound ADP promotes their detachment. This conclusion further suggests that there might be several populations of detached bridges that all have bound ADP and phosphate but which differ with regard to amount of ATP hydrolysis energy remaining. Evidence for these populations can be found in the additional observation that ADP and phosphate abolish an intermediate plateau of high relative force that is maintained for a brief period when isometric sarcomeres are suddenly driven to shorten at a constant velocity.

Tu-PM-D8

WATER IS THE REAL ACTOR IN BIOLOGICAL ENGINES. THE PROTEINS ARE MERELY THE STAGE. (Avraham Oplatka) Weizmann Institute of Science, Rehovot, Israel (Spon. by P.C. Leavis)

A wealth of data suggests that water bound to actomyosin is actively involved in muscular contraction. Thus, during an isomerization which occurs at the end of the ATPase cycle, an increase in volume of ΔV=110 c.c./mole myosin heads was detected, largely ascribed to a change in state of bound water (Coats *et al.*, Biochem. J., 1985). The ratio of $\Delta V(>o)$ and the volume of released water (V) for polymerization is the same for flagellin and for tobacco mosaic virus protein, which is typical of a phase transition. Applying this ratio to actomyosin I found that 25 water molecules are released per head. Dividing the enthalpy change of the reaction (>o) by 25 the value of 1.5 kT was obtained per water molecule, which is the translational kinetic energy of a gas or a liquid molecule. Employing the ideal gas equation P=cTR to half an A-band with a crossectional area of 1cm^2 we obtain P=1.46 kN/m^2, which is in the usual range of values of the maximal isometric tension. It is proposed that the water molecules are ejected towards the center of the sarcomeres thus exerting a pressure which is detected as tension. Substituting the above value of ΔV in $\Delta V/V = -\kappa P$ relating the change in volume of a liquid to applied hydrostatic pressure we obtain P = 1.61 kN/m^2. Data is presented which suggests that the same mechanism operates also in microtubule-based engines.

Tu-PM-D9

POSITIVE EFFECT OF EJECTION IN ISOLATED RAT CARDIAC TRABECULAE

((Pieter P. de Tombe)) Bowman Gray School of Medicine, Winston-Salem, NC 27157.

It has been shown previously in isolated canine ventricles that ejection can prolong the duration of pressure development, and it has been suggested that this is a property of the cardiac sarcomere. The purpose of the present study was to evaluate this hypothesis in isolated rat cardiac trabeculae. Muscle length (ML) was controlled by a motor; force (F) was measured by a silicon strain gauge; and sarcomere length (SL) was measured by laser diffraction techniques. To simulate contractile events at the sarcomere level, the ventricle was modeled as a thick-walled sphere. F was converted to ventricular pressure ("P"), applied to a simulated afterload impedance (3-element Windkessel) to derive ventricular volume ("V"), which was next converted to SL. An iterative adaptive algorithm was then used to drive ML such that desired SL was followed during the twitch. The figure shows the experimental protocol (left panel) which consisted of isovolumic beats at varied preload, and ejecting beats at varied afterload. The right panel shows measured "P" during ejection at intermediate afterload (M); "P" calculated from instantaneous "V" and isovolumic "P" time-courses (C); and the difference M-C (D). During early ejection, "P" was lower than predicted from the isovolumic beats as would be expected considering the force-velocity relation. However, during late ejection, measured "P" was higher than calculated "P", reaching a maximum at the onset of relaxation. This maximum "pressure difference" was largest at the lowest afterload (not shown).

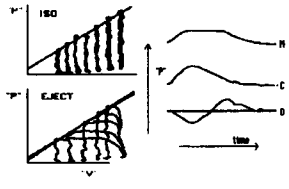

We conclude that 1) ejection causes an increase in the duration of pressure development, and 2) this phenomenon *is* a property of the cardiac sarcomere.

Tu-PM-D10

STEADY-STATE CALCIUM FORCE RELATIONSHIP IN INTACT TWITCHING CARDIAC MUSCLE: EVIDENCE FOR DESENSITIZATION BY ISOPROTERENOL ((L.E. Dobrunz, P. Backx, and D.T. Yue)), Johns Hopkins School of Medicine, Baltimore MD 21205.

ß-adrenergic stimulation may desensitize the myofilaments in cardiac muscle, shifting the steady-state $[Ca^{2+}]_i$-tension relationship to higher $[Ca^{2+}]_i$. While the biochemical evidence is consistent with this idea, there is little direct evidence for this mechanism in intact muscle. To test this hypothesis directly, we developed a strategy for deriving steady-state $[Ca^{2+}]_i$-tension relations in twitching muscle. Application of cyclopiazonic acid (50 μM) and ryanodine (1 μM) (potent inhibitors of SR $[Ca^{2+}]_i$ uptake and release, respectively) produced a striking slowing of twitch contraction, as gauged by the prolongation of $[Ca^{2+}]_i$ and tension transients measured in rat trabeculae injected with FURA-2 (A vs. B). Contraction was slowed to the extent that tension and $[Ca^{2+}]_i$ approached steady state late in the twitch (t > *), as shown by the superposition of $[Ca^{2+}]_i$-tension curves derived from this portion of twitches with different $[Ca^{2+}]_i$ (C, Ctrl). We then tested the effect of isoproterenol (1 μM) and found it shifted the $[Ca^{2+}]_i$-tension relationship significantly rightward (C, Iso). Hill equation fits to the data in C point to a 1.6-fold increase in the $[Ca^{2+}]_i$ required for half-maximal activation. This method allows measurement of steady-state $[Ca^{2+}]_i$-tension relations within a single contraction, and provides direct evidence that ß-adrenergic stimulation decreases myofilament $[Ca^{2+}]_i$ sensitivity in intact cardiac muscle.

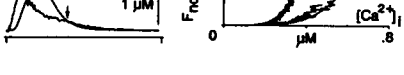

EXCITATION-CONTRACTION COUPLING: CARDIAC MUSCLE

Tu-PM-E1

Steady-State Force-pCa Relationship in Intact Rat Cardiac Trabeculae measured using microinjected Fura-2 Salt

Peter H Backx, Michelle D. Azan-Backx, Eduardo Marban. Faculty of Medicine, Johns Hopkins Unversity, Baltimore MD

The steady state relationship between force (F) and the cytosolic $[Ca^{2+}]$ was studied in intact cardiac trabeculae from the rat tetanized in the presence of 10μM ryanodine. $[Ca^{2+}]$ was estimated using iontophoretically microinjected Fura-2 salt (*Backx & ter Keurs AJP: in press*). The F-$[Ca^{2+}]$, at an end-systolic sarcomere length of 2.1-2.2 μm, could be fit with Hill equation. The fitted estimate of the half maximal activation (K_D) were 569nM and the Hill coefficient (n) equalled 3.87 (N=5). This contrasts to estimates obtained in skinned fibers (i.e. $K_D \approx 5\mu$M and $n \approx 2$-5, *Chapman, Am J Physiol 245:H535-H552,1983*). The maximum force (F_{max}) recorded with ryanodine tetani with an extracellular $[Ca^{2+}]$ of 10-20mM was 112mN/mm^2 in the intact trabeculae versus 105mN/mm^2 in the same trabeculae following skinning and maximal activation with 40μM $[Ca^{2+}]$. Our results support the finding (*Yue, Marban & Wier, J Gen Physiol 87:223-242, 1986*) that the intact F-pCa is shifted leftward by about one pCa unit when compared to skinned fibers, and that maximal stress obtained in the intact ryanodine tetanized muscle is identical to that obtained in the skinned fibers.

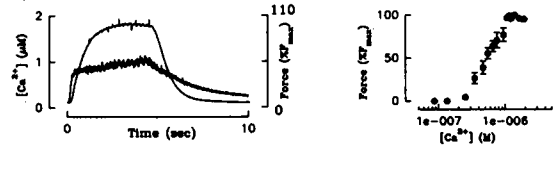

Tu-PM-E2

CHARACTERIZATION OF THE CALCIUM PUMP OF THE CARDIAC SARCOPLASMIC RETICULUM *IN SITU*.

((T.M. Egan, W.G. Wier, C.W. Balke)) University of Maryland, Baltimore, MD 21201

In mammalian cardiac muscle, relaxation occurs as a result of the decline of the cytoplasmic free calcium ion (Ca^{2+}) concentration ($[Ca^{2+}]_i$) as Ca^{2+} is sequestered by the sarcoplasmic reticulum (SR) Ca^{2+}-ATP-ase and extruded by the Na^+/Ca^{2+} exchanger. In order to quantitatively describe SR Ca^{2+}-uptake, we studied the declining phase of the $[Ca^{2+}]_i$ under experimental conditions (Na^+-free) where the fall of the $[Ca^{2+}]_i$ was due to the sequestration of Ca^{2+} by the SR Ca^{2+}-ATP-ase and to the complexation of Ca^{2+} by intracellular Ca^{2+}-ligands as described by equation (1). Peak whole-cell L-type calcium currents ($I_{Ca\text{-}L}$) and

(1) $$d[Ca^{2+}]_i/dt = -V_{max}/(1+(K_M/[Ca^{2+}]_i)^2) - \Sigma\{d[CaL]_n/dt\} + F_{leak}$$

$[Ca^{2+}]_i$ were obtained in single rat ventricular cells by 200 msec depolarizations to -10 mV from a holding potential of -50 mV. The cells were internally perfused with indo-1 (salt). Na^+/Ca^{2+} exchange was eliminated with Na^+-free solutions internally and externally. With the quantitative characterization of the Ca^{2+}-binding ligands and the assumption that SR Ca^{2+}-release is over after repolarization, the K_M, V_{max}, and F_{leak} were computed by multi-parametric fitting of the declining phase of the $[Ca^{2+}]_i$ to equation (1). Under a variety of experimental conditions, the K_M = 0.50 µM, and V_{max} = 7.5 pmoles/cm^2/s. These values are consistent with values of K_M & V_{max} obtained for the SR Ca^{2+}-ATP-ase from biochemical studies and indicate that equation (1) adequately describes the declining phase of the $[Ca^{2+}]_i$ *in vivo*.

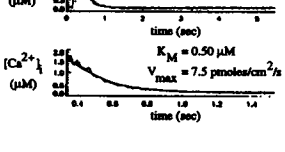

Tu-PM-E3

CALCULATION OF THE EFFLUX OF CALCIUM FROM THE CARDIAC SARCOPLASMIC RETICULUM

((C. W. Balke, T.M. Egan, W.G. Wier)) University of Maryland, Baltimore, MD 21201

The experimental evaluation of new theories of excitation-contraction coupling in mammalian cardiac muscle has been hampered by the lack of quantitative information regarding sarcoplasmic reticulum (SR) Ca^{2+}-release ($F_{SR,rel}$). We calculated $F_{SR,rel}$ from measurements of the cytoplasmic free Ca^{2+} concentration ($[Ca^{2+}]_i$), the whole-cell L-type Ca^{2+}-current (I_{Ca-L}), verified assumptions regarding Ca^{2+}-binding ligands, and the computed uptake of Ca^{2+} via the SR Ca^{2+}-ATP-ase (abstract: Egan *et al. Biophys J*, in press) according to equation (1).

(1) $F_{SR,rel}=d[Ca^{2+}]_i/dt-V_{max}/((1+K_M)/[Ca^{2+}]_i)^2)+\Sigma\{d[CaL]n/dt\}-F_{leak}-FI_{Ca-L}$

I_{Ca-L} & $[Ca^{2+}]_i$ were elicited by a 200 ms depolarization to a range of test potentials from -30 mV to +80 mV from a holding potential of -50 mV in single rat ventricular cells perfused with the fluorescent Ca^{2+}-indicator, indo-1. Na^+/Ca^{2+} exchange was eliminated with Na^+-free solutions internally and externally. The figure illustrates the calculation of FI_{Ca-L}, $F_{SR,rel}$, and $F_{SR,uptk}$ derived from the peak I_{Ca-L} & $[Ca^{2+}]_i$ during a depolarization to -10 mV. Like I_{Ca-L}, $F_{SR,rel}$ has a bell-shaped dependence on test potential. $F_{SR,rel}$ was also terminated with stopping I_{Ca-L}, and was elicited by Ca^{2+}-current "tails" on repolarization from positive test potentials.

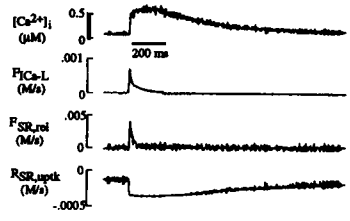

Tu-PM-E4

GREATER PARTICIPATION OF Na-Ca EXCHANGE IN RELAXATION OF RABBIT THAN OF RAT CARDIAC MYOCYTES.

((Rosana A. Bassani, José Wilson M. Bassani and Donald M. Bers)) Loyola University, Maywood, IL 60153.

Rapid relaxation in cardiac muscle depends on myoplasmic Ca removal by the sarcoplasmic reticulum Ca-pump (SR) and Na-Ca exchange (Na-CaX). To compare the participation of these mechanisms during relaxation of rabbit and rat cardiac cells, we determined the half-times of relaxation ($t_{1/2}$) of steady-state twitches (0.5 Hz) and caffeine-induced contractures (CafC) in control (NT) and 0Na,0Ca solutions. Comparable results were obtained with cell shortening and Ca_i transients (using indo-1). Twitches relaxed faster in rat ($t_{1/2}$ = 0.08 ± 0.01 s) than in rabbit (0.18 ± 0.01 s, P< 0.01). In contrast, the $t_{1/2}$ of relaxation when the SR and Na-CaX were inhibited (CafC in 0Na,0Ca solution) was similar in both species (rat: 10.16 ± 0.97 s; rabbit: 8.83 ± 0.44 s). During CafC with Na_o, Na-CaX is primarily responsible for relaxation which was slower in rats (2.09 ± 0.30 s) than in rabbits (0.60 ± 0.09 s, P< 0.01). This may indicate that the Na-CaX is ~3 fold slower in rat. Thus, we might expect the rat twitch to relax 3 times slower (rather than 2.2 times faster). The faster relaxation indicates that the SR must be more powerful in the rat and that it more than compensates for the slower Na-CaX.

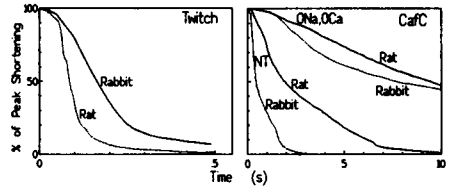

Tu-PM-E5

SR Ca UPTAKE AND THAPSIGARGIN SENSITIVITY IN PERMEABILIZED RABBIT AND RAT VENTRICULAR MYOCYTES.

((L. Hove-Madsen and D.M. Bers)) Dept. of Physiology, Loyola University Chicago, Maywood, IL 60153.

Ca uptake and thapsigargin (TG) sensitivity was measured with Ca selective minielectrodes in suspensions of digitonin permeabilized myocytes isolated from rat and rabbit ventricle (10-20 mg/ml protein). In the presence of 25 μM ruthenium red and 10 mM oxalate, the maximal Ca uptake rate was 2.4 times higher in rat than in rabbit. The left figure shows SR Ca uptake after a Ca addition in rat myocytes with successive increments in TG concentration. A submaximal [TG] of 2 μM (0.1 nmol/mg) slowed the uptake rate 5-10 fold, but the cells could still lower free [Ca] below 150 nM. Addition of 5 nmol TG/mg cell protein abolished Ca uptake completely in both species in less than 15 sec. The right figure compares the [TG] dependence of Ca uptake rate. The $K_{1/2}$ for Ca pump inhibition for rabbit and rat was 55 and 390 pmol/mg, respectively. If the K_d for TG is much lower than the [pump sites], then the number of pump sites can be estimated as twice the $K_{1/2}$. This gives densities of pump sites for rabbit and rat of 7.7 μmol /kg wet wt 54.6 μmol/kg wet wt respectively. We conclude that TG can rapidly and completely inhibit the SR Ca pump, and that there may be more SR Ca pump sites in rat than in rabbit ventricle.

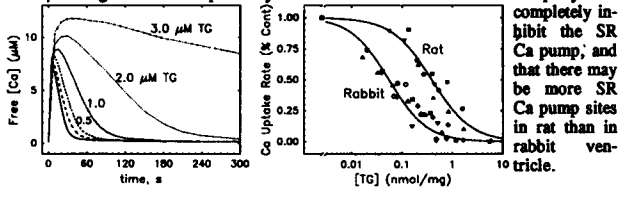

Tu-PM-E6

EFFECT OF TEMPERATURE ON VOLTAGE-TENSION RELATION OF GUINEA PIG HEART: ROLES OF ICA AND NA/CA EXCHANGE

((M.Vornanen, N.Shepherd and G.Isenberg))Univ. Köln 5000 Köln 41, GER. & VAMC, Durham, NC, 27705, USA.

Ventricular cells were fixed to a force transducer, perfused with a fast-solution-switching device & voltage-clamped at a steady rate to insure constant SR Ca-loading (1 Hz, 200 ms pulses to +5 mV, HP=-45 mV). The voltage-tension (V-F) relation for test pulses from -35 mV to +100 mV (Vt) was bell-shaped at 24°C but was N-shaped at 35°C (Na_i=0-20 mM). Contraction at 35°C at all Vt was a fast twitch (FT) followed by a 'tonic' phase (time to peak of FT ≈ 90 ms). A brief pulse of 5 mM caffeine applied just before a test pulse strongly reduced peak tension for all Vt, implying that SR Ca is needed for contraction. 300 uM Cd, applied only during a test pulse, 1) blocked FT for all Vt at 35 °C, 2) blocked all force at 24°C & 3) blocked a fast inward current, presumably I_{Ca}, for all Vt at both temperatures. Since the FT at +100 mV at 35°C depends on I_{Ca} & SR Ca but does not need Nai, Na/Ca exchange cannot play a role in triggering the FT, though it may be important for the slower 'tonic' component. Thus, different V-T relations at 24 & 35 °C may result from the slower, smaller I_{Ca} at 24°C.

Tu-PM-E7

FK-506 BINDING PROTEIN IS ASSOCIATED WITH THE RYANODINE RECEPTOR FROM CANINE HEART SARCOPLASMIC RETICULUM.

((A.P. Timerman#, T. Jayaraman*, Y. Kijima#, L.H. Jeyakumar#, E.M. Ogunbumni#, A-M. Brilliantes*, G. Wiederrecht+, A. Marks*, and Sidney Fleischer#)). #Dept. Molecular Biology, Vanderbilt University, Nashville, TN 37235; *Brookdale Center for Molecular Biology, Mount Sinai School of Medicine, New York, NY 10029; +Dept. Immunology Research, Merck Research Laboratories+, Rahway, NJ 07065.

Recently, we have shown that an immunophilin, FK-506 binding protein (FKBP), is associated with the ryanodine receptor of rabbit skeletal muscle terminal cisternae (J. Biol. Chem. 267, 9474, 1992). Western blot analysis using antiserum against the N-terminal amino acid sequence of FKBP-12 indicates the presence of FKBP in both sarcoplasmic reticulum and partially purified cardiac ryanodine receptor preparations isolated from dog heart. The stoichiometry of FKBP to ryanodine receptor in canine heart sarcoplasmic reticulum, as estimated by binding of ^{3}[H] FK-816 (a dihydropropyl derivative of FK-506) versus ^{3}[H] ryanodine, is approximately 1 FKBP per foot structure. This is about one-half the content of FKBP per foot structure found in rabbit skeletal muscle sarcoplasmic reticulum. These results provide the first demonstration that the cardiac ryanodine receptor is also associated with FKBP.

Supported in part by grants from NIH HL32711 and Muscular Dystrophy Association to S.F. APT is a NRSA receipient from the NIH.

Tu-PM-E8

PARALLEL CALCIUM RELEASE AND REUPTAKE BY CORBULAR AND JUNCTIONAL SR IN BEATING HEART.

((John McD. Tormey and Randi C. Goodnight)) Dept. of Physiology, UCLA, Los Angeles, CA 90024.

Corbular SR (CSR) consists of ~75 μm diameter bulbous evaginations of network SR in cardiac muscle. It has most of the ultrastructural and cytochemical properties of junctional SR (JSR), and contains elevated Ca (Jorgensen *et al* '88).

Rabbit papillary muscles were superperfused at 28°C and stimulated by paired-pulses at 0.3 Hz while force was recorded isometrically. Stimulation and recording continued until the instant when each muscle was "slam" frozen. Three groups were analyzed by electron probe x-ray microanalysis (EPMA): (a) *End Diastole* - frozen 10 ms before the next stimulus; (b) *Mid-rise* - frozen when developed force rose to 50% of peak (~150 ms after stimulation); (c) *Peak* - frozen at max. force.

The results indicate parallel Ca release and reuptake during a heartbeat:

	End Diastole	*Mid-rise*	*Peak*
JSR	8.99 ±0.86 (95)	3.91 ±0.50 (99)	4.96 ±0.85 (34)
CSR	3.92 ±0.34 (130)	2.15 ±0.24 (111)	2.55 ±0.46 (47)

Results are [Ca] in mmol/kg dry wt ± s.e.m. (N). End Diastole results differ significantly from others. (Lower values of [Ca] in CSR are due to its smaller dimensions relative to section thickness and electron beam.)

Additional evidence indicates the total amount Ca released is sufficient to explain developed force, but the JSR accounts for only a fraction of this amount. This suggests that CSR adds significantly to the functional capacities of the SR *in toto*. *(Supported in part by NIH grant HL31249)*

Tu-PM-E9

FUNCTIONAL COUPLING BETWEEN THE DIHYDROPYRIDINE RECEPTORS AND THE RYANODINE RECEPTORS OF CARDIAC MYOCYTES.

((J.S.K. Sham, L. Cleemann, and M. Morad)) Department of Physiology, University of Pennsylvania, Philadelphia, PA 19104-6085.

In skeletal muscle, dihydropyridine receptors appear to be functionally coupled to ryanodine receptors of the sarcoplasmic reticulum in the triadic or diadic junctional complexes. In cardiac muscle, a direct physical or functional coupling has not been as yet demonstrated. We tested the "functional coupling" hypothesis in whole cell-clamped and fura-2 dialysed cardiac myocytes by comparing the efficacy of Ca^{2+} in gating Ca^{2+} release, when Ca^{2+} enters the myocyte via the Ca^{2+} channels, the Na^+-Ca^{2+} exchanger, and the Ca^{2+}-transporting Na^+ channels. The Ca^{2+} influx through the Ca^{2+} channel and the Na^+-Ca^{2+} exchanger were activated by depolarizing pulses to 0 and +80 mV, respectively. The Ca^{2+} influx via the Na^+ channels was activated by depolarizing pulses to -40 or -30 mV in Na^+-free external solution containing 50 nM atrial natriuretic peptide (ANP), which increases the Ca^{2+} selectivity of the Na^+ channel (Sorbera and Morad, Science 247:969-972, 1990). The Ca^{2+} influx through the different transporters were quantified by integrating the current through the Ca^{2+} channel, the Na^+-Ca^{2+} exchanger, and the Ca^{2+} current passing through the ANP-transformed Na^+ channels. We found that Ca^{2+} transported via the Ca^{2+} channels was 20-160 times more effective than Ca^{2+} influx through Na^+-Ca^{2+} exchanger in gating Ca^{2+} release. Delivery of equivalent amount of Ca^{2+} through the ANP-transformed Na^+ channels failed to trigger significant Ca^{2+} release. Sustained delivery of Ca^{2+} via the ANP-transformed Na^+ channels in the veratridine-treated myocytes was accompanied with a slow rise in $[Ca^{2+}]_i$ which either failed to trigger Ca^{2+} release or activated only marginal and slow release when intracellular Ca^{2+} stores were overloaded. The high efficacy of Ca^{2+} influx through the Ca^{2+} channel in activating the ryanodine receptors suggests that the Ca^{2+} channels have *privileged access* to the Ca^{2+}-activation-site of the ryanodine receptors, and provide functional evidence for a close association between the two sets of receptors, most likely within the diadic junctions of cardiac myocytes. (Supported by HL16152 and AHA, Southeastern Pennsylvania Affiliate)

SMOOTH MUSCLE BIOCHEMISTRY AND PHYSIOLOGY

Tu-PM-F1

SINUSOIDAL ANALYSIS OF CROSS-BRIDGE INTERACTION IN SMOOTH MUSCLE FIBERS.

((A. Arner, M. Kawai*, Y. Zhao*)) Dept Physiol. and Biophys., Lund University, S-223 62 Lund, Sweden; and *Dept Anatomy, University of Iowa, Iowa City, IA 52242.

The elementary steps in the cross-bridge interaction in skinned smooth muscle fibers were studied using the sinusoidal analysis technique (Kawai & Halvorson 1989, Biophys. J. 55:595; Kawai & Halvorson 1991, Biophys. J. 59:329). Skinned fibers from guinea pig taenia coli (TC) and rabbit rectococcygeus (RC) were maximally activated with thiophosphorylation and studied at 22 °C in the presence of varying concentrations of ATP, ADP and phosphate (Pi). In the contracting muscle two exponential advance processes could be observed with approximate rate constants of 0.2-0.4 s^{-1} (slow) and 2-3 s^{-1} (fast). In this study we have characterized the faster exponential process. Addition of Pi resulted in a concentration-dependent decrease in force and increase in the rate constant of the faster process. The effect of Pi on the rate constant was more pronounced in the RC compared to the TC muscle and at 24 mM Pi the rate constant in RC was 1.5-2 times higher than in TC. Increasing [ATP] in the range 1 to 10 mM in the presence of 24 mM Pi decreased force and increased the rate constant. Increasing ADP at constant Pi and ATP decreased the rate constant. The results are consistent with the cross-bridge scheme proposed for striated muscle and we conclude that the observed faster exponential process reflects cross-bridge detachment steps after ATP binding.

Tu-PM-F2

INHIBITION OF SPONTANEOUS TONE BY CYANIDE IN SMOOTH MUSCLE OF RAT PORTAL VEIN: ROLE OF ATP-REGULATED POTASSIUM CHANNELS.

((P. Hellstrand, K.H. Swärd and M.-L. Lydrup)) Dept of Physiology and Biophysics, Univ. of Lund, S-226 53 Lund, Sweden. (Spon. by S. Forsén)

Vascular smooth muscle tone is dependent on oxidative metabolism, a phenomenon of potential importance for the metabolic regulation of blood flow to tissues. The response of the rat portal vein to inhibition of cell respiration by cyanide is a reduced amplitude of its spontaneous phasic contractions, mimicking hypoxic vasodilatation. The trains of action potentials triggering the contractions are reduced in duration, while the frequency of trains is often somewhat increased as the membrane is slightly depolarized in the intervals between spike trains. Glibenclamide (glib; 0.1 μM) did not affect electrical or mechanical activity of oxygenated portal veins in the absence of cyanide, but significantly increased activity in its presence (0.5 mM). This was associated with a less reduced duration of the spike trains, while the membrane depolarized slightly more than with cyanide alone. Basal cytosolic Ca was increased by cyanide, while the Ca transients associated with phasic contractions were reduced in duration, and this latter effect was partially reversed by glib. We conclude that the effects of inhibited cell respiration on spontaneous activity reflect a depolarizing drive, possibly caused by inhibited active ion pumping, modified by a repolarizing drive from ATP-sensitive K channels causing reduced duration of the spike trains.

Tu-PM-F3

MECHANISM OF CA^{2+} SENSITIZING EFFECT OF PROTEIN KINASE C ON SMOOTH MUSCLE.

((T. Kitazawa*, S. Reardon+, M. Ikebe+ and M. Masuo*)) *Dept. of Physiol., Univ. of Virginia, Charlottesville, VA 22908 and +Dept. of Physiol. and Biophys., Case Western Reserve Univ., Cleveland, OH 44106.

The mechanism of Ca^{2+} sensitization of myosin light chain (MLC) phosphorylation and force by PKC was studied in permeabilized arterial smooth muscle in comparison with GTPγS effect. PKC activators (phorbol esters, short chain synthetic diacylglycerols and a DAG kinase inhibitor) significantly increased MLC phosphorylation and force at constant Ca^{2+} as observed with GTPγS. Major phosphorylation site during Ca^{2+} sensitization by PDBu or GTPγS was the same MLC kinase-specific site (Ser-19) as that by Ca^{2+} alone. In the absence of kinase activity PDBu decreased the rate of MLC dephosphorylation to half of the control value, as did GTPγS. However, PDBu inhibited more strongly the rate of relaxation than GTPγS. When MLC phosphatase was not active, the effects of PDBu and GTPγS on MLC phosphorylation and force development were not observed. These results clearly demonstrate that PKC, like activation of GTP binding protein, increases Ca^{2+} sensitivity of MLC phosphorylation and force through inhibition of MLC phosphatase.

Tu-PM-F4

THE EFFECTS OF EXTRACELLULAR MAGNESIUM ON INTRACELLULAR CALCIUM ACTIVITY AND SMOOTH MUSCLE CONTRACTION.

((F.A. Lattanzio, P.H. Ratz and D.K. Bartschat)) Eastern Virginia Medical School, Norfolk, VA 23501.

A recent report described an increase in intracellular calcium activity (Ca_i) in isolated rat aortic smooth muscle cells caused by the reduction of extracellular magnesium (Mg_o) (Zhang et al., Biochem. Biophy. Acta 1134:25-9, 1992). To investigate this effect, fura-2 loaded rat aortic rings were exposed to 0mM Mg_o for 20 min at 37°C, a manipulation which increased the fura-2 signal but had minimal effect on contraction as compared with increases occurring when 110 mM KCl or 10 micromolar phenylephrine were added. The removal of Mg_o did not change intracellular Mg activity as measured by mag fura-5 or mag green, two new fluorescent Mg indicators whose properties were evaluated in this study. The removal of Mg_o slightly acidified the cell (pH change -0.1 units) as determined by measurements with the fluorescent pH indicator BCECF. This acidification was unlikely to have desensitized the myofilaments to the increase in Ca_i predicted from the fura-2 measurements. The absence of Mg_o during the addition of KCl or phenylephrine did not uncouple the force response seen with these agents. These data suggest that the increase in fura-2 signal may be due to a change in Ca_i at a site which is not in communication with the contractile apparatus, but which may be associated with the plasmalemmal membrane.

Tu-PM-F5

H-CALDESMON PHOSPHORYLATION BY MITOGEN-ACTIVATED PROTEIN KINASE. ((L.P. Adam and D.R. Hathaway)) Krannert Institute of Cardiology, Indiana University, Indianapolis, Indiana.

Caldesmon is a potent modulator of actomyosin ATPase activity and because of this property has been proposed to modulate smooth muscle contractility. Although the precise mechanisms underlying this modulation are poorly understood, the evidence that caldesmon is phosphorylated in contracting muscle suggests that phosphorylation of the protein may regulate its function in living tissue. In order to investigate this process, we have previously identified the sequences of the sites phosphorylated in the intact tissue, in the hopes of identifying the responsible kinase. The two sites are both on serine residues that are followed by proline in their primary amino acid sequence. Two types of 'proline-directed protein kinases' have been identified recently: $p34^{cdc2}$ and mitogen-activated protein kinase (MAPK). We now report that, of these two kinases, only MAPK is present in vascular smooth muscle. Furthermore, purified MAPK will phosphorylate caldesmon to a level of 1.7 mole phosphate/mole protein. In addition, 61% of the phosphate incorporated into porcine stomach caldesmon by MAPK, in vitro, is located on one of the sites phosphorylated in the intact tissue (i.e., peak B sequence in FEBS 302:223-226). Based upon the evidence that 1) caldesmon is phosphorylated in the intact tissue, 2) the level of phosphorylation varies in response to pharmacologic manipulation, 3) the sites phosphorylated are on 'proline-directed' sites, 4) MAPK, and not $p34^{cdc2}$, is present in vascular smooth muscle and 5) purified MAPK will phosphorylate caldesmon on at least one of the sites phosphorylated in the intact tissue, these data suggest that the function of caldesmon is regulated through reversible means by a MAPK or MAPK-like phosphorylation-dependent mechanism.

Tu-PM-F6

INVOLVEMENT OF CALPONIN AND CALDESMON IN SUSTAINED CONTRACTION OF ARTERIAL SMOOTH MUSCLE AND MYOFIBRILS. ((M. Bárány and K. Bárány)) Depts. of Biochem., and Physiol. and Biophys., Col. of Med., University of Illinois, Chicago, IL, 60612.

The molecular mechanism of smooth muscle contraction was approached by a novel method, covalent ^{14}C-labeling. Intra- and intermolecular protein interactions during contractile activity are reflected by changed reactivity of protein side chains which can be detected by covalent ^{14}C-labeling. The incorporation of $^{14}CH_2ICONH_2$ into proteins of 1-hour histamine contracted versus resting porcine carotid arterial muscles was determined. (Bárány, et al., Biochem. Biophys. Res. Commun. 187, 847-852, 1992). Out of fourteen ^{14}C-labeled proteins analyzed, only two showed a change in reactivity during sustained contraction. The incorporation of $^{14}CH_2ICONH_2$ into calponin and caldesmon in contracted muscles was about 66% of that into these same proteins in resting muscles. About 60% incorporation of $^{14}CH_2ICONH_2$ into calponin and caldesmon was observed when crude arterial myofibrils were contracted by MgATP and Ca^{2+}, by comparison to resting myofibrils in the presence of ATP and EGTA at physiological ionic strength. These results suggest that, during smooth muscle or myofibrillar contraction, an intramolecular change takes place in calponin and caldesmon implicating their involvement in regulation.

Tu-PM-F7

CALDESMON INHIBITS ACTIN-TROPOMYOSIN ACTIVATION OF MYOSIN MgATPase BY REDUCING VMAX AND ACTIN ACTIVATION BY INCREASING KM ((S. Marston & C.S. Redwood))
Dept of Cardiac Medicine, NHLI, Dovehouse st.,LONDON SW3 6LY, UK.

Caldesmon inhibition of actin-tropomyosin activation of myosin MgATPase activity was investigated.>90% inhibition of ATPase activation correlated with 0.035-0.1 caldesmon bound per actin monomer over a wide range of conditions. Caldesmon inhibited sheep aorta actin-tropomyosin activation of skeletal muscle heavy meromyosin(HMM) by 85% but had no effect on the binding affinity of HMM.ADP.Pi to actin. At ratios of 2 and 0.12 subfragment-1(S1):1 actin, addition of caldesmon inhibited the ATPase activation by up to 95%, but did not alter the fraction of S1.ADP.Pi associated with actin-tropomyosin. We concluded that caldesmon inhibited Atm.myosin ATPase by slowing the rate limiting step of the activation pathway (product release). An expressed mutant of caldesmon comprising just the C-terminal 99 amino acids bound actin 10 times weaker than whole caldesmon but otherwise inhibited actin-tropomyosin activation with the same potency and same mechanism as intact caldesmon. Thus the entire inhibitory function of caldesmon resides in its extreme C-terminus.

In the absence of tropomyosin much larger quantities of caldesmon were required to inhibit acto-S1 ATPase, such that 90% inhibition correlated with one caldesmon bound per 0.7-1.0 actin (compare with 0.07 CD/Atm). S1.ADP.Pi and caldesmon binding to actin were measured simultaneously at both 0.5μM S1/50μMA and 8μMS1/4μMA. Inhibition was directly proportional to S1.ADP.Pi displacement from actin. Thus caldesmon inhibits actin by competing with S1.ADP.Pi for a binding site on actin.

We conclude that tropomyosin in smooth muscle thin filaments is essential to propagate the inhibitory signal (reduction in Vmax) from a single actin-caldesmon contact to up to 14 other actins and that inhibition in the absence of tropomyosin involves a competition between caldesmon and S1.ADP.Pi for a site on actin, which is not physiologically relevant.

Tu-PM-F8

CALDESMON AND CALPONIN REGULATE RECRUITMENT OF CROSS-BRIDGES IN AN *IN VITRO* MOTILITY ASSAY ((J.R.Haeberle)) Department of Physiology & Biophysics, The University of Vermont, Burlington, VT, 05405

The regulatory properties of caldesmon and calponin have been investigated using a motility assay in which the interaction of fluorescently-labeled actin filaments with a fixed surface of monomeric thiophosphorylated smooth muscle myosin (TSMM) is visualized. We found previously that the C-terminal domain of caldesmon inhibits binding of actin to myosin, whereas, intact caldesmon tethers actin filaments by forming an actin-caldesmon-myosin complex without inhibiting filament velocity (Haeberle, *et al.* J.Biol.Chem. 267, 23001). In the present study we have shown that calponin (CaP) dramatically increases the binding of actin to TSMM and decreases the velocity of actin filaments. These results suggest that CaP may inhibit either the release of ADP and/or the binding of ATP to myosin. In support of this, mixing NEM-modified skeletal muscle myosin (NEM-myosin) with TSMM has almost the same effects on filament motion as the addition of CaP to the motility buffer with TSMM. Both increase filament binding at 80 mM KCl, increase filament fragmentation at low concentration, and inhibit or slow filament motion at high concentrations. In contrast, with dephosphorylated smooth muscle myosin (DSMM), NEM-myosin inhibits motility while CaP promotes low velocity motion (0.3-0.5 μm/sec). Moreover CaP antagonizes the inhibitory effects of NEM-myosin. 2% NEM-myosin completely blocks the motion of DSMM and the addition of 1 μM CaP restores motion, but at a velocity that is <0.1 μm/sec. The subsequent addition of 4 μM CaD inhibits motion. These results suggest that NEM-myosin inhibits motion of filaments with DSMM by presenting a mechanical load to the filaments. CaP recruitments slowly-cycling cross bridges by decreasing the off-rate. The low velocity motion indicates that the filaments are now moving under loaded conditions. CaD derecruits cross bridges by inhibiting binding.

Tu-PM-F9

ACTIN-CALDESMON-MYOSIN COMPLEXES PROMOTE MYOSIN ASSOCIATION WITH THE CYTOSKELETON DURING PLATELET ACTIVATION ((M.E. Hemric and J.R. Haeberle)) Department of Physiology & Biophysics, University of Vermont, Burlington, VT 05405 USA.

Caldesmon is a smooth muscle and nonmuscle protein that can bind actin and myosin simultaneously to form an actin-caldesmon-myosin complex. Using an *in vitro* motility assay, we have previously shown that caldesmon promotes actomyosin interaction and crossbridge cycling at near physiological ionic strengths. During platelet activation, the association of soluble, cytoplasmic myosin with the actin cytoskeleton increases and this association is linked to platelet shape change. In the present study, we have tested the hypothesis that endogenous caldesmon is necessary for this increased actomyosin interaction by using the NTCB, myosin-binding fragment of caldesmon as a competitive inhibitor of myosin binding to cytoskeleton-associated caldesmon. Platelets were activated either by the addition of thrombin or by saponin permeabilization in the presence of calcium and ATPγS. Activation was terminated by treatment with 1% Triton-100, 5 mM EGTA, 1 $^{mg}/_{ml}$ leupeptin, 1 mM PMSF, and 0.1 $^{NIH\ units}/_{ml}$ hirudin either in the absence or presence of the myosin-binding fragment of caldesmon. The platelet cytoskeleton was collected by low speed centrifugation and the protein content analyzed by SDS polyacrylamide gel electrophoresis. As the concentration of fragment was increased from 5 to 100 μM, the amount of myosin associating with the cytoskeleton decreased 10 to 70% in a concentration dependent manner. These results suggest that actin-caldesmon-myosin complexes are required for the reversible association of myosin with the cytoskeleton during platelet activation.

Tu-PM-G1

SOLVENT STRUCTURE AT THE LIPID BILAYER-SOLVENT INTERFACE: COMPARISON BETWEEN DLPE AND DMPC BASED BILAYERS.((Kenneth M. Merz Jr. and K. V. Damodaran)) 152 Davey Laboratory, Department of Chemistry, The Pennsylvania State University, University Park, PA 16802.

A molecular dynamics (MD) trajectory has been generated for the dimyristoylphosphatidylcholine (DMPC) based lipid bilayer using a united atom model with explicit solvent (water) molecules. Fully hydrated DMPC has a large (~27Å) interlamellar distance due to the hydration repulsion. The orientational ordering in the interlamellar water has been probed and compared with similar results from previous simulations (1) of dilauroylphosphatidylethanolamine (DLPE) which has relative small interlamellar distance (~5Å). From this comparison insights into water structure near a lipid bilayer-solvent interface has been obtained. The DLPE bilayer is found to have less water penetration than does the DMPC based bilayer and there are significant differences in the diffusional properties of water near these two bilayer-solvent interfaces.

1. Damodaran, K. V., Merz, K. M., Jr., and Gaber, B. P. 1992. Structure and Dynamics of the Dilauroylphophatidylethanolamine Lipid Bilayer. *Biochemistry*. 31: 7656-7664

Tu-PM-G2

ADHESION OF LIPOSOMES CAUSED BY GLYCOLIPID-GLYCOLIPID INTERACTIONS. ((J.M. Boggs and R.J. Stewart)) Research Institute, Hospital for Sick Children and Department of Clinical Biochemistry, University of Toronto, Toronto, Canada M5G 1X8

Liposomes containing galactosylceramide (GC) adhere to liposomes containing galactosylceramide I^3-sulfate (CBS) in the presence of divalent cations as measured from an increase in light scattering. Since these two glycolipids are present in high concentrations in myelin, this interaction may be involved in the adhesion of the extracellular surfaces of compact myelin. We have investigated the effect of ceramide composition on this interaction using semi-synthetic molecular species of GC and CBS which occur in myelin. Aggregation of the liposomes increases with an increase in the fatty acid chain length of either or both glycolipids. This is due to increased exposure of the carbohydrate on the bilayer surface. Aggregation also increases if the fatty acid chain of either or both glycolipids is α-hydroxylated. Since the α-hydroxy group has been found to decrease exposure of the carbohydrate, this effect must be caused by something other than exposure. The α-hydroxy group also contributes to intermolecular hydrogen bonding interactions and dehydration of CBS. It may also result in increased interlamellar hydrogen bonding and dehydration of the bilayer surface thus augmenting adhesion and aggregation.

Tu-PM-G3

ERYTHROCYTE PELLETS AS A MODEL SYSTEM: OSMOTIC PHENOMENA, ELECTROPORATION, ELECTROFUSION, MEMBRANE INTERACTIONS
I.G.Abidor[*†], Lin Hong Li[+], S.W.Hui[+]; [+]Dept. Biophysics, Roswell Park Cancer Institute, Buffalo, NY 14263; [*]A.N.Frumkin Institute of Electrochemistry, Russian Academy of Sciences, Moscow

Compact pellets of erythrocytes have properties similar to those of porous bodies and gels. The pellet structure and osmotic equilibrium between supernatant, cells and intercellular space should be considered in detail to explain a variety of osmotic phenomena observed in cell pellets after electroporation or changing supernatant tonicity. Osmotic swelling leads to notable changes in the pellet electrical resistance, R_p. It also plays an important role in cell electrofusion and prevents pelleted cells from electrohemolysis.

Cell pellets give an unique opportunity for directly measuring interactions between intact cell membranes. For rabbit erythrocytes, the pellet porosity, ε, i.e. intercellular:total volume ratio, estimated from R_p, varies from ~0.5 to 8% depending on a compressive force, P_{ext}, either mechanical (centrifugation) or osmotic (due to electroporation or adding PEG or dextran in supernatant). Unlike conventional porous bodies with cylinder-like pores, cell pellet "pores" are narrow gaps surrounding every cell. The average intermembrane distance calculated from ε decreases from ~600 (i.e. ~twice the glycocalyx thickness) to 20-30 Å with an increase of P_{ext} from 10^{-1} to 10^{6} Pa. To the first approximation, this dependence agrees with the balance between external, Van der Waals, electrical (due to charges distributed over opposing glycocalicies) and hydration forces.

Tu-PM-G4

SLOW LATERAL DIFFUSION OF LIPID PROBES IN YEAST CELL MEMBRANES. ((Miriam L. Greenberg[1] and Daniel Axelrod[2])) [1] Dept. of Biological Chemistry, and [2] Biophysics Research Division and Dept. of Physics, University of Michigan, Ann Arbor, MI 48109

We have measured the lateral mobility of two fluorescent lipid probes dioctadecylindocarbocyanine (diI) and tetramethyl rhodamine phosphatidylethanolamine (R-PE) in the plasma membranes of *Saccharomyces cerevisiae ino1* and *opi3* spheroplasts. These are well-characterized strains with mutations in the inositol and phosphatidylcholine biosynthetic pathways. Membrane phospholipid composition was altered by growing these mutants in the presence or absence of inositol and choline. Lateral mobility was measured by fluorescence recovery after photobleaching (FRAP). Microscopic fluorescence polarization employing CCD digital imaging produced an ordered orientation distribution of the lipid probe diI, confirming that at least one of the probes is largely incorporated into the bilayer membrane. Our results demonstrate the existence of anomalously slow mobility of both lipid probes for both mutants, regardless of whether the lipid composition is near normal or dramatically altered in relative composition of phosphatidylinositol and phosphatidylcholine. Trypsinization of the spheroplasts to remove surface proteins results in markedly increased lateral mobility. However, even in trypsinized spheroplasts, mobility is still somewhat lower than the mobility observed in the membrane of mammalian cells, such as rat smooth muscle culture cells tested here for comparison. Supported by NIH NS14565 and NSF DMB8805296 (to D.A.) and NIH GM37723 (to M.G.).

Tu-PM-G5

NEUTRON REFLECTIVITY STUDIES OF MITOCHONDRIAL OUTER MEMBRANE. ((S. Krueger[*], J.F. Ankner[*], S.K. Satija[*], C.F. Majkrzak[*], D. Gurley[†] and M. Colombini[†])) [*]Reactor Radiation Division, National Inst. of Standards and Technology, Gaithersburg, MD 20899; [†]Department of Zoology, U. of Maryland, College Park, MD 20742.

The neutron reflectivity technique is being used to study the structure of the outer membrane of Neurospora crassa mitochondria. These membranes contain VDAC (voltage-dependent anion-selective channel) proteins which respond to an electrical potential. At low potentials, the channels are in the open state, with an effective pore diameter estimated at 3 nm. When the appropriate potential is applied across the membrane, the channels close, reducing the effective pore diameter to 1.8 nm. One current model for the membrane structure suggests that approximately one-third of the protein mass is ejected from the channels onto the surface of the membrane as the channel closes. In order to test this model, neutron reflectivity measurements have been performed on a single bilayer membrane (~4.5 nm thick) containing VDAC deposited on a single crystal silicon substrate. Measurements were made in aqueous solvent with and without a potential applied across the membrane. Neutron scattering length density profiles perpendicular to the bilayer surface have been generated from fits to the data. Initial results show that a single bilayer containing VDAC can be successfully measured with the sensitivity needed to observe the small conformation changes which are expected to occur as a function of channel opening and closing.

Tu-PM-G6

Measurements of Plasma Membrane Architecture During Hypoxia in Rat Hepatocytes.

[(X. F. Wang, J. Gordon, J. J. Lemasters, and B. Herman)] Department of Cell Biology & Anatomy, University of North Carolina at Chapel Hill, Chapel Hill, NC 27599.

There is increasing evidence that changes in the physical state of the plasma membrane is a major factor in the evolution of irreversible hypoxic injury. We wished to understand in more detail the changes in plasma membrane lipid structure (e.g. lipid order, lateral diffusion, domain structure) during the evolution of hypoxic injury in rat hepatocytes. Following hypoxic injury, TEMPO quenching and Fluorescence Resonance Energy Transfer (FRET) imaging were used to detect and monitor lipid domain formation and topography during hypoxic injury, Fluorescence Recovery After Photobleaching (FRAP) was used to monitor plasma membrane lipid and protein diffusion, and phospholipase A_2 activity was observed using a novel microscopic imaging approach during hypoxic injury. Our data indicates that initially, hypoxic injury causes major alterations in the morphology of the cell (formation of blebs), and an increase in the fluidity of the plasma membrane. Subsequently as injury progresses, membrane lipids undergo a shift from a fluid to more rigid, gel state. The formation of these lipid domains and transition from fluid to more rigid lipid is pH-dependent and is associateed with high phospholipase A_2 activity in the plasma membrane. Formation of these lipid domains leads to eventual weakening of plasma membrane integrity barrier, loss of this barrier and consequently cell death.

Tu-PM-G7

A BIOPHYSICAL STUDY OF INTEGRAL MEMBRANE PROTEIN FOLDING. ((John F. Hunt, Olaf Bousché‡, Krishna Kalghatgi Kariyne Reilly, Csaba Horváth, Kenneth J. Rothschild‡, and Donald M. Engelman)) Yale University and (‡) Boston University.

The transmembrane domain of many integral membrane proteins is believed to contain exclusively α-helical secondary structure. Based on simple thermodynamic arguments, it has been proposed that the individual α-helices in such domains should be stable in the transmembrane configuration even in the absence of the remainder of the protein structure. This hypothesis suggests that the folding of these domains could proceed by a particularly simple mechanism in which the individual α-helices are inserted into the membrane independently and prior to the formation of helix - helix contacts. In order to test these ideas, we have synthesized seven polypeptides corresponding to all of the individual transmembrane α-helices in the native structure of the integral membrane protein bacteriorhodopsin. We have reconstituted each polypeptide individually into phospholipid membranes and characterized its structure using CD spectroscopy, polarized FTIR spectroscopy, and protease protection experiments. Our results show that five of the seven polypeptides form stable transmembrane α-helices (in isolation from the remainder of the BR molecule). However, the polypeptide corresponding to the "F" helix does not form any stable or well-oriented secondary structure, while the polypeptide corresponding to the "G" helix seems to form a stable transmembrane β-sheet. These observations have important implications for the thermodynamic analysis of integral membrane protein structure and folding.

Tu-PM-G8

Perturbation of Lipid Membranes by Cholesterol as Observed by High Pressure Spectroscopy. Suzanne F. Scarlata, Dept. of Physiol.& Biophysics, SUNY Stony Brook, Stony Brook, NY 11794-8661.

High pressure fluorescence spectroscopy was used to determine the effect of cholesterol on the physical properties of phosphatidylcholine and phosphatidic acid membranes. When not in membranes, pressure will promote the dissociation of a proton from a fluorescent pH indicator due to electrostriction. If the indicator is then placed in an environment that is unable to expand to allow for further hydration, such as the surface of a bilayer, then dissociation will be inhibited (Biochem. 29, 10233). We have found that the presence of cholesterol will expand the membrane surface and reverse this inhibition. To assess the formation of cholesterol-rich domains, we monitored the fluorescence anisotropy of two probes in different membrane locations. In unsaturated lipids our data indicate aggregates of cholesterol that become more extensive as pressure is applied. Supported by NIH GM39924.

PROTEIN STRUCTURE AND FUNCTION

Tu-PM-H1

HPLC-PURIFICATION OF FUNCTIONAL CHIP28 WATER CHANNELS FOR DETERMINATION OF SECONDARY STRUCTURE BY CD AND FTIR SPECTROSCOPY. ((AN van Hoek, MC Wiener, S Bicknese, J Biwersi, L Miercke, RM Stroud and AS Verkman.)) Cardiovascular Research Institute and Dep. of Biochemistry & Biophysics, UCSF, CA 94143

The integral membrane protein CHIP28 is an important water channel in erythrocytes and kidney tubule epithelia. CHIP28 is a member of a family of channel/pore homologues that includes lens protein MIP26. The purpose of this study was to purify functional delipidated CHIP28 to homogeneity, and to test the validity of the α-helical structure predicted by hydropathy analysis. CHIP28 was delipidated by ion exchange chromatography following solubilization of N-lauroylsarcosine-stripped erythrocyte membranes (AN van Hoek and AS Verkman (1992), J. Biol. Chem. 267, 18267-18269) with β-octylglycoside (OG)/CHAPS. Size exclusion HPLC revealed a single peak of monomeric (28kDa) CHIP28 in 50 mM OG. Proteoliposomes reconstituted with purified CHIP28 were water permeable.

Circular Dichroism (CD) of CHIP28 in 50 mM OG showed a spectrum typical for α-helical structures: a maximum at 192 nm and minima at 208 and 222 nm. Spectral deconvolution by singular value decomposition (SVD) gave 40% α-helix, 35% β-sheet and turn, and 30% 'other' structures. For comparison, CD of ion exchanged purified MIP26 in 50 mM OG gave 50% α-helix, 25% β sheet and turn, and 25% other structures. Attenuated Total Reflectance (ATR) Fourier Transform Infrared (FTIR) spectroscopy was used for independent evaluation of secondary structure. ATR-FTIR of air-dried multilayers of both stripped membranes and reconstituted CHIP28 showed a maximum at 1648 cm^{-1} (MIP26: 1652 cm^{-1}). SVD gave 27% α-helix and 52% β sheet and turn. ATR-FTIR of MIP26 gave 35% α-helix and 42% β-sheet and turn. The lower values of α-helix in ATR-FTIR might reflect differences in secondary structures between solubilized (used in CD) and native or reconstituted-active protein (used in FTIR). Preliminary CD analysis of CHIP28 reconstituted in cholesterol-containing proteoliposomes indicate a cholesterol induced structural change towards β sheet and turn. These results establish a procedure to obtain purified CHIP28 in functional form and provide spectroscopic evidence to support the multi-spanning α-helical structure predicted for CHIP28 and MIP26.

Tu-PM-H2

A POINT MUTATION AT CYSTEINE 189 BLOCKS THE WATER PERMEABILITY OF RAT KIDNEY WATER CHANNEL CHIP28k ((R. Zhang, A.N. van Hoek and A.S. Verkman)) Cardiovascular Research Institute, U.C.S.F., San Francisco, CA 94143

CHIP28k is an important water transporting protein in kidney proximal tubule and thin descending limb of Henle (Zhang, Skach, Hasegawa, Van Hoek and Verkman, *J. Cell Biol.*, in press) that is homologous to human erythrocyte CHIP28 (Preston and Agre, Proc. Natl. Acad. Sci. 88:11110-4, 1991). Oligonucleotide-directed mutagenesis was used to identify the cysteine(s) involved in inhibition of the water transporting function of CHIP28k by the mercurial $HgCl_2$. Each of the 4 cysteines (at positions 87, 102, 152, and 189) was mutated to serine individually, or in combinations. *In vitro* transcribed cRNA was expressed in Xenopus oocytes for measurement of osmotic water permeability (P_f) in the absence or presence of 0.3 mM $HgCl_2$. P_f (in cm/s x 10^{-4} measured at 10 °C) was 7 ± 1 in water-injected oocytes. In wild-type CHIP28k, P_f was 58 ± 7 (-$HgCl_2$) and 10 ± 1 (+$HgCl_2$). Mutation of cysteines 87, 102, or 152, individually or in combinations, did not affect oocyte P_f or the inhibition by $HgCl_2$. Mutation of cysteine 189 to serine or glycine decreased P_f to 14 ± 2 (-$HgCl_2$) and 9 ± 1 (+$HgCl_2$). Western blot analysis of oocyte plasma membranes using a polyclonal anti-CHIP28 antibody indicated that the differences in P_f were not due to differences in protein expression. These result indicate that cysteine 189: (a) is involved in the water transporting function of CHIP28k, (b) is the site of action of $HgCl_2$, and (c) may be involved in the tetrameric assembly of CHIP28k in kidney and erythrocyte membranes.

Tu-PM-H3

NMR STRUCTURE OF THE VILLIN TAIL, A DOMAIN CONSERVED AMONG ACTIN-SEVERING PROTEINS. ((M. A. Markus*+, T. Nakayama#, K. Chandrasekhar,* P. T. Matsudaira# and G. Wagner*,+)) *Department of BCMP, Harvard Medical School, 240 Longwood Avenue, Boston, MA 02115, +Department of Biophysics, Harvard University, 7 Divinity Avenue, Cambridge, MA 02138, #Whitehead Institute for Biomedical Research and Department of Biology, Massachusetts Institute of Technology, Nine Cambridge Center, Cambridge, MA 02142.
(Spon. by D. J. Lockhart)

The actin-severing proteins are built upon one domain of approximately 130 amino acids with no detected sequence homology to any known structure. To complement mutational analysis, we are characterizing the structure of the amino-terminal domain of villin by solution NMR. The first domain (126 amino acids) of chicken villin has been overexpressed in *E. coli* and produced with and without uniform ^{13}C and ^{15}N enrichment. Sequential backbone assignments have been made based on triple resonance experiments and confirmed with ^{15}N-resolved NOESY. Side chain assignments have been based on ^{15}N-resolved TOCSY and extended with heteronuclear crosspolarization experiments. The secondary structure of the protein is mostly β-sheet with a short α-helix around residues 79-92. Initial structural characterization is in progress and will be presented.

Tu-PM-H4

THE AMINO-TERMINAL DOMAIN OF VILLIN: MOLECULAR ANALYSIS OF VILLIN-ACTIN INTERACTION. ((T. Nakayama, M. Way, A. Weeds*, and P. Matsudaira)) Whitehead Inst., Dept. of Biology, M.I.T., Cambridge, MA 02142 and *MRC Laboratory of Molecular Biology, UK. (Spon. by P. S. Kim)

Villin (95 kDa) is a major actin-binding protein in the brush-border cells of intestine and kidney. Villin cross-links actin filaments into bundles at low Ca^{2+} concentration but severs them at high Ca^{2+} concentration. Sequence analysis predicts that there are six repeats of 37-51 amino acids (domains 1-6). Proteolysis results suggest that these domains are structural units. To understand the nature of villin-actin interactions, we have investigated structure and function relationships of domain 1 by replacing every 10th amino acid from the N-terminus by cysteine. The functionally active domains 1-3, that contain mutations in domain 1, were expressed in E. coli and purified. Effects of mutations on severing, capping, and monomer actin binding were measured by fluorescence spectroscopy. All the mutants showed wild-type capping and monomer binding activities. However, the mutants, F100C, F110C, and G120C, showed significantly reduced severing activity. We also found that copper-phenanthroline induced the formation of a disulfide bond in the S90C/monomer actin complex. The resulting disulfide bond was between Cys-90 in villin (domains 1-3) and Cys-374 in actin, suggesting that these residues are in close proximity in the complex.

Tu-PM-H5

THE EFFECT OF LOCAL DISORDERING ON PROTEIN FUNCTIONS: INHOMOGENEOUS REACTION KINETICS.

((A.P.Demchenko)) Palladin Institute of Biochemistry, Kiev 252030, Ukraine.

The experimental data on non-Arrhenius temperature function and non-exponential time dependence of different ligand-binding and photoinitiated charge-transfer reactions require the interpretation of reaction mechanisms beyond the classical transition-state theory. Inhomogeneous kinetics is one of the features of these reactions. It is observed when the reaction rate depends strongly upon the interaction of the reactant with the surrounding and this surrounding exhibits distributions in its interactions and does not relax faster than the motion along the reaction coordinate. The inhomogeneous kinetics mechanism is supported by our recently obtained results on photoinduced electron transfer in a complex of bianthryl with different proteins and by the calculation of reaction trajectories for the model charge-transfer reaction in the conditions of distributions and fluctuations of the electric field.

Tu-PM-H6

Protein conformational changes probed by Classical Raman Difference Spectroscopy

G. Weng, D. Manor and R. Callender. Physics Dept. City College of CUNY, New York, NY 10031

A number of key cellular functions (proliferation, hormone response, neurotransmission and protein biosynthesis) are regulated *in vivo* by members of a family of guanine nucleotide binding proteins, the so called G-proteins. These proteins share strong functional and structural homologies. Elongation Factor Tu and *ras*-p21 are members of this family. The proteins are normally bound to either GDP or GTP, and the two forms differ drastically in both their biological activity and their conformations. We used Classical Raman Difference Spectroscopy to investigate the differences of these protein-nucleotide complexes. The differences between the two nucleotide complexes were found to be correlated with GTP hydrolysis. The S-H vibrations of cysteine residues on EF-Tu are affected by the nature of the bound ligand (GDP .vs. GTP). The difference spectra will be presented and their relevance to protein conformational changes and mechanisms of action will be discussed.

Tu-PM-H7

STRUCTURE AND FUNCTION IN *E. coli* THIOREDOXIN: DETERMINATION BY RAMAN SPECTROSCOPY OF THE pK VALUES OF ACTIVE-CENTER CYSTEINES, CYS32 AND CYS35.

((H. Li, C. Hanson, C.K. Woodward and G.J. Thomas, Jr.)) School of Biological Sciences, U. Missouri, Kansas City, MO and Department of Biochemistry, U. Minnesota, St. Paul, MN.

Hydrogen bonding interactions and ionizations of the two sulfhydryls (Cys32 and Cys35) at the redox-active center of *E. coli* thioredoxin have been determined by Raman spectroscopy. Quantitative Raman intensity measurements on thioredoxin over the range $4.0<pH<12.2$, and correlation of the data with results on model compounds, indicate the following: (i) Both SH groups of the native protein are relatively robust hydrogen-bond donors, but one is a stronger donor than the other. (ii) The sulfhydryl which donates the weaker hydrogen bond, assigned tentatively as Cys32, is titrated preferentially to the thiolate ion (S^-) as the solution pH is increased from 4 to 7. (iii) The sulfhydryl which donates the stronger hydrogen bond (Cys35) is bonded to a highly electronegative acceptor and resists substantial ionization until roughly 50% of the more accessible sulfhydryl has been titrated. (iv) The Raman titration data indicate $pK_1 = 7.1 \pm 0.2$ and $pK_2 = 7.9 \pm 0.2$ for the two thiol-thiolate equilibria in thioredoxin. Conformation-sensitive Raman bands of the thioredoxin main chain and of several side chains have also been analyzed, and likely acceptors for the SH hydrogen-bond donors are proposed. [Supported by NIH Grant AI11855.]

Tu-PM-H8

3-NITROSOBENZAMIDE (NOBA) REACTS WITH THE ZINC-FINGER SEQUENCES OF HIV-1 NUCLEOCAPSID PROTEIN (P7) AND PHAGE T4 GENE 32 PROTEIN (GP32)

((J.R. Casas-Finet[1], R.C. Sowder[2], X. Yu[3], J. Mendeleyev[4], C. Fenselau[3], E. Kun[4], J.W. Erickson[1], and L.E. Henderson[2])) [1]Struct. Biochem. and [2]AIDS Vacc. Progs., NCI-FCRDC, Frederick, MD 21702; [3]Chem. Dept., UMBC, Baltimore, MD 21228; [4]Envir. Toxic. & Chem. Lab., SFSU, Tiburon, CA 94920 (Spon. by E. Kun)

NOBA, a C-nitroso compound known to inactivate poly(ADP-ribose) polymerase by attack on its Zn-finger sequence, was studied to assess its reaction mechanism and specificity. NOBA appears to be a Cys-specific reagent, as a collapse of the doublet peak in its near-UV absorption spectrum (λ_{max} = 280 nm, 303 nm) to a single, less intense peak in the 286-296 nm range was observed with 2-ME, DTT and reduced glutathione, but not with oxidized glutathione, Met or Trp. NOBA reaction with thiols resulted in the formation of a minor fluorescent side-product (identified as azoxo-3,3'-benzamide) with maximal excitation at 320 nm and emission at 460 nm; Zn-finger sequences yielded this product in significantly higher amounts.
NOBA reaction with the single-stranded DNA-binding protein gp32 resulted in a biphasic decrease of its Trp fluorescence. A first step, leading to ~20% Trp quenching, was complete after 20 min and was assigned to the reaction of NOBA with the sole free thiol in gp32 (Cys 166). A slower reaction occurred with the 3 Cys thiolates of the Zn-finger sequence; over several hrs, a red-shift of the fluorescence emission λ_{max} from 339 to 359 nm indicated increased solvent exposure of the Trp chromophores resulting from the disruption of the Zn coordination sphere. A blue-shifted, broader excitation spectrum suggested the formation of gp32-NOBA adducts. Qualitatively similar changes in p7 Trp fluorescence were observed upon NOBA reaction. Reverse phase HPLC showed an early-eluting p7 peak and p7 species with altered UV spectra that nearly co-eluted with intact p7. Electrospray mass spectrometry (ESMS) showed that the early-eluting p7 had a MW of 4 amu smaller than apo-p7, suggesting formation of internal -S-S-bridges (as confirmed by 2-ME treatment). The composite HPLC peak was found to contain p7 adducts with 1 and 2 NOBA moieties, as ESMS exhibited species with increased MW by 150 and 300 amu (MW of NOBA is 150 amu); a 32 amu increase in MW was attributed to formation of Cys sulfone (also observed in model systems). NOBA reaction with p7 bound to a DNA oligo- or RNA polynucleotide resulted in a decrease in affinity or structural alteration of the complex. These effects correlated with metal loss from p7, and suggest that NOBA or related compounds may be of therapeutic use as anti-HIV agents.

Tu-PM-H9

PROBING THE CONTACT ZONE BETWEEN α-BUNGAROTOXIN AND A PORTION OF THE α-SUBUNIT OF THE NICOTINIC RECEPTOR BY 2-D NMR.

((L.N. Gentile, V.J. Basus*, Q-L. Shi and E. Hawrot)) Section of Molecular and Biochemical Pharmacology, Brown University, Providence, RI 02912. * Dept. of Pharmaceutical Chemistry, UCSF, San Francisco, CA 94143.

Binding studies with the nicotinic acetylcholine receptor (nAChR) suggest that the agonist and antagonist binding sites reside in large part on the N-terminal extracellular portion of the α-subunit. A major determinant of the binding site for the competitive antagonist, α-bungarotoxin (BGTX), appears to be located in the region containing residues 181-200 of the α-subunit. We have been studying the interaction between BGTX and peptide fragments of the α-subunit localized to this region.
We have determined the residues in BGTX which are greatly perturbed ($\Delta\delta > 0.15$ ppm) upon binding to an 18mer peptide (α181-198). A ROESY spectrum of the 2:1 complex of BGTX:18mer provides exchange cross peaks between bound and unbound BGTX. When compared to the previously assigned 2-D NMR spectrum of unbound BGTX, the ROESY cross peaks provide a framework for assigning the HOHAHA and NOESY cross peaks of "bound" BGTX in the corresponding 1:1 complex of BGTX and 18mer. The binding-induced chemical shift perturbations thus revealed in BGTX are consistent with our previous NMR studies of BGTX binding to a 12mer (α185-196) peptide from this same receptor region. Not unexpectedly, due to the higher binding affinity of the 18mer peptide, the perturbations induced by 18mer binding appear to involve more BGTX residues than those perturbed upon 12mer binding. In both cases however, it is clear that both the N-terminal and the middle toxic loops of BGTX are important for the molecular recognition of the nAChR
(Supported by NIH-GM32629, NSF-IBN-9021227 and NSF-DMB-9104794.)

Tu-PM-H10

FLUORESCENCE ENERGY TRANSFER IN TRYPTOPHANASE: MECHANISM AND EFFECTS OF QUASISUBSTRATES.

((A. Markel[1], T. Ben-Kasus[1], G. Gdalevsky[3]. D. Gill[2], Yu. M. Torchinsky[3], R.S. Phillips[4], A.H. Parola[2])) Dept. of Chemistry[1], and Physics[2], Institutes for Appl. Res.[3], Ben-Gurion University of the Negev, Beer-Sheva 84105, Israel, and Dept. of Chemistry and Biochemistry, University of Georgia[4], Athens, Georgia 30602, U.S.A.

Tryptophanase is a bacterial, pyridoxal phosphate (PLP)-dependent, 208-kd tetrameric enzyme; it displays two PLP absorption bands at 337 and 420 nm. Excitation of tryptophanase at 290 nm evokes two emission peaks, one at 335 nm, arising from Trp residues, and one at 500 nm which is due to energy transfer (ET) from tryptophans to PLP (Tokushige et al., BBRC, 96, 863). We were puzzled by the fact that the 500-nm peak is located so far from the maximal overlap of tryptophan emission and PLP absorption at 337 nm, whereas excitation in the PLP band at 337 nm evokes emission at 380 nm. Taking into account these facts and the asymmetry of the 335-nm peak, we suggested that this peak actually consists of two bands: a strong band of tryptophan emission and a weaker ET band. The existance of the latter band is supported by measurements of polarization fluorescence spectra. The excitation spectrum with λ_{em} = 500 nm showed that the 500-nm peak can be induced by both ET and direct excitation at 337 nm. We suggested that an excited PLP molecule captures a proton, and that the protonated species emits at 500 nm in the same manner as the enzyme excited at 420 nm. It seems likely that the ET from tryptophans induces the 500-nm peak through the same intermediate protonation step. The pH dependence of the ET spectra agrees with our suggestion. Formation of enzyme complexes with L-threonine and 3-phenyl-DL-serine reduces the 500-nm peak. The fluorescence of these complexes, excited in the PLP bands, is also weaker than that of the free enzyme. These differences may result from reorientation of the PLP ring upon formation of the enzyme-quasisubstrate complexes.

Tu-PM-I1

A NEW TECHNIQUE FOR IN SITU MEASUREMENT OF FREE CALCIUM IN INTRACELLULAR INSP3-SENSITIVE STORES.

((A.M. Hofer & T.E. Machen)) University of California at Berkeley, Berkeley, CA 94720.

We report here a novel technique for directly monitoring [Ca] within the inositol 1,4,5-trisphoshate ($InsP_3$)-senstitive store in single gastric epithelial cells. The AM-ester derivative of the fluorescent dye mag-fura-2 (which is sensitive to [Ca] above 5μM) accumulates into subcellular compartments where it reports changes in free [Ca]. In permeabilized cells incubated in an intracellular buffer, 1μM $InsP_3$ caused [Ca] to decrease from ~130μM to ~80μM, and this effect was blocked by the $InsP_3$ receptor antagonist, heparin. Ca sequestration into this internal store was ATP-dependent and blocked by thapsigargin, a specific inhibitor of the Ca-ATPase of the $InsP_3$-sensitive pool. We used this technique to investigate the effects of Cl on the release and reloading of the internal store, and found that Ca uptake was reduced in Cl-free solutions, suggesting an important role for Cl in the refilling of this store.

Tu-PM-I2

RANGE OF MESSENGER ACTION OF CALCIUM ION AND INOSITOL 1,4,5-TRISPHOSPHATE.

((N.L. Allbritton, T. Meyer and L. Stryer)) Dept. of Cell Biology, Stanford University, Stanford CA 94305 (N.L.A. and L.S.) and Dept.of Cell Biology, Duke University, Durham, NC 27710 (T. M.).

The range of messenger action of a point source of Ca^{2+} or inositol 1,4,5-trisphosphate (IP_3) was determined from measurements of their diffusion coefficients in a cytosolic extract from *Xenopus laevis* oocytes. Breakdown of IP_3 was inhibited by inclusion of 30 mM EDTA in the extract for IP_3 diffusion and sequestration of Ca^{2+} by intracellular organelles was abolished by addition of 1 μM FCCP and 40 μM thapsigargin in the extract for Ca^{2+} diffusion. The diffusion coeficient (D) of ^3H-IP_3 was 283 μm^2/sec. D for Ca^{2+} increased from 13 to 65 μm^2/sec when the free calcium concentration was raised from about 90 nM to 1 μM. The slow diffusion of Ca^{2+} in the physiologic concentration range results from its binding to slowly mobile or immobile buffers. The calculated effective range for free Ca^{2+} (prior to buffering), buffered Ca^{2+}, and IP_3 determined from their diffusion coefficients and lifetimes were 0.1 μm, 5 μm, and 24 μm, respectively. Thus, for a transient point source of messenger in cells smaller than 20 μm, IP_3 is a global messenger, whereas Ca^{2+} acts in restricted domains. Experiments by others indicate that D of the propagating messenger for calcium waves in cells is between 300 and 600 μm^2/sec. Hence IP_3 but not Ca^{2+} is an attractive candidate for the mobile messenger in calcium wave propagation.

Tu-PM-I3

EXPRESSION OF A CA^{2+}-ATPASE ENHANCES IP_3-MEDIATED CA^{2+} WAVE ACTIVITY IN *XENOPUS LAEVIS* OOCYTES.

((P. Camacho and J.D. Lechleiter)) Department of Neurosciences, University of Virginia, Charlottesville, VA 22908.

Inositol 1,4,5 trisphosphate receptors (IP_3Rs) play a critical role in signal transduction pathways stimulated by neurotransmitter and/or hormone receptors. When IP_3Rs are activated, Ca^{2+} is released from intracellular stores in excitatory propagating waves which annihilate each other upon collision. Annihilation, as well as the frequency of pulsatile Ca^{2+} waves, is thought to be due to an underlying refractory period. To test whether enhanced Ca^{2+} pumping activity can alter the refractory state of Ca^{2+} release, we expressed a Ca^{2+}-ATPase (SERCA1) mRNA in *Xenopus laevis* oocytes. IP_3 was used to elicit Ca^{2+} release which was visualized with Ca^{2+}-Green using confocal microscopy. Compared to control oocytes, the frequency of Ca^{2+} waves was dramatically enhanced in SERCA1 expressing oocytes. Additionally, individual Ca^{2+} waves were narrower in width. The results are consistent with a shortened refractory period for excitability introduced by the activity of the SERCA1 pump. The effect of SERCA1 on wave frequency occurs both at low (0.1μM) and high (1μM) IP_3 concentrations. Furthermore, IP_3 levels determined the length of time during which Ca^{2+} activity was observed. A monoclonal antibody against SERCA1 corroborated the expression of this Ca^{2+}-ATPase. A polyclonal antibody which recognizes the endogenous IP_3R in *Xenopus* oocytes was also used to demonstrate that the levels of IP_3R expression were not altered in oocytes expressing SERCA1 mRNA. Based on these data, we suggest that Ca^{2+} ATPases play an active role in Ca^{2+} signalling pathways.

Tu-PM-I4

THE MECHANISMS INVOLVED IN INTRACELLULAR Ca^{2+} OSCILLATIONS IN PANCREATIC β-CELLS.

((Teresa Ree Chay)) Department of Biological Sciences, University of Pittsburgh, Pittsburgh, PA 15260.

Pancreatic β-cells exhibit simple as well as complex (bursting) types of $[Ca^{2+}]_i$ oscillations in response to glucose, hormones, and neurotransmitters. While some of these oscillations occur in close conjunction with electrical bursting, others occur even at the resting potential, suggesting that an intracellular Ca^{2+} store is involved in the genesis of these oscillations. By cross-coupling the membrane model (Chay, 1990. Am. J. of Physiol., 258: C955-C965) with the intracellular store model (Cuthbertson & Chay, 1991. Cell Calcium, 12: 97-109), we have studied the mechanisms involved in the $[Ca^{2+}]_i$ oscillations in response to various types of external signals. The *membrane model* contains a slowly inactivating component of the Ca^{2+}-sensitive currents (*i.e*, SK- and Ca^{2+}-sensitive Ca^{2+}-channels) and a cluster of L-type Ca^{2+}-channels which induce a heterogeneous cellular Ca^{2+} distribution (*i.e.*, hot spots). In this model, the Ca^{2+}-sensitive currents are responsible for a slow underlying wave, while the compartmentalized Ca^{2+} ions in the hot spots are responsible for the fast spikes. In *the intracellular store model*, the action of phospholipase C (PLC) is controlled by g-proteins as well as intracellular Ca^{2+} ions. The Ca^{2+} channel in the intracellular store is not only sensitive to inositol 1,4,5-trisphosphate (IP_3) but also to $[Ca^{2+}]_i$ in that it opens when the cellular Ca^{2+} is low and closes when it is high enough. In this model, the GTP-bound g-protein oscillates due to a receptor-bound PLC which acts as GTPase activating protein (GAP). The cross-coupled model produced many interesting patterns of $[Ca^{2+}]_i$ oscillations observed in both excitable and non-excitable cells.

Tu-PM-I5

VOLTAGE-DEPENDENCE OF CYTOSOLIC $[Ca^{2+}]$ OSCILLATIONS IN GONADOTROPHS: Ca^{2+} ENTRY THROUGH L-TYPE CHANNELS SUSTAINS ENDOPLASMIC RETICULUM FUNCTION.

((M. Kukuljan, S.S. Stojilkovic, K.J. Catt and E. Rojas)) NIDDK and NICHD, NIH, Bethesda, MD 20892.

Inositol (1,4,5) trisphosphate ($InsP_3$)-initiated Ca^{2+} release from the endoplasmic reticulum (ER) is involved in the regulation of cytosolic Ca^{2+} concentration ($[Ca^{2+}]_i$) in many cell types. Although the $InsP_3$-mediated elevation of $[Ca^{2+}]_i$ is independent of extracellular Ca^{2+}, the eventual depletion of the ER stores necessitates the activation of Ca^{2+} entry mechanisms that support the sustained elevation of $[Ca^{2+}]_i$. In response to gonadotropin-releasing hormone (GnRH), gonadotrophs display high amplitude, $InsP_3$-initiated, $[Ca^{2+}]_i$ oscillations, that can be monitored by measuring a Ca^{2+}-activated, voltage-independent, K^+ current ($K_{(Ca)}$). In cells held at V_m=-100 mV, GnRH-initiated Ca^{2+} oscillations are maintained for up to 10 min, with a progressive decrease in their amplitude. Holding the membrane potential (V_m) at values positive to -35 mV leads to a marked increase of the amplitude of the oscillations; the time constant of this process depends on V_m, with a minimum value near 20 mV. To avoid errors associated with changes in the driving force for the $K_{(Ca)}$ current as well as from the activation of other K^+ channels, we studied the oscillations observed at V_m=-100 mV immediately after a depolarizing pulse. The amplitude and the area of the transients, representing the maximal $[Ca^{2+}]_i$ and the total amount of Ca^{2+} mobilized respectively, showed a Boltzmann's dependence on the V_m during the depolarizing pulse. The peak $[Ca^{2+}]_i$ and the total mobilized Ca^{2+} were proportional to the duration of the pulse. Activation of the oscillations by depolarization was abolished by removal of extracellular Ca^{2+} and exposure to Co^{2+} (5 mM), Cd^{2+} (2 mM) or nifedipine (5 μM). BK8644 shifted the V_m-dependence to more negative V_m values. We conclude that Ca^{2+} entry through L-type channels is the main mechanism for the sustained function of the ER in the $[Ca^{2+}]_i$ response of GnRH-stimulated gonadotrophs.

Tu-PM-I6

BOTH INTRA- & EXTRACELLULAR Ca^{2+} SOURCES REGULATE GLUCOSE-INDUCED Ca^{2+} TRANSIENTS IN MOUSE ISLETS.

((M.W. Roe, M.E. Lancaster, R.J. Mertz, J.F. Worley & I.D. Dukes.)) Glaxo Research Institute, RTP, NC 27709.

Using Fura-2-AM loaded mouse islets, we examined the influx and efflux pathways for Ca^{2+} during exposure to glucose. In the presence of 2mM glucose, $[Ca^{2+}]_i$ was maintained at low levels (< 100nM). Exposure to 12mM glucose caused a triphasic effect; within the first two minutes, $[Ca^{2+}]_i$ consistently fell by 30-40nM, rising rapidly thereafter to a level of ~450nM that was maintained for 30-50s, following which $[Ca^{2+}]_i$ began to oscillate at a frequency of 2-3Hz. On removal of glucose, $[Ca^{2+}]_i$ rapidly returned to near control levels. Removal of $[Ca^{2+}]_o$, or addition of Cd^{2+}, Co^{2+} or verapamil all suppressed the glucose-induced $[Ca^{2+}]_i$ transients, indicating that Ca^{2+} channel openings, secondary to glucose-induced phasic depolarizations were involved. However, rapid exposure to 5mM caffeine also reversibly suppressed the $[Ca^{2+}]_i$ transients, suggesting that $[Ca^{2+}]_i$ stores also played a role. Exposure to thapsigargin inhibited the initial glucose-induced drop in $[Ca^{2+}]_i$ and increased the amplitude of the Ca^{2+} oscillations. Replacement of extracellular Na^+ with Li^+ caused a reversible, sustained rise in Ca^{2+} either in the presence or absence of glucose. We conclude that glucose induced rises in $[Ca^{2+}]_i$ arise secondary to CICR from ER storage sites, and that both the ER Ca^{2+}-ATPase and Na^+-Ca^{2+} exchange play important roles in the removal of Ca^{2+} from the cytosol.

Tu-PM-I7

CALCIUM INFLUX AND EFFLUX PATHWAYS IN INSULIN-SECRETING CELLS. ((I.D. Dukes)) Glaxo Res. Inst., R.T.P. NC 27709.

Using combined Fura-2 and membrane current measurements, the mechanism underlying voltage dependent $[Ca^{2+}]_i$ transients in insulinoma (HIT-T15) cells was investigated. Depolarizations positive to -50mV produced time dependent rises in $[Ca^{2+}]_i$, which were maintained for 10s. The rise in $[Ca^{2+}]_i$ exhibited a bell-shaped relationship with voltage with a maximum at 0mV. The accompanying ionic currents revealed a slowly inactivating calcium current, whose time and voltage dependence mirrored that of the Ca^{2+} transients. The Ca^{2+} signals and I_{Ca} were simultaneously inhibited by removal of $[Ca^{2+}]_o$ or rapid application of Cd^{2+}, and integrations of I_{Ca} were superimposable upon the $[Ca^{2+}]_i$ transients, suggesting that I_{Ca} was responsible for the $[Ca^{2+}]_i$ signals. However, exposure to 5mM caffeine induced a large, long lasting Ca^{2+} transient - indicating release of Ca^{2+} from ER storage sites - and in the continued presence of caffeine, the depolarization-activated $[Ca^{2+}]_i$ transients were largely suppressed, suggesting that calcium induced calcium release from the ER, under tight control of I_{Ca}, was the primary regulator of the Ca^{2+} transients. The efflux pathways for Ca^{2+} were also examined, and two separate removal mechansims for $[Ca^{2+}]_i$ were detected. In the range of voltages from +60mV to +100mV and -60mV to -40mV, removal of $[Ca^{2+}]_i$ at a constant rate ($\tau \sim 7s$) could be observed; at voltages from -60mV to -110mV a further voltage dependent removal system seemed to additionally operate ($\tau \sim 2.5s$).

Tu-PM-I8

CYCLIC GMP STIMULATES DEPLETION-ACTIVATED CALCIUM ENTRY IN RAT PANCREATIC ACINAR CELLS. ((T.D. Bahnson, S.J. Pandol and V.E. Dionne°)) Departments of Medicine and Pharmacology°, UCSD, La Jolla, CA 92093-0636. (Spon. V.E. Dionne)

In the rat pancreatic acinar cell, hormonal stimulation causes a rise in the intracellular free Ca^{2+} concentration ($[Ca^{2+}]_i$) by activating the inositol-1,4,5-trisphosphate (IP_3) mediated release of Ca^{2+} from intracellular stores. The released Ca^{2+} is, for the most part, extruded from the cell, necessitating a mechanism for Ca^{2+} entry to replenish the stores. However, neither the mechanism of depletion-activated Ca^{2+} entry, nor the signal which activates it are known. A sustained inward current of depletion-activated Ca^{2+} entry can be measured in acinar cells using patch recording methods. The current can be activated by adding either 10 μM 1,4,5-IP_3 or 10 μM 2,4,5-IP_3 to the recording pipet with low $[Ca^{2+}]_i$. The addition of 1,3,4,5-IP_4 did not activate Ca^{2+} entry, suggesting that IP_4 is not the intracellular signal that stimulates the depletion-activated current. However, the depletion-activated current can be induced in the absence of Ca^{2+} depletion by perfusing the cell with 10 μM cGMP (but not cAMP), can be blocked by the guanylyl cyclase inhibitor LY83583, and can be reactivated by 8-bromo-cGMP after inhibition of the cyclase. We conclude that cGMP may be an intracellular messenger which regulates depletion-activated Ca^{2+} entry.

SPECTROSCOPIC STUDIES (OTHER)

Tu-PM-J1

FEMTOSECOND DYNAMICS OF THE *CIS-TRANS* ISOMERIZATION IN RHODOPSIN; THE FIRST STEP IN VISION.((Q. Wang, R.W. Schoenlein, L.A. Peteanu, R.A. Mathies, C.V. Shank)) Lawrence Berkeley Laboratory and Chemistry Department,University of California , Berkeley, CA 94720.

We report femtosecond studies of the ultrafast photo-induced *cis-trans* isomerization in rhodopsin[1]. This reaction is the first step in the process of vision. Using a novel femtosecond laser system, we excite the *11-cis* prosthetic group of the rhodopsin molecule with a 35-fs optical pulse at 500 nm. The molecule is then probed by either a 10-fs green pulse centered at 500 nm, or a 10-fs red pulse centered at 620 nm. Two sets of pump-probe data are combined to give a complete picture of the dynamic spectral response from 450 to 650 nm with femtosecond resolution. Differential spectral measurements over the photoproduct absorption range demonstrate that the formation of the photoproduct is essentially complete in only 200 fs. This time scale is comparable to typical vibrational dephasing and relaxation times, suggesting that the photochemistry occurs from a vibrationally coherent or nonstationary system. Vibrational oscillations having a period of several hundred femtoseconds are clearly observed at 590, 610 and 620 nm. We also observe a decay of the photoproduct absorption on the picosecond time scale which is consistent with vibrational cooling and conformational relaxation. In summary, the spectral dynamics of the primary step in vision are resolved with 35 fs time resolution using a two-color pump-probe technique, showing it to be one of the most rapid biochemical reactions ever studied.

1. An early version of this work was presented in, R.W.Schoenlein L.A.Peteanu, R.A.Mathies, C.V.Shank, *Science* 254, 412 (1991)

Tu-PM-J2

TEMPERATURE DEPENDENCE OF THE PHOSPHORESCENCE QUANTUM YIELD OF HEN EGG-WHITE LYSOZYME AND VARIOUS ALPHA-LACTALBUMINS.
((C.A. Smith and A.H. Maki)) Department of Chemistry, University of California, Davis, CA 95616.

The radiative quantum yield, ϕ_p°, of the triplet state of hen egg-white lysozyme (HEWL), and the structurally analogous α-lactalbumins from human (HLA), bovine (BLA) and guinea pig (GPLA), have been measured in the temperature range between 6 K, and the softening temperature of the aqueous glass (ca. 150 K). For HEWL, HLA, and BLA, ϕ_p° has little temperature dependence below ca. 30 K, but above this it decreases sharply with increasing temperature. The temperature dependence is fitted by a two state model in which the phosphorescence originates primarily from a donor (trp 108 in HEWL; trp 104 in HLA, BLA) whose population is coupled to an acceptor (trp 63 in HEWL; trp 60 in HLA, BLA) by a thermally activated triplet-triplet energy transfer process. The acceptor undergoes radiationless deactivation by a proximal disulfide while the donor has no analogous extrinsic quencher. In contrast with HEWL, HLA and BLA, GPLA exhibits a nearly temperature-independent ϕ_p° up to the softening point of the glass which supports of the proposed quenching model. GPLA contains trp 104 but has phe in place of the putative trp acceptor.

Tu-PM-J3

DIELECTRIC DISPERSION OF WATER-POLYPENTAPEPTIDE SYSTEM IN THE GHZ RANGE. ((J.-Z. Bao[1], K.W. Rhee[1], C.C. Davis[1], K.U. Prasad[2], D.W. Urry[2] and M.L. Swicord[3])) [1]Department of Electrical Engineering, University of Maryland, College Park, MD 20742. [2]University of Alabama at Birmingham, Laboratory of Molecular Biophysics, VH300, Birmingham, AL 35294. [3]FDA/CDRH, Rockville, MD 20857. (Spon. by J.-Z. Bao)

The complex permittivity of the water-polypentapeptide of elastin (Val^1-Pro^2-Gly^3-Val^4-Gly^5)$_n$ system is determined in the frequency range from 200MHz to 26.5GHz and for temperatures from 5 to 80°C by measuring reflection coefficients with the open-ended coaxial probe technique using a HP 8510 Network Analyzer. A calibration procedure, which involves three standard measurements, corrects the systematic errors and gives reliable results even for small quantities of sample (~ .1 ml). The synthetic poly(VPGVG) is soluble in water below 25°C, while aggregation occurs above 25°C with formation of a viscoelastic coacervate. The water molecules associated with the hydrophobic side chains are very different from the free water and give a lower dielectric dispersion than that of free water. To analyze the dispersion, we apply the Havriliak-Negami (HN) dielectric response: $\epsilon(\omega) = \Delta\epsilon/[1 + (j\omega\tau)^\alpha]^\beta$, which is an empirical function. Such non-Debye behavior is usually ascribed to the presence of a distribution, possibly of a fractal nature, of some physical quantity in space, time, or energy although there exists no specific theory yielding this power-law relation. At each temperature, the parameters of the HN function are determined by means of a Complex Nonlinear Least Squares (CNLS) fit, which fits the real and imaginary parts simultaneously. We acknowledge the support of ONR and FDA.

Tu-PM-J4

STRUCTURE AND STACKING BEHAVIOR OF THE DEOXYOLIGONUCLEOTIDE d(A-G)$_{10}$ INVESTIGATED BY ULTRAVIOLET RESONANCE RAMAN SPECTROSCOPY.
((I. Mukerji*, M.C. Shiber, H. Klump, T.G. Spiro* and J.R. Fresco)) Depts. of Chemistry* and Molecular Biology, Princeton University, Princeton, NJ 08544.

Guanine-rich regions occur at both the ends of chromosomes and within them at recombination hot spots. These guanine-rich regions have been proposed to play an important functional role in meiosis by initiating the alignment of four chromatids through the formation of a guanine tetrad. The deoxyoligonucleotide d(A-G)$_{10}$ may serve as a simple model for these guanine-rich regions. UV absorption as a function of temperature demonstrates that hypochromicity is observed for d(A-G)$_{10}$, indicative of base stacking at lower temperatures and that melting is cooperative, suggesting a helical structure. UV Resonance Raman spectroscopy has been used to investigate the behavior of d(A-G)$_{10}$ from 4 to 80 °C. Comparison of the melting behavior with that of dAMP and dGMP indicates that Raman hypochromism parallels absorption hypochromism. Selective excitation at either 240 nm or 250 nm enhances the Raman signal from guanine or adenine residues, respectively. The results suggest that adenine residues unstack preferentially between 4 and 20 °C, whereas guanine unstacking occurs between 20 and 60 °C. Structural models will be presented to account for these spectroscopic observations.

Tu-PM-J5
RESONANCE RAMAN SPECTROELECTROCHEMISTRY OF TRANSIENT METALLOPORPHYRIN AND AROMATIC AMINO ACID RADICALS.
((Michael L. McGlashen, Milton E. Blackwood and Thomas G. Spiro))
Department of chemistry, Princeton University, Princeton New Jersey, 08544

Resonance Raman (RR) spectroscopy has played a fundamental role in elucidating the structural features of metalloporphyrins. The mechanisms of RR enhancement are now well understood, as are the compositions of the porphyrin normal modes. Resonance Raman spectra have also been obtained for the stable cation and anion radicals of several metalloporphyrin derivatives and the structural details of electron transfer in this interesting class of molecules are beginning to emerge. Not all porphyrin radicals are stable, however, and new techniques are necessary to obtain RR spectra at higher time resolution in order to follow these reactive species. In addition, the study of anion radicals requires that the sample cell be anaerobic, inert ot non-aqueous solvents and cooled to prevent sample decomposition. We will discuss RR spectra obtained using a spectroelectrochemical cell which employs microelectrodes for transient radical generation. We will also discuss recent ultraviolet RR studies of models of the galactose oxidase active site.

Tu-PM-J6
INFRARED AND RAMAN MICROSCOPY OF CELLULAR PROTEINS IN HUMAN TISSUE SPECIMENS. Jose A. Centeno, Cesar A. Moran, Florabel G. Mullick, and Timothy J. O'Leary. Departments of Environmental and Toxicologic Pathology, Pulmonary and Cellular Pathology, Armed Forces Institute of Pathology, Washington, D.C. 20306-6000.

The presence of intracellular proteins such as mucins in certain neoplasms of the lung have been commonly associated in cases of adenocarcinoma. However, in many of these cases the histochemical differentiation of this neoplasm is not so obvious, presumably due to the empirical nature of the stains and the intrinsic variable sensitivity of the stain within laboratories. For this reason, structural information is needed to obtain a most accurate diagnosis. In this study, infrared microscopy and laser Raman microprobing (RMP) have been used to probe the structure of various matrix protein components in normal and neoplastic lung tissue specimens. Infrared and Raman bands originating from carboxylic acid groups were identified. In addition, the amide I, II, and -A vibrations of intracellular mucin (adenocarcinoma) are clearly discernable at 1650, 1546, and 3295 cm^{-1}, respectively; while for the mucin protein in mesothelioma, these lines were observed at 1632, 1550, and 3305 cm^{-1}. In the latter case the mucin displayed a characteristic beta-pleated structure. The intracellular mucin amide frequencies are consistent with a less ordered structure presumably an alpha-helix conformation. The data obtained herein indicates that a combination of infrared and Raman microscopy provides two powerful new tools for a quick identification, characterization, and differentiation of intracellular protein components in human tissue specimens.

Tu-PM-J7
SPECTROPHOTOMETRIC ABSORBANCE OF PROTEIN CHROMOPHORES TO DIFFERENTIATE NORMAL FROM PATHOLOGICAL CONDITIONS. ((Germille Colmano)), Va-Md Regional College Veterinary Medicine, Dept Biomedical Sciences, VPI & SU, Blacksburg, VA 24061-0442, and BioSpectra Co., 609 Broce Dr NW, Blacksburg VA, 24060-2801.

Differences in UV-VIS absorption spectra of protein chromophores (color carriers) from biological fluids can differentiate not only specific bacterial cultures contaminating food products, but also normal healthy from abnormal pathological conditions in different animals, and humans. Spectral patterns followed quail mercury poisoning, detected low levels of carbaryl contamination in poultry plasma and goldfish bile or aquarium water, and detected differences between three specific enteric human pathogens Salmonellae (typhimurium, enteritidis, Arizona), Listeria, and Campylobacter jejuni mixed with non-pathogenic bacteria. Then, differences, in specific spectral absorbaces of biological fluids, separated the normal healthy humans from pregnant patients, and also from the abnormal pathological patients with cancer of the stomach, heart, ulcer, and arthritis. SAS and SPSS-X (discriminant analysis), were used to differentiate changes in the digitized UV-VIS absorption spectra of the protein chromophores (color carriers). The experiments in the experimental section are given to illustrate our main technical approach, which, excluding proprietary parts, we consider innovative enough to be presented.

Tu-PM-J8
STATIC AND DYNAMIC LIGHT SCATTERING STUDIES OF FILIPIN IN AQUEOUS MEDIA AND ITS INTERACTION WITH CHOLESTEROL
((M.A.R.B.Castanho[1], W. Brown[2], M.J.E.Prieto[1])) 1-Centro Química Física Molecular, Complexo I, 1096 Lisboa codex, Portugal; 2-Institute of Physical Chemistry, Univ. Uppsala, Box 532, 751 21 Uppsala, Sweden.

Aggregation of filipin in an aqueous medium and filipin-induced changes in cholesterol micelles have been studied using intensity and dynamic light scattering. The dependencies of filipin aggregate dimensions on concentration, solvent and temperature were studied and revealed that the aggregates do not have a well defined geometry, i.e. a critical micelle concentration cannot be detected and stable structures are not formed. The aggregates are of size Rg=110 nm, Rh=63 nm referring to the radius of gyration and hydrodynamic radius, respectively. In the concentration range studied (1-30 μM), a low molecular weight species (monomer or dimer) is always present together with the aggregates.
No pronounced effect of filipin on the structure of the cholesterol micelles was observed (a small increase in Rg and Rh is noted). These results rule out any "specificity" for the filipin interactions with cholesterol, which has been considered a key event on the filipin biochemical mode of action as an antibiotic A re-evaluation of this question is suggested and some alternatives are advanced.

ELECTRON TRANSFER SYSTEMS

Tu-PM-K1
CYANIDE BINDING TO CYTOCHROME OXIDASE
((M. Brunori, G. Antonini, F. Malatesta, P. Sarti and M.T. Wilson*)) Biochemistry, University of Rome, IT; *Chemistry, University of Essex, Colchester, UK.

Inhibition of respiration by cyanide binding to cytochrome oxidase proceeds via rapid complex formation to partially reduced states of the enzyme; however the redox intermediate which is highly reactive towards cyanide remains controversial. Transient spectroscopy and SVD analysis has been employed to provide an answer to the following questions: (i) how many electrons are necessary and sufficient to populate this intermediate?; (ii) what is the redox state of cyt.a/CuA/Cyt.a3/CuB in the intermediate?; (iii) which is the cyanide-binding metal in this intermediate? The data show that entry of 1-1.3 electron into the cyt.a/CuA centres leads to rapid cyanide binding to an enzyme in which cyt.a3 is oxidized; however the inhibitor is not bound to cyt.a3 but to oxidized CuB, and the access to this site is conditioned by the entry of a single electron into the enzyme. The relevance of these results for the primary intermediate in the reaction of oxygen (and CO) with the reduced binuclear center is discussed.

Tu-PM-K2
NEW INTERMEDIATE STATE INVOLVED IN CO REBINDING TO CYTOCHROME OXIDASE. ((H. James Harmon)) Oklahoma State University, Stillwater, OK 74078.

Successive ("kinetic") spectra of cytochrome oxidase were recorded following the photolysis of ferrous carboxyoxidase and during CO recombination in beef heart mitochondria at low temperatures (to -114 C) using a conventional dual wavelength spectrophotometer or a rapid scanning monochromator (OLIS). At pH 7 and lower values, a change in absorbance at 412-415 nm is recorded during the rebinding of CO. Both the increase and decay in 415 nm absorbance after photolysis occur on a faster time scale than the decrease in 446 nm or increase in 430 nm absorbance as CO rebinds, the decrease in 415 absorbance occurring as 430 nm absorbance increases but while 446 absorbance does not decrease. This suggests that protonated unliganded ferrous oxidase forms with spectral properties suggestive of a low-to-high-to-low spin state change.

Supported by a grant from the Health Research program of the Oklahoma Center for the Advancement of Science and Technology.

Tu-PM-K3

FINDING ELECTRON TRANSFER PATHWAYS IN PROTEINS

((J.J. Regan[1], D.N. Beratan[2], J.N. Onuchic[1]))

[1] Department of Physics, University of California at San Diego, La Jolla, CA 92093. [2] Department of Chemistry, University of Pittsburgh, Pittsburgh, PA 15260.

A model of electron transfer is reviewed which characterises a molecule as a network of sigma bonding orbitals and lone pair orbitals through which an electron can transfer with a rate proportional to the square of the electronic coupling mediated by the orbitals. A tight binding Hamiltonian and Dyson's equation method are used to compute the tunneling matrix elements between the electron donor and acceptor orbitals. The Green's function matrix elements of the bridge are computed using a strategy that builds up the orbital chain one orbital at a time, allowing inclusion of all alternative orbital pathways in the resulting computed coupling factor, taking into account backscattering and multiple pathway interference. The inclusion of these effects should substantially improve theoretical prediction of electron transfer rates in proteins.

This model can be investigated to answer a number of questions. Is an electron transfer reaction mediated by a single distinct path through orbitals, or is a network of interfering paths involved? Given a donor orbital, what is the relative accessibility of all the other orbitals in the protein? In a given transfer reaction, is there a critical orbital such that the deletion or addition of the orbital results in a large change in the coupling (and thus the transfer rate) between two orbitals?

Work supported by the NSF (grant MCB-9018768) and by the NIH (training grant 5T32 GM08326-03).

Tu-PM-K4

LONG RANGE INTERMOLECULAR ELECTRON TRANSFER REACTIONS IN THE METHYLAMINE DEHYDROGENASE-AMICYANIN COMPLEX.

((H.B. Brooks and V.L. Davidson)) Univ. of Miss. Med. Ctr., Jackson MS 39216

A quinoprotein, methylamine dehydrogenase, and a type I copper protein, amicyanin, form a physiologically relevant complex in which electrons are transferred from tryptophan tryptophylquinone [TTQ] to copper. From x-ray crystallographic studies (Chen, et al. Biochemistry 31:4959) of an actual complex of these proteins, it is known that the distance from the edge of TTQ to copper is 9.5Å. The reoxidation of MADH by amicyanin has been studied by stopped-flow spectroscopy. At 30°C, the association constant for complex formation was $5 \times 10^8 M^{-1}$ and the rate of conversion of TTQ from the reduced to semiquinone form was 44 s^{-1}. The temperature-dependence of the latter reaction was analyzed using the Eyring equation and yielded values of +12 kcal·mol^{-1} and -12 cal·mol^{-1}·°K^{-1}, respectively, for the enthalpy and entropy of activation. Using Marcus theory, it has been possible to calculate from these data the reorganizational energy and electronic coupling for this intermolecular electron transfer reaction and compare these values with those reported for intramolecular electron transfer reactions. From these structural and kinetic data it is possible to predict the likely pathway of electron transfer from TTQ to copper and speculate as to what conformational changes within the protein complex may occur to facilitate the electron transfer. Supported by NIH grant GM-41574.

Tu-PM-K5

EVIDENCE THAT AN INTRINSIC MEMBRANE PROTEIN IN THYLAKOIDS IS NECESSARY FOR MAINTAINING LOCALIZED $\Delta\tilde{\mu}_{H^+}$ ENERGY COUPLING.

((M. Renganathan and R.A. Dilley)) Dept. of Biological Sciences, Purdue University, West Lafayette, IN 47907-1392

Previous work has led us to postulate that chloroplast thylakoids can maintain a sequestered H^+ gradient in domains in which can form a localized energy coupling $\Delta\tilde{\mu}_{H^+}$, but certain conditions such as overfilling the sequestered domains allow delocalized coupling. We earlier identified several thylakoid proteins that contribute low pK_a lysines to the sequestered domains, including the chlorophyll a/b binding light-harvesting complex (1). A barley mutant lacking LHCII (chlorina f2) has been found to be unable to maintain the localized $\Delta\tilde{\mu}_{H^+}$ and those thylakoids carry out delocalized energy coupling under all conditions tested. The wild type barley shows either localized or delocalized $\Delta\tilde{\mu}_{H^+}$ energy coupling. We have other evidence suggesting that the two coupling possibilities depend on treatments which either maintain Ca^{++} gating of H^+ fluxes at the CF_0 or displace Ca^{++} from the CF_0 gating site. The barley mutant data are consistent with a hypothesis that visualizes several thylakoid proteins providing acid-base ionizable groups buried in sequestered domains with those domains collectively providing a localized H^+ diffusion pathway into the CF_0. The absence of the LHCII protein could produce a "leaky" H^+ diffusion pathway allowing entry of domain H^+ ions into the lumen before they reach the CF_0, and the lumenal H^+ accumulation could open the CF_0 H^+ flux gate by displacing the putative gating Ca^{++} allowing delocalized energy coupling

(1) Laszlo, J.A., Baker, G.M. and Dilley, R.A. (1984) *Biochim. Biophys. Acta 764*, 160.

Tu-PM-K6

MYOCARDIAL ADAPTIVE STRATEGIES IN ANAEMIA AS A MODEL OF CHRONIC HYPOXIA

((M. L. Field, J. F. Clark and G. K. Radda)) Dept. of Biochemistry, South Parks Road, Oxford University, OX1 3QU, U.K.

Exposure of the rat myocardium to a chronically hypoxic environment leads to a series of adaptive and maladaptive morphological, ionic and metabolic alterations. Chronic anaemia may be used as a model of hypoxia with the qualification that its aetiology is complicated by volume overload hypertrophy and iron dependent enzyme deficiencies. Table 1 describes alterations in the metabolic capacity of heart from anaemic rats. Maximal extracted citrate synthase (CS), total creatine kinase (CK), mitochondrial CK and phosphofructokinase (PFK) activities are expressed as IU/g wet wt/min. Respiratory capacities of mitochondria in saponin skinned fibers are expressed as ng O_2/mg dry wt/min.

	CS	*CK*	*PFK*	*MITO CK*	*BASAL RS*	*ADP‡ RS*	*Cr‡‡ RS*
Control	63.0 ±2.3	260 ±8.8	11.0 ±0.1	59.0 ±4.0	4.6 ±0.4	8.4 ±0.7	12.5 ±0.9
Anaemic	85.0* ±4.4	361* ±8.9	18.0* ±0.9	96.0* ±2.5	6.9* ±0.7	12.1* ±1.3	17.4* ±1.0

Values are means +/- SE. C, control; A, anaemic; RS, respiration; Cr, creatine; ‡, 0.1mM; ‡‡, 40mM.*P<0.05 using Students t test.

In response to chronic hypoxia the myocyte will increase its metabolic efficacy by elevating the sensitivity of ADP and Cr control of respiration rather than altering maximal respiratory capacity (2mM ADP). Integral to this altered sensitivity may be an increased mitochondrial CK activity as part of an overall CK foetal shift (increased total CK and a decreased M to B subunit ratio). The capacity for glycolytic ATP production is greatly enhanced in the anaemic fibers by the elevated PFK activity thus allowing the myocyte to respire in the hypoxic environment *in situ*. Higher basal metabolism of anaemic fibers is probably a consequence of the experimental conditions (higher pO_2 than *in situ*) and reflects an increased relative sensitivity to $[O_2]$.

Tu-PM-K7

CRYSTALLIZATION OF MITOCHONDRIAL CYTOCHROME *b*-c_1 COMPLEX IN GEL.

((C.A.Yu[a], A.J. Weaver[b], J. Deisenhofer[b] and L. Yu[a])) [a]Oklahoma State University, Stillwater, OK 74078 and [b]Howard Hughes Medical Institute, Dallas, TX 75235

Cytochrome *b*-c_1 complex (ubiquinol-cytochrome *c* reductase) of beef heart mitochondria has been crystallized. The crystals, grown in capillary tubes, diffracted X-ray to 7Å resolution in the presence of mother liquor. Preliminary experiments on a Xuong/Hamin area detector indicate that they belong to tetragonal system; the space group is probably $P4_122$ (or $P4_322$) with cell constants a=b=158.7Å, c=593Å. Assuming one cytochrome *b*-c_1 complex dimer per asymmetric unit, the crystals would have a solvent content of 70%. Removal of the mother liquor from crystals causes severe loss of diffraction quality. On the other hand, movement of crystals in the capillary tube makes the data collection impossible. To circumvent these difficulties, we have recently developed a method to crystallize cytochrome *b*-c_1 complex in the gel state. Purified cytochrome *b*-c_1 complex, 20 mg/ml in 50 mM MES buffer, pH 7.0 containing 0.67 M sucrose was mixed, at 18 °C, with an equal volume of precipitating solution containing 0.08% decanoyl-N-methyl-glucamide, 3.6% heptanetriol, and 0.5M sodium chloride, 12% polyethylene glycol and 0.8-0.4% low gelling temperature agarose. The mixture was then placed in capillary tubes, cooled to 4 °C, overlaid with equilibrating solution, and incubated in a shock-free environment at 4 °C. Under these conditions the cytochrome *b*-c_1 complex crystals were formed within 2-4 weeks. The sizes, shapes and diffraction quality of these crystals approach those obtained in the liquid state. Supported in part by grants from NIH (GM 30721 to CAY) and by the Howard Hughes Medical Institute (JD).

Tu-PM-L1

EPIDERMAL GROWTH FACTOR (EGF)-RECEPTOR CLUSTERING MONITORED BY FLUORESCENCE RESONANCE ENERGY TRANSFER USING DONOR PHOTOBLEACHING AND LIFETIME-RESOLVED FLUORESCENCE IMAGING MICROSCOPY. ((T. W. J. Gadella Jr., R. Clegg, D. J. Arndt-Jovin and T. M. Jovin)) Department of Molecular Biology, Max Planck Institute for Biophysical Chemistry, Postfach 2841, W-3400 Göttingen, Federal Republic of Germany.

Microclustering of the epidermal growth factor (EGF)-receptor is generally believed to be the first event in EGF-mediated cellular activation. With fluorescence resonance energy transfer (FRET) using fluorescein- and rhodamine-labelled EGF as the donor/acceptor pair, the distance between the EGF-receptors can be monitored. Donor photobleaching microscopy [1] and lifetime-resolved fluorescence imaging microscopy [2] coupled to image analysis and processing [3] are convenient techniques to determine FRET in a spatially resolved manner on intact cells. Using these techniques, we observed that after a brief exposure at room temperature to 50 nM labelled-EGF at a donor/acceptor ratio of 1:2 , about 20% FRET-efficiency was achieved. Data analysis and modeling [4] indicates that EGF triggers at least 40% of the receptors to dimerize (oligomerize) and that the maximal distance between the donor/ acceptor pair (i.e. the two dimerized receptor molecules) is $\leq$ 6 nm. This is compatible with an elongated rather than a globular receptor structure.

[1] Jovin, & Arndt-Jovin (1989) in *Cell Structure and Function by Microspectrofluorometry*, pp.99-117. [2] Clegg et al. (1992) *SPIE Proc 1640*, 448-460.[3,4] Gadella Jr. et al.,manuscripts in preparation.

Tu-PM-L2

QUANTITATIVE ESTIMATION OF PDGF-INDUCED NUCLEAR FREE CALCIUM OSCILLATIONS IN SINGLE CELLS PERFORMED BY CONFOCAL MICROSCOPY WITH FLUO-3 AND FURA-RED.

((P.A. Diliberto and B. Herman)) Department of Cell Biology & Anatomy, University of North Carolina at Chapel Hill, Chapel Hill, NC 27599. (Spon. B. Chazotte).

Upon binding to its receptor(s), Platelet-derived Growth Factor (PDGF) initiates a rapid, transient elevation in intracellular free calcium concentration thought to be important in the promotion of cell growth. We have recently identified oscillations in nuclear free calcium (Ca^{2+}_n) elicited by PDGF isoforms in BALB/c3T3 fibroblasts (Diliberto et al., EMSA Proceedings, p.228, 1991), and are currently characterizing these alterations using confocal laser scanning microscopy to examine optical sections of cells that pass through the center of the nucleus as a function of time. In cells loaded with Fluo-3-AM, the oscillations involve stimulation of Ca^{2+}_n from resting levels lower than those observed in the cytoplasm to levels apparently equal to or higher than those of the surrounding cytoplasm. Differences in the propensity of AA- and BB- PDGF isoforms to elicit these oscillations have been found. Additionally, agents acting on Ca^{2+} pools and the distribution of intracellular Ca^{2+} (i.e. caffeine, EGTA) were found to affect the occurrence and frequency of the oscillations. We are now developing a method to quantitate, as well as verify, the Ca^{2+}_n oscillations observed with Fluo-3 alone by co-loading cells with Fluo-3 and Fura-Red with subsequent measurement of the fluorescence intensity ratio of these two Ca^{2+}-sensitive indicators. Preliminary data indicate that this method can detect the Ca^{2+}_n oscillations induced by PDGF, and effectively normalize, in a quantitative manner, accessible volume, pathlength, and cell-to-cell heterogeneity in fluorescence intensities thought to arise from differences in indicator concentrations.

Tu-PM-L3

SPATIAL AND TEMPORAL CHANGES IN THE HIPPOCAMPAL DISTRIBUTION OF A FLOURESCENT PHOSPHOLIPASE SUBSTRATE.

(D.S. Lester, J.L. Olds, P.L. Huddie and D.L. Alkon) NSS, NINDS, NIH, Bethesda, MD. 20892

Intact hippocampal slices have been principally employed in electrophysiological studies. Such slices largely preserve cytoarchitecture and the integrity of the tri-synaptic circuit and hence have been useful in delineating physiology. Here, slices were used to visualize distribution of a fluorescent substrate for phospholipase before and after muscarinic receptor challenge. Uptake of the fluorescent substrate (1-NBD-phosphatidylcholine [PC]) was relatively constant across control slices (N=9). The probe manifested itself (low power X2.5) heterogeneously in the pyramidale cells (stratum pyramidale, oriens and radiatum) of Amon's Horn and in the granule cell somata and dendrites of the dentate gyrus. Epifluorescence-microscopy at higher power (X20 objective) revealed labelling at distinct subcellular loci within neurons. The pattern seen with NBD-PC was reproducible (N=12) when compared to incorporation of another fluorescent lipid probe, BODIPY phorbol ester (N=4). Bath perfusion of carbachol (5 uM) resulted in a decrease in quantum yield, two-fold greater than photobleaching, as quantitated by a low-light image analysis system. This shift was largely blocked by concurrent perfusion of the muscarinic receptor antagonist, atropine (10 uM). This technique may prove to be a powerful complement to extant morphological labelling procedures in living tissue.

Tu-PM-L4

PHOTOCHROME AND TRIPLET- PHOTOCHROME LABELING IS A NOVEL METHOD OF RECORD SENSITIVITY IN STUDY OF BIODYNAMICS .

((G.I. Likhtenshtein[1], V.M. Mekler[2],D.V. Khudjakov[2] and V.R. Vogel[2])) [1]Department of Chemistry, Ben-Gurion University of the Negev, Beer Sheva 84105,Israel.[2]Institute of Chemical Physics, Russian Academy, Chernogolovka, Moscow Region 142432 Russia. (Spon. by A.H. Parola)

Spin and lumenescent labels,that have progressively been brought into use in molecular biology, have, along with there advantages, number of limitations. The theoretical consideration and experimentalevidences indicate that quantitative study of photochromicprocesses in labeled objects open up new possibilities for investigating microviscosity, conformational transition and dynamic contactacts between molecules, including proteins.We now report that the rate of photoisomerization of a photochrome label, a stilben derivative in this case, in solution and being attached to myoglobin is limited by the rate of rotation of the exited molecule fragment. However, it correlates with a spin label rotation in identical conditions. Secondly, we proposed a method for registration of very rare collisions based on monitoring kinetics of photochrome reaction between PL and trilet label (TL), erithrosin, both bound to chymotrypsinogene. The photochrome reaction is initited with triplet-triplet energy transfer from TL to PL. The lowest frequency of collisions was 1s .Both methods feature a record sensitivity, simplicity and accesability for many laboratories.

Tu-PM-L5

Quantitation of Absorption And Scattering of Small Biological Samples by Substitution Using Time-Resolved Spectroscopy. **H. Liu, B. Chance, N. G. Wang, M. Miwa, University of Pennsylvania, Dept. of Biochem/Biophys., Phila., PA 19104**

Applying near infrared time- and frequency-resolved tissue spectroscopy to biomedical imaging and medicine is of great interest recently. While the optical properties of large-size biomedical materials can be successfully characterized by photon diffusion approximation, the semi-infinite boundary condition limits the direct measurement of small samples due to photon escape and results in the difficulty to establish analytical solutions for heterogenious media. Using time resolved spectroscopy, we developed experimental approaches by substitution to measure the absorption and scattering coefficients of small samples so as to overcome photon escape from the small sample. The method is based on introducing the small sample to a large tank containing an initial concentration of intralipid with a certain absorption. By matching the optical properties of the sample and the intralipid, the absorption and then scattering coefficients are characterized. On the other hand, the perturbation of the introduced sample will alter the photon migration patterns, resulting in discontinuity of photon kinetics. Specifically, using this method, we have measured the optical properties of human fingers of fifteen people. The results show that the absorption coefficients of human fingers vary from person to person and the direct measurement may give incorrect answer due to photon escape. This method may be useful for detection of pathological properties of diseased tissue samples and for measurements of cell and organelle properties.

Tu-PM-L6

QUANTITATION OF $[Ca^{2+}]_i$ DURING HYPOXIA IN PERFUSED RAT HEARTS USING INDO-1 FLUOROMETRY.

((R. Brandes*, V.M. Figueredo, S.A. Camacho, A.J. Baker & M.W. Weiner)) *Loyola Univ. Chicago, IL 60153 & Univ. Calif. San Francisco, CA 94121.

Fluorometric detection of intracellular $[Ca^{2+}]$, $[Ca^{2+}]_i$, in intact tissue is complicated by wavelength-dependent tissue light absorbance, resulting in different *in-vitro* and *in-vivo* calibration parameters. Furthermore, changes in tissue absorbance during hypoxia could cause errors in calculated changes of $[Ca^{2+}]_i$. To overcome the first problem, *in-vitro* calibration parameters were first obtained from a reference solution containing a mixture of proteins; *in-vivo* parameters were then calculated by correcting for heart light absorbance which was determined by a novel method (based on the relationship between Indo-1 fluorescence intensities measured at two wavelengths). The Figure shows calculated $[Ca^{2+}]_i$ in a beating heart during normoxia and hypoxia: before and after correcting for absorbance changes. These results demonstrate a method by which $[Ca^{2+}]_i$ can be estimated in intact tissue using *in-vitro* calibration parameters. Furthermore, the example demonstrate that, in the absence of a correction for changing absorbance, $[Ca^{2+}]_i$ could appear to increase during hypoxia, although systolic $[Ca^{2+}]_i$ actually decreased.

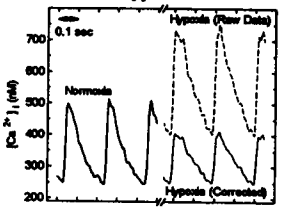

Tu-PM-L7

THE STRUCTURE OF BIOLOGICAL MEMBRANES PROBED BY K-SPACE PULSED FIELD GRADIENT SPIN ECHO NMR. ((*K. Svoboda*[1,2], *L.L. Latour*[3], *P.P. Mitra*[1], *and C.H. Sotak*[3,4])) *Harvard University*[1], *Rowland Inst. for Science*[2], *Cambridge, MA; Worcester Polytechnic Inst.*[3], *U. Mass. Med. Sch.*[4], *Worcester, MA. (Spon. by S.M. Block)*

Packed red blood cells (RBCs) are ideally suited as a model system for the study of water diffusion through biological membranes. We investigated the effects of RBC packing density, membrane permeability, and buffer ionic strength on the pulsed field gradient spin echo (PFGSE) amplitude, $M(k)$. Using a modified pulse sequence that removes the effects of inhomogeneous fields, we measured $M(k)$ at long diffusion times (*100 ms*) as a function of the wavevector $k = \gamma G\delta$ (γ, gyromagnetic ratio; G, gradient pulse amplitude; δ, gradient pulse width). Bovine RBCs at *150 mM* ionic strength (*pH 7.4*) were centrifuged in NMR tubes at *23,000 g x 15 min*. $M(k)$ in these samples showed a large first-order coherence peak at $k_{max} = 1.93 \times 10^{-4}$ *cm*$^{-1}$. Assuming a face-centered cubic (fcc) lattice packing this corresponds to a cell-to-cell spacing of *4.1 μm*. Within experimental error, this number agrees with independent estimates derived from i) cell-counting of a known volume of packed blood cells, using a hemacytometer counting chamber, and ii) differential interference contrast (DIC) microscopy. To increase the cell-to-cell spacing we prepared packed cells in *100 mM* buffer. For this sample, $M(k)$ showed a peak at $k_{max} = 1.65 \times 10^{-4}$ *cm*$^{-1}$, corresponding to a cell-to-cell spacing of *4.68 μm*, in agreement with our estimate from cell counting. Measurements on larger human RBCs yielded equally accurate results. We compare our data to Monte Carlo simulations and analytical studies of $M(k)$ and find good agreement. To investigate the effect of membrane permeability on $M(k)$, we compared samples packed at *2700 g x 4 min* (volume fraction of extracellular fluid ~ *0.25*) with and without *1 mM* pCMBS (at *150 mM* ionic strength). pCMBS is known to inhibit the channel-based water transport through RBC membranes. Both samples showed a less pronounced coherence peak than those packed at *23,000 g*, independent of pCMBS. The position of the peak was in agreement with cell-to-cell distance measurements. $M(k)$ for cells treated with pCMBS had a larger amplitude, due to the increased localization of water in these samples. Our results show that $M(k)$ is a sensitive probe of the structure (resolution < *0.1 μm*) and permeability of biological membranes.

Tu-PM-L8

SURFACE-TO-VOLUME RATIO AND MEMBRANE PERMEABILITY DERIVED FROM TIME-DEPENDENT DIFFUSION OF WATER THROUGH BIOLOGICAL MEMBRANES. ((*K. Svoboda*[1,2], *L.L. Latour*[3], *P.P. Mitra*[1], *and C.H. Sotak*[3,4])) *Harvard University*[1], *Rowland Inst. for Science*[2], *Cambridge, MA; Worcester Polytechnic Inst.*[3], *U. Mass. Med. Sch.*[4], *Worcester, MA.*

Packed red blood cells (RBCs) are ideally suited as a model system for the study of water diffusion through biological membranes. We used a modified pulsed field gradient spin echo (PFGSE) NMR technique to measure the time-dependent diffusion constant, $D(t)$, in packed samples of RBCs, over times ranging from *2 ms* to *50 ms*. $D(t)$ started to fall sharply at early times, as recently predicted[1] and in contrast to previous reports. For short times the equation

$$D(t) = D_o\left\{1 - 4/\left(9\sqrt{\pi}\right)\sqrt{D_o t}(S/V) + o(D_o t)\right\}. \quad (1)$$

provides a new measure of V/S, the volume-to-surface ratio of the cell. For packed human RBCs at *100 mM* ionic strength (*pH 7.4*) that were centrifuged in NMR tubes at *23,000 g x 15 min*, a fit of $D(t)$ to equation (1) gave $V/S = 0.7\ \mu m$, in agreement with light microscopy. The long time diffusion constant, D_∞, depends on membrane permeability. Using our value for this constant and a new effective medium theory that takes into account the effects of extracellular as well as intracellular fluid, we computed the membrane permeability, κ. For bovine RBCs packed as above with and without prior treatment with pCMBS, we obtained $\kappa = 0.7 \times 10^{-2}$ *cm/s* and $\kappa = 1.3 \times 10^{-2}$ *cm/s*, respectively, assuming a negligible fraction of extracellular fluid. pCMBS is known to inhibit channel-based water transport through RBC membranes. These permeabilities are close to previous estimates derived from studies of cell suspensions. For RBCs packed at *2,700 g x 4 min* (volume fraction of extracellular fluid ~ *0.25*) we obtained significantly larger values for D_∞ than for those packed at higher speed.(0.42×10^{-5} *cm*^{2}*/s* vs. 0.23×10^{-5} *cm*^{2}*/s*). Our results show that PFGSE measurements may be used to determine V/S and permeability of biological membranes, and also that D_∞ in such systems depends sensitively on parameters such as packing and the ratio of extracellular to intracellular fluid. An important advantage to this technique is that it is noninvasive, and so can be carried out *in vivo*.

[1]P. P. Mitra *et al.* Phys. Rev. Lett. 68, 3555 (1992).

Tu-PM-L9

MEASURING TISSUE FIBER DIRECTION USING DIFFUSION NMR ((P.J. Basser, D. LeBihan and J. Mattiello)) BEIP, NCRR, NIH, Bethesda, MD 20892. (Spon. by P.J. Basser)

We exploit the phenomenon of anisotropic diffusion to determine noninvasively the local fiber direction in tissues. A tissue's three orthotropic directions coincide with the principal coordinate axes of the effective self-diffusion tensor, $\underline{D}^{eff}$, estimated from NMR pulsed-gradient, spin-echo experiments. The diffusivites and mean diffusion distances in these orthotropic directions are the eigenvalues and the square root of the eigenvalues of $\underline{D}^{eff}$, respectively. A diffusion ellipsoid is constructed in each voxel to depict both the local fiber direction and mean diffusion distances. Three scalar invariants of $\underline{D}^{eff}$, which are independent of the tissue sample's orientation in the laboratory frame of reference, differ significantly among brain gray matter, brain white matter, and fat (*in vitro*), and may reflect changes in tissue microstructure and in membrane, interstitial, and intracellular permeabilities. Finally, we suggest that $\underline{D}^{eff}$ can be used both to align and to adjust the magnetic field gradients used in diffusion NMR imaging and spectroscopy. Inherently, $\underline{D}^{eff}$ contains information about tissue structure and function *within a voxel*, which scalars (such as T_1, T_2, and proton density) do not. The estimation of tensors that describe transport processes in anisotropic media presents new opportunities in functional MR imaging, development, diagnosis, physiology, and nondestructive testing.

Tu-PM-L10

ROTATIONAL RESONANCE NMR STUDIES OF HYDROPHOBIC PEPTIDE SECONDARY STRUCTURE. ((Olve B. Peersen, Saburo Aimoto and Steven O. Smith)) Department of Molecular Biophysics and Biochemistry, Yale University, 260 Whitney Ave., New Haven, CT 06511 and Institute for Protein Research, 3-2 Yamadaoka, Suita, Osaka, Japan.

Rotational resonance (RR) NMR provides an experimental approach for extracting internuclear distances between specific ^{13}C labeled sites in integral membrane proteins and protein micro-crystals. A number of such distances can provide structural constraints and allow determination of secondary and possibly tertiary structure in these systems. Using a model peptide whose high resolution X-ray crystal structure has been determined, we have shown that RR NMR can detect $^{13}C\cdots^{13}C$ distances as long as 6.8Å and with a resolution of ~0.5Å for distances in the 5Å range (Peersen et al., *J. Am. Chem. Soc.*, **114**, 4332-35, 1992). The RR NMR data can be theoretically simulated by considering the internuclear distance and relative orientations of the ^{13}C labeled sites. These parameters are readily calculated from the structure of the peptide, providing an ideal system for evaluating simulations of long distances.

These studies have also been extended to longer peptides corresponding to the transmembrane domains of the red cell protein glycophorin A and the *neu* receptor. RR NMR measurement of these peptides reconstituted into lipid bilayers are being used to address local secondary structure and protein-lipid interactions in native membrane environments.

PHOTOSYNTHESIS II

Tu-PM-M1

CONFORMATIONAL SURFACES OF PHOTOSYNTHETIC CHROMOPHORES. PLANAR AND RUFFLED CONFORMERS OF PYROPHEOPHORBIDE DERIVATIVES. ((K.M. Barkigia, E. Gudowska-Nowak, M.W. Renner, F.Y. Shiau, K.M. Smith and J. Fajer)) Brookhaven National Laboratory, Upton, NY 11973

Recent structural data for porphyrins and (bacterio)chlorins as isolated molecules and in proteins illustrate the considerable flexibility of the chromophores. We report here examples of such multiple conformations in two Ni(II) derivatives of pyrochorophyll a in which the usual 3-vinyl substituent has been replaced by ethyl (1) or formyl (2) groups. The macrocycle of 1 is planar with maximum deviation of any core atom from the average macrocycle plane ≤0.1Å. In contrast, 2 is severely ruffled with deviations from the average plane as large as 0.6Å. Besides offering further evidence of the significant flexibility of the chlorophyll macrocycle, the crystallographic data provide the basis for molecular orbital and dynamics calculations of photosynthetic conformers. Molecular dynamics calculations indicate that the energy difference between the relaxed planar and ruffled conformations of 1 and 2 is ~7 kcal. Recent results for nonplanar porphyrin derivatives clearly demonstrate that the optical, redox and excited state properties of the molecules are affected by core distortions. The modest energy differences between the planar and ruffled conformers of 1 and 2 suggest that conformational distortions provide facile structural mechanisms for modulating the properties of the chromophores in vitro and in vivo. (Work supported by U.S. DOE contract No. DE-AC02-76CH00016.)

Tu-PM-M2

STRUCTURE-FUNCTION RELATIONSHIPS IN AN ANTENNA PROTEIN OF PHOTOSYSTEM II. ((Julio de Paula[1], Sarina Hinsley[1], Ann Liefshitz[1], Wei Lin[1], Scott Betts[2], Charles Yocum[2], and Scott Williams[3])) [1]Department of Chemistry, Haverford College, Haverford, PA 19041; [2]Department of Biology, The University of Michigan, Ann Arbor, MI 48109; and [3]Regional Laser and Biotechnology Laboratory, The University of Pennsylvania, Philadelphia, PA 19104.

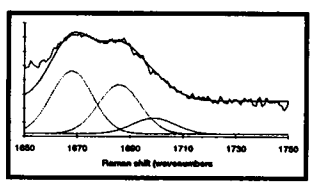

The chlorophyll *a* (Chl) molecules bound to the 47 kDa antenna protein from photosystem II were studied by resonance Raman spectroscopy at 441.6 nm. We observed three populations of Chl, which were distinguished by the extent to which the C_9=O group of Chl interacts with the medium (see figure). We will show that these interactions modulate the energies of π-π^* transitions and, consequently, the roles of Chl in energy transfer. The Chl fluorescence decay in the 47 kDa protein was fitted with three exponentials (lifetimes of ~200 ps, ~2.5 ns, and ~4.5 ns). The fluorescence data are, thus, also indicative of three functionally distinct populations of Chl bound to the protein. A kinetic model will be presented whose aim is to correlate the Raman and fluorescence data. *Supported by ACS-PRF and Research Corporation.*

Tu-PM-M3

NEW INSIGHT INTO THE RELATIONSHIP OF CHLOROPHYLL *a* FLUORESCENCE YIELD TO THE CONCENTRATION OF ITS QUENCHERS Q_A AND $P680^+$.

((V.Shinkarev and Govindjee)) Dep. of Physiol. and Biophys. UIUC, Urbana, IL 61801

Both the oxidized primary quinone, Q_A, and the oxidized primary donor, $P680^+$ (for short, P^+), are known to be quenchers of chlorophyll *a* fluorescence yield (ϕf) of photosystem II (PSII) of photosynthesis. Thus, it is usually assumed that $[PQ_A^-]$ controls ϕf of PSII. The ratios of the ϕf of PSII, induced by alternate flashes, were measured in spinach thylakoids as a function of time, at pH 6. The observed time dependence of the ratio of ϕf after flash 3 to that after flash 1 (or flash 5) can be explained if we suggest $1/\phi f \propto a\cdot[PQ_A^-] + b\cdot[P^+] + c$, where a, b and c - are constants. However, these data cannot be explained by $\phi f \propto [PQ_A^-]$. We thank NSF (91-16838) for support.

Tu-PM-M4

ULTRAFAST SPECTROSCOPY OF THE PRIMARY ELECTRON AND ENERGY TRANSFER PROCESSES IN THE REACTION CENTER OF PHOTOSYSTEM II.

(A.R. Holzwarth, M. Hucke, G. Gatzen, G. Schweitzer and K. Griebenow) Max-Planck-Institut für Strahlenchemie, D-4330 Mülheim a.d. Ruhr, Germany

The reaction center of photosystem II from higher plants has been isolated in 1987. It is composed of the D1-D2-cyt-b559 complex containing 4-6 chlorophyll a, 2 pheophytin a and cytochrome b559. The nature and kinetics of the primary processes in this reaction center particle have been discussed controversially recently. It is not clear whether the primary charge separation occurs within a time of 3 ps or about 20 ps. Both of these possibilities have been proposed based upon ultrafast spectroscopic studies by different groups. We present new data from both femtosecond transient absorption and from picosecond fluorescence kinetics in order to further elucidate the kinetics of energy transfer and the primary charge separation. New insight can be obtained by varying the excitation wavelength and the temperature in the experiments. The data have been analyzed by global target analysis and various possible kinetic models will be discussed.

Tu-PM-M5

RECOMBINATION DYNAMICS OF THE RADICAL PAIR P^+H^- IN PHOTOSYSTEM II, M. Gilbert, G. Rousseau, M. Richter, A. Ogrodnik, M. Volk and M.E. Michel-Beyerle, Institut für Physikalische und Theoretische Chemie, Technische Universität München, 8046 Garching (Germany)

$D_1D_2Cytb_{559}$ reaction centers (RCs) of Photosystem II in *Spinacia oleracea* were prepared according to the procedures of [1] with slight modifications. Since these RCs lack quinone, the radical pair P^+H^- (P: primary donor, H: pheophytin) recombines on the ns timescale either to the groundstate P with the rate k_S or, after hyperfine induced singlet-triplet-mixing (STM), to the triplet state $^3P^*$ with k_T, as in RCs of purple bacteria. An external magnetic field hinders STM, thus reducing the yield Φ_T of $^3P^*$ and slowing the recombination of P^+H^-. At low temperature (90K) the absorbance bleaching at 681nm and 544nm was measured at times between 1ns and 10ms. The magnetic field dependent recovery of the absorbance mirroring the recombination of P^+H^- is consistent with previous results obtained at 820nm [2]. Due to the higher S/N ratio of our experiments the determination of k_S and k_T became possible. The effective lifetime τ_{RP} of P^+H^- was ≃100ns (0G) and ≃200ns (700G). The deviations from monoexponentiality observed arise from the statistical orientation of the nuclear spins causing STM and sample heterogeneities. From the magnetic field dependence of τ_{RP} and Φ_T the rate $k_S \simeq 0.002\text{-}0.005 ns^{-1}$ can be deduced. This is smaller than in bacterial RCs (≃0.015) [3]. The difference probably reflects the larger free energy gap between P^+H^- and PH. Due to lifetime broadening of the radical pair levels Φ_T decreases with increasing magnetic field with a halfwidth of 270G. From this width the value of k_T can be estimated to be $3\text{-}5 ns^{-1}$, which is larger than the value observed in bacterial RCs ($0.5\text{-}2 ns^{-1}$) [3].

[1] McTavish et al. (1989) Plant Phys. 89, 452; Chapman et al. (1988) Biochim. Biophys Acta 933, 423; [2] Hansson et al. Current Res. in Photosyn. (ed. Baltscheffsky), Kluwer 1990; [3] Ogrodnik et al. (1988) Biochim. Biophys. Acta 936, 361.

Tu-PM-M6

ELECTRIC FIELD INDUCED DECREASE OF QUANTUM YIELD OF CHARGE SEPARATION IN PHOTOSYNTHETIC REACTION CENTERS

T. Langenbacher, G. Bieser, U. Eberl, M. Volk, A. Ogrodnik and M.E. Michel-Beyerle, Institut für Physikalische und Theoretische Chemie, Technische Universität München, 8046 Garching (Germany)

Electric field effects on light induced absorption changes have been detected on the picosecond time scale at 90K in reaction centers from *Rb. sphaeroides* isotropically embedded in polyvinylalcohol films. Various cofactors have been probed, i.e. the ground state absorption of the special pair P (850-880nm), the bacteriopheophytins at the A- and B-branch in their Q_x transitions, H_A (545nm) and H_B (533nm), the bacteriochlorophylls in their Q_y transitions, B_A and B_B (780-815nm), and the broad absorption of P^+ and $^1P^*$ at 558nm. Upon application of a field of $7\cdot10^6$V/cm the signal at 545nm decreases by 11% within 30ps after excitation revealing a corresponding reduction of the quantum efficiency of $P^+H_A^-$ formation. An analogous electric field effect on the absorption of P (870nm) is not observed immediately after excitation, but develops with a time constant of ≃900ps. We conclude that the loss channel leads to an intermediate state involving an excited form of P (P^* or P^+) the decay of which is reflected in the ground state recovery with the measured lifetime of ≃900ps. Field induced formation of $P^+H_B^-$ is excluded by the observation that the decrease of the bleaching at 545nm is not accompanied by a corresponding increase of bleaching at 533nm. Immediately after excitation a field effect was also detected around 780nm (indicating a change in the electrochromic blueshift of the 800nm band due to a change in $P^+H_A^-$), while a field induced recovery of the bacteriochlorophyll absorption with a time constant ≃900ps was observed between 808nm and 815nm. This rules out formation of a long living form of $^1P^*$ as possible intermediate. Instead, indication for field induced formation of $P^+B_B^-$ is given. The alternative formation of $P^+B_A^-$ with slow recombination to the groundstate in the electric field is rather unlikely.

Tu-PM-M7

Photosynthetic Water Oxidation: the Reactivity of the Tetramanganese Cluster and Its Mn Electronic Configurations

Ming Zheng and G. C. Dismukes
Princeton University, Henry H. Hoyt Laboratory, Princeton, NJ 08544

Photosynthetic water oxidation and concomitant oxygen evolution in higher plants is one of the most fundamental reactions on the earth. It is carried out by a tetramanganese cluster through a mechanism which is not well understood. This can be judged by the fact that no synthetic Mn cluster has been characterized which is capable of oxidizing water. The unusual reactivity of the Mn tetramer adopted by Nature must center around its ability to activate two bound water molecules(H_2O, OH^- or O^{2-}) for O-O bond formation. This chemistry depends critically on the Mn-O bonding and hence on the electronic structure of Mn. Our recent EPR results have shown that the Mn tetramer possesses Mn(III) ions which exhibit the extremely rare $d_\pi^3 d_{x2\text{-}y2}^1$ configuration in which the oxo ligand atoms are directed at the antibonding $d_{x2\text{-}y2}$ orbital, in contrast to nearly all oxo bridged Mn clusters which possess the $d_\pi^3 d_{z2}^1$ configuration at Mn(III). We have recently identified a synthetic $Mn_2(\mu\text{-}O)_2$ dimer which has biologically relevant ligands(acetate) and the $d_\pi^3 d_{x2\text{-}y2}^1$ configuration. Its physical characterization, chemical reactivity and implications for water oxidation will be presented.

NIH GM-39932

Tu-PM-M8

PHOTOSYNTHETIC MITOCHONDRIA : INTEGRATION OF A LIGHT-DRIVEN PROTON PUMP INTO MITOCHONDRIAL INNER MEMBRANE

((Astrid Hoffmann, Volker Hildebrandt and Georg Büldt))
Freie Universität Berlin, Dept. of Physics, Biophysics Group, Arnimallee 14, W-1000 Berlin 33, Germany

The functional genetic transfer of the light-driven proton pump bacteriorhodopsin (BR) into the mitochondrial inner membrane of yeast, *Schizosaccharomyces pombe*, was successfully acheaved. Thus it is possible to replace or to increase the proton gradient usually formed by the respiratory chain. To target BR to the mitochondrial inner membrane signal-sequences of proteins, naturally located in this membrane, were fused to the N-terminal end of the gene of bacterio-opsin. Expression products were regenerated to BR by addition of retinal to the culture medium. Immunogold-labelling experiments revealed that BR was incorporated into mitochondrial membranes. Western-blot-analysis of purified mitochondria also indicated that BR was transported into these organelles, where it was processed releasing the signal-peptid. Protease digestion studies on mitoplasts give evidence that BR is incorporated into the mitochodrial inner membrane with the processed N-terminus exposed to the intermembrane space and the C-terminus towards the matrix. The pH sensitive dye BCECF was used to monitor the increase of pH in the matrix of isolated mitochodria when protons are translocated over the mitochodrial inner membrane after light excitation. Under anaerobic conditions, glucose uptake of *S.pombe* cells, containing BR in the mitochondrial inner membrane, was decreased after light excitation. This indicates that these cells use BR as an additional pump producing a light-induced proton gradient for ATP synthesis.

Tu-PM-M9

SPECTRAL HOLE BURNING AS A PROBE OF AMORPHOUS DISORDER IN THE PRIMARY ELECTRON TRANSFER OF BACTERIAL REACTION CENTERS

Stephen V. Kolaczkowski, Paul A. Lyle and Gerald J. Small Ames Laboratory USDOE and Department of Chemistry, Iowa State University, Ames, Iowa 50011

The mechanism of the primary electron transfer (PET) in bacterial reaction centers continues to be the focus of significant debate. Experimental evidence currently supports both the single-step and two-step ET models to form P^+BH^- as the primary charge separated state. Complicating this issue are the repeated observations of non-exponential electron transfer rates for $P870^*$. These observations have pointed towards the possibility of structural heterogeneity as the source of the non-exponential PET rates. Hole burning studies have identified a 120-150 cm^{-1} inhomogeneous width, Γ_i, of P870 that describes the energy range, i.e. degree of heterogeneity, of the protein induced substates. Γ_i, when used solely as a measure of the range of energy gaps between $P870^*$ and P^+BH^- is unable to account for the non-exponential PET rates.[1] This result raises the question of a range of electronic coupling matrix element values, V; ($k=4\pi^2/h|V|^2FC$), as the source of the non-exponential PET rates. The variation and correlation of the V-values to Γ_i is obtained from the PET rate, measured as ZPH width/2; γ (cm^{-1})= $(2\pi c)^{-1}$, over Γ_i. The data presented for four burn energies (ω_b) indicate no difference in the PET rates or V-values across Γ_i and will be the topic of discussion. (1) Small, G. J. *et al., J. Phys. Chem.* 1992, 96, 7499.

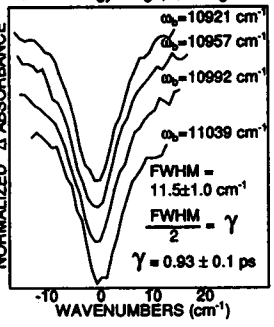

VISUAL RECEPTORS II

Tu-PM-N1

A NOVEL SUBUNIT OF THE CYCLIC NUCLEOTIDE-GATED CATION CHANNEL IN RETINAL RODS. ((T.-Y. Chen, Y.-W. Peng, R.S. Dhallan, B. Ahamed, R.R. Reed and K.-W. Yau)) Howard Hughes Med. Inst. and Depts. of Neurosci., Biomed. Eng., and Mol. Biol. and Genetics, Johns Hopkins Univ. Sch. of Med., Baltimore, MD 21205.

The cGMP-gated cation channel mediating phototransduction in retinal rods has been purified from bovine retina and molecularly cloned; when expressed in Xenopus oocytes the cloned protein gives ion channels that are activated by cGMP (Kaupp et al., Nature 342, 762, 1989). These findings have prompted a notion that the native cGMP-gated channel is perhaps a homo-oligomer. We have very recently cloned the human homolog of the bovine protein which likewise forms cGMP-gated channels by itself. We now report, however, the molecular cloning of another protein from human retina that shows only about 30% overall identity to the rod channel subunit. This protein does not form functional channels by itself, but when co-expressed with the rod channel clone in a cell line it introduces rapid flickers to the channel openings that are highly characteristic of the native channel. Furthermore, the hetero-oligomeric channel shows a high sensitivity to the blocker L-cis-diltiazem much like the native channel. Finally, immunocytochemistry with a peptide antibody has located this protein to all rod outer segments in the human retina. Thus, this new protein appears to be another subunit of the native rod channel and it imparts a specific functional property to the latter. That the rod channel is a hetero-oligomer also means that it is no exception to a common motif shared by other known ligand-gated channels.

Tu-PM-N2

MONO- AND DIVALENT CATION SELECTIVITY OF CATFISH CONE OUTER SEGMENT cGMP-GATED CHANNELS. ((L.W. HAYNES)) Department of Medical Physiology and Neuroscience Research Group, University of Calgary, Calgary, Alberta, Canada.

The cGMP-gated channels of cone and rod photoreceptors have different single-channel conductances and patterns of rectification, suggesting that there must be differences in cation permeation in the two types of channels. Inside-out patches were excised from channel catfish (*Ictalurus punctatus*) cone outer segments and current-voltage relations under bilonic conditions were obtained by applying paired ±120 mV s^{-1} ramps. The resulting currents at each voltage were averaged to reduce capacitive artifacts. Net currents were obtained by subtracting the averaged currents before and after cGMP from the currents with cGMP. For monovalent cations, the pipet contained (in mM): 120 NaCl, 0.1 NaEGTA, 0.1 NaEDTA, 5.0 NaHEPES (pH 7.6). The bath contained the corresponding NH_4, Na, Li, K, Rb or Cs salts with the addition of 1 mM cGMP free acid when required. The permeability ratios followed the sequence NH_4 > Li = K > Na > Rb > Cs (2.2 : 1.12, 1.12 : 1 : 0.94 : 0.73) while the conductance ratios at +50 mV followed the sequence Na > NH_4 > K > Rb > Li > Cs (1 : 0.87 : 0.80 : 0.61 : 0.40 : 0.33). Organic monovalent cations (TMA, TEA, TPrA, TBuA, TPeA, choline, guanidine) showed no measurable permeability, but substantially reduced inward Na current. For divalent cations, the pipet contained (in mM): 40 $CaCl_2$, 5.0 CaHEPES (pH 7.6). The bath contained the corresponding Ca, Mg or Ba salts with the addition of 1 mM cGMP free acid when required. The current-voltage relations showed the typical rectification observed under physiological conditions (an exponential increase in current at both positive and negative voltages). The permeability ratios were Ca > Ba > Mg (1 : 0.74 : 0.63), but the conductance ratios at +60 mV were in the order of Ca > Mg >> Ba (1 : 0.74 : 0.1). Relative to Na, the permeabilities were Ca > Ba > Mg > Na (70 : 32 : 15 : 1) with conductance ratios at +50 mV in the order of Na >> Ca = Mg > Ba (1 : 0.01, 0.01 : 0.009). [Supported by the MRC of Canada and Alberta Heritage Foundation for Medical Research].

Tu-PM-N3

IN RETINAL RODS, MEMBRANE DEPOLARIZATION IN DARKNESS REDUCES THE cGMP-DEPENDENT CONDUCTANCE: IMPLICATIONS FOR Ca-DEPENDENT REGULATION OF PDE. Juan I. Korenbrot and James L. Miller, Department of Physiology, University of California, San Francisco, CA 94143-0444.

We measured outer segment currents under voltage-clamp in both intact cells and in detached outer segments of rods isolated from tiger salamander or catfish retinas. In darkness, steps changes in voltage from a holding value of -30 mV to voltages more positive than +20 mV generated an outward current that inactivated with an exponential time course and reached a steady-state value in 8 to 10 secs. This dark, voltage-inactivated current, DVIC, was entirely suppressed by light, and its current-voltage characteristics and reversal potential were the same as those of the light-sensitive currents. DVIC, therefore, arises from the closure in darkness of the light-sensitive, cGMP-gated channels of the rod outer segment. The Ca buffer BAPTA, loaded into the cytoplasm of the rod outer segment, strongly attenuates or blocks DVIC. We propose that DVIC arises from a voltage-dependent decrease in cytoplasmic Ca concentration that results in a net reduction in outer segment cGMP. In rods, cytoplasmic Ca concentration can be continuously calculated from the balance between passive Ca influx via the cGMP-gated channel and its active efflux via a Na/Ca,K exchanger. Membrane depolarization should result in a decrease in influx of Ca and, therefore, a decrease in its cytoplasmic concentration. Since decreased Ca concentration is known to activate guanylate cyclase, the observed reduction in outer segment current in the presence of an increased rate of cGMP synthesis suggests that lowering cytoplasmic Ca also leads to increased PDE activity. Moreover, the increase in PDE activity is sufficient to overcome the Ca-dependent activation of cyclase and generates a net reduction of cGMP in the outer segment. This finding stands in strong contrast to results in cones (Miller and Korenbrot, Biophys Soc. Abstr., 1993) and suggests that a profound difference between rods and cones lies in the features of the regulation by Ca of PDE activity.

Tu-PM-N4

IN RETINAL CONES, MEMBRANE DEPOLARIZATION IN DARKNESS ACTIVATES THE cGMP-DEPENDENT CURRENT: IMPLICATIONS FOR CA HOMEOSTASIS. James L. Miller and Juan I. Korenbrot, Department of Physiology, University of California, San Francisco, CA 94143-0444.

We measured currents under voltage-clamp in solitary, single cone photoreceptors isolated from the retina of striped bass. In darkness, changes in membrane voltage to values more positive than 10 mV activate a time- and voltage-dependent outward current in the outer segment. This dark, voltage-activated current, DVAC, increases in amplitude with a sigmoidal time course up to a steady-state value, reached in 0.75 to 1.5 s. DVAC is entirely suppressed by light, and its current-voltage characteristics and reversal potential are the same as those of the light-sensitive currents. DVAC, therefore, arises from the activation by voltage in the dark of the light-sensitive, cGMP-gated channels of the cone outer segment. Since these channels are not directly gated by voltage, we explain DVAC as arising from a voltage-dependent decrease in cytoplasmic Ca concentration that, in turn, activates the enzymes that regulate cytoplasmic cGMP concentration and results in net synthesis of the nucleotide. This explanation is supported by the finding that the Ca buffer BAPTA, loaded into the cytoplasm of the cone outer segment, strongly attenuates or blocks DVAC. We develop a quantitative model that assumes cytoplasmic Ca concentration can be continuously calculated from the balance between passive Ca influx via the cGMP-gated channel and its active efflux via a Na/Ca,K exchanger and that further presumes guanylate cyclase is activated by decreasing cytoplasmic Ca concentration. DVAC is well simulated by assuming that the Ca flux through the cGMP-gated channel does not obey the independence principle and that the Ca dependence of guanylate cyclase in cones, previously untested, is quantitatively identical to that described for rods in the literature. The specific Ca conductance of the cGMP-gated channel at voltages between +30 and +60 mV is predicted to be 4- to 8-fold larger than expected from the independence principle.

Tu-PM-N5

A NON-EFFECTOR ACTIVATOR OF TRANSDUCIN GTPASE IN BOVINE ROD OUTER SEGMENTS ((Joseph K. Angleson, and Theodore G. Wensel*)) Verna & Marrs McLean Department of Biochemistry, Baylor College of Medicine, Houston, Texas.

The slow (tens of seconds) hydrolysis of GTP by transducin under single turnover conditions in dilute bovine rod outer segments (ROS) is accelerated dramatically when the concentration of ROS is increased, as reported previously [Arshavsky, V. Yu. *et al.*, (1989) *FEBS Lett.* 250:353-356; Dratz, E. A. *et al.* (1987) *Biochem. Biophys. Res. Comm.* 146: 379-386]. We have found that the first order rate constants for hydrolysis of GTP and for GTPase-dependent inactivation of transducin's effector, cGMP phosphodiesterase (PDE), both increase 4- to 6-fold when the ROS concentration is increased from 4 μM to 50 μM rhodopsin. This effect is not mimiced by PDE or by its inhibitory subunit, PDE_γ, in either the presence or absence of cGMP. PDE_γ, but not holo-PDE, does increase the rate at which PDE inactivates after transducin activation, but this inhibitory effect is not correlated with GTP hydrolysis and does not depend on it. Very little, if any, effect on transducin GTPase was observed using either native PDEγ isolated from rod outer segments, or a recombinant fusion protein form of PDEγ. The inhibitory effect of PDE_γ is cumulative with successive additions of sub-stoichiometric GTP, suggesting that the extra PDE_γ may induce formation of a "refractory" form of transducin. PDE_γ accelerates PDE inactivation even at concentrations of ROS sufficient to saturate the GTPase effect. These results indicate that bovine ROS contain a GTPase activating, or "GAP"-like activity, but that this activity is not due to PDE_γ.

Tu-PM-N6

PDE*/R* GAIN IN RETINAL ROD LIGHT ADAPTATION. ((D.R. Pepperberg[1], J. Jin[2], and G.J. Jones[2])) [1]Dept. of Ophthalmol. & Visual Sciences, Univ. of Illinois, Chicago, IL 60612; and [2]Dept. of Physiology, Boston Univ. School of Medicine, Boston, MA 02118.

Background light shortens the periods of photocurrent saturation induced by bright flashes. This effect cannot be mediated by an increase in guanylate cyclase activity (cyc*), as cyc* is expected to be maximal during saturation. We have measured the background-dependence of the saturation period (T) and present a new model of adaptation based on the data obtained. We find that light- and dark-adapted responses to weak flashes are linked in simple fashion through a gain parameter, $\phi = \exp(-\Delta T/\tau)$, where τ is the slope of the line relating T and ln flash intensity ($\ln I_f$), and ΔT is the background-induced change in T at fixed I_f (ref. 1). This finding is readily explained in terms of a reduced efficiency with which photoactivated rhodopsin (R*) generates activated cGMP phosphodiesterase (PDE*). The results suggest that a decrease in PDE*/R* gain is the primary mechanism of rod light adaptation, i.e., that "cyc* feedback" operates within the framework of a sensitivity level established within the R*⟶PDE* chain of reactions. Supported by grants EY05494, EY-01792, and EY01157. (1) Visual Neurosci. 8:9 (1992).

Tu-PM-N7

A SINGLE CLASS OF LIGHT-ACTIVATED CHANNEL CAN YIELD BIPHASIC LIGHT-INDUCED CURRENTS AT E_{REV} ((Peter M. O'Day[1], Edwin C. Johnson[2], & Stephany Freeman[1])) [1]Institute of Neuroscience, University of Oregon; and [2]SIBIA Inc., La Jolla, CA.

It has been proposed that there are two or more classes of light-activated channel in invertebrate photoreceptors, since light-induced currents recorded under voltage-clamp possess complicated waveforms. In particular, the currents near reversal potential of the light response (E_{hv}) can be biphasic (*i.e.* outward-to-inward, or vice-versa).

We have rejected this logic using a theoretical approach, analyzing data from *Limulus* and *Drosophila*. Although multiple classes of channel are possible, the data are consistent with the more parsimonious notion of a single class. Biphasic currents can result from alteration of E_{hv} during the response itself due to modulation of the following currents.

1. ***Na^+/Ca^2 exchange currents***, I_X, are activated quickly as a result of light-induced elevation of $[Ca_i^{2+}]$. They vary with membrane voltage, V_m, reversing at $E_X = nE_{Na} - 2E_{Ca}$, which changes constantly during illumination as $[Ca_i^{2+}]$ changes. Since $E_X \neq E_{hv}$, I_X can be much larger than light-activated channel currents, I_{hv}, which are small when $V_m \approx E_{hv}$. Simulations yield biphasic net light-induced currents (I_X+I_{hv}) when $V_m \approx E_{hv}$.
2. ***Light-activated channel currents***, I_{hv}, if they are carried by both Na^+ and Ca^{2+}, should be complex, due to unequal shifts in E_{Na} and E_{Ca} as $[Ca_i^{2+}]$ rises. Simulations yield biphasic I_{hv} when $V_m \approx E_{hv}$.
3. ***Voltage-gated channel currents***, I_K^V and I_{Ca}^V, are inhibited by light-induced $[Ca_i^{2+}]$-elevation; this can result in biphasic net currents when $V_m \approx E_{hv}$ if these channels are active during excitation.

In these three cases the biphasic nature of the net current is intensity- and $[Ca_i^{2+}]$-dependent, consistent with observation. We conclude that bright flashes should induce biphasic currents near E_{hv} in a Ca^{2+}-dependent fashion, even if only a single class of light-activated channel exists.

MUSCLE REGULATORY PROTEINS

Tu-Pos1

FUNCTIONAL SIGNIFICANCE OF THE N-TERMINAL HELIX OF TROPONIN C. ((L. Smith, N. Greenfield, and S.E. Hitchcock-DeGregori)) Dept. of Neuroscience and Cell Biology, Robert Wood Johnson Medical School, Piscataway, NJ 08854. (Spon. by S.M. Shea)

Troponin C is a calcium binding protein that is homologous to calmodulin. One difference is that TnC has a 14 residue helix at the N-terminus that is absent in calmodulin. To investigate the importance of the N-terminal helix, we deleted res. 1-15 (ASMTDQQAEARAFLS, Δ15) using site-directed mutagenesis. The biophysical properties of Δ15 were analyzed using circular dichroism. The results showed that the far-UV spectrum in the presence of divalent cations was very similiar to that reported for TnC isolated from muscle, displaying a large increase in α-helix in the Ca^{2+} or Mg^{2+} bound forms. The thermal denaturation profile, however, was significantly different. The T_m of Δ15 was 20 °C lower than wildtype TnC when 0, 2, or 4 sites were occupied by divalent cations. To determine the function of the mutant, we assayed its ability to relieve troponin IT inhibition of the actomyosin ATPase in the presence of Ca^{2+}. Δ15 relieved inhibition only to 20-35% of the wildtype level, even at very high concentrations. That is, the mutant is defective in switching the thin filament from the relaxed to the active state. These results are the first to demonstrate the possible significance of the N-helix in TnC, suggesting that it is important for stability and may play a vital role in the Ca^{2+} switching mechanism. Supported by NIH.

Tu-Pos2

FUNCTIONAL CONSEQUENCES OF INSERTIONS IN AND DELETION OF THE TROPONIN C CENTRAL HELIX. ((S.Ramakrishnan and S.E. Hitchcock-DeGregori)) Dept. of Neuroscience and Cell Biology, UMDNJ-Robert Wood Johnson Medical School, Piscataway, NJ 08854. (Spon. by J. Lenard)

To investigate the role of the troponin C central helix, a series of insertion and deletion mutants were constructed and the purified proteins expressed in *E.coli* were studied. In one deletion mutant the entire central helix region (^{87}KEDAKGKSEEE^{97}) was removed so that the calcium binding domains sit on top of each other. Qualitative binding assays indicated that this mutant has higher affinity for TnI in the absence of Ca^{2+}, than wild type or other mutants. In addition this mutant partially relieved TnIT inhibition of the actomyosin ATPase in the absence of Ca^{2+}, unlike wild type. Activation in the presence of Ca^{2+} is normal suggesting that the removal of the central helix impairs the switching off of the thin filament. To begin to investigate the importance of length and flexibility of the central helix for TnC function, two insertion mutants were constructed. 1. Length of the helix is increased by two turns by inserting 7 residues with probability of forming α-helix (EELAKSE) between residues 93 and 94. 2. A non-helical insert of 9 residues (GSGKGEGWG) was inserted at the same site. This would make the helix more flexible so that the calcium-binding domains can 'flip' upon each other. Both mutants are deficient in relieving TnIT inhibition of the actomyosin ATPase in the presence of Ca^{2+} (about 50% and 80% of the wild type in the case of 9 and 7 residue insertion respectively). Supported by NIH.

Tu-Pos3

Ca^{2+} AND RIGOR ACTIVATION OF FORCE AND $cTnC_{IAANS}$ FLUORESCENCE FROM A MONOCYSTEIN DERIVATIVE OF CARDIAC TROPONIN IN SKINNED SKELETAL MUSCLE FIBERS.

((W.G.L. Kerrick*#, J.D. Potter*, J.A. Putkey)) Dept of Biochem. and Mol. Biol., Univ. of Texas Med. Sch., Houston, TX 77225, and Depts of *Mol. & Cell. Pharm. and #Physiol. & Biophys., Univ. of Miami. Sch. of Med., Miami, FL 33136.

Skinned rat soleus and rabbit adductor magnus fibers were used to compare changes in $cTnC_{IAANS}$ fluorescence associated with Ca^{2+} or rigor activation of force. Genetically engineered $cTnC_{IAANS}$ used in this study contained a single cysteine located at position 84 in the amino acid sequence and was incorporated into skinned fibers. In rat soleus (slow-twitch muscle) and rabbit adductor magnus (fast twitch muscle) fibers changes in Ca^{2+} activated $cTnC_{IAANS}$ fluorescence showed a close correlation between changes in force and fluorescence as reported for cardiac muscle (Biophys. J. 59:583a,1991). Both muscle fiber types showed an increase in $cTnC_{IAANS}$ fluorescence when the muscles were exposed to rigor conditions in the absence of Ca^{2+} and the fluorescence increased further in the presence of Ca^{2+}. If the muscle fibers were put into the rigor state in the absence of Ca^{2+} by slowly removing ATP from the bathing solution there was three phases of fluorescence changes. The first phase was a small decrease in fluorescence associated with decreasing ATP to a level which began to initiate activation of the fibers. The second phase was an increase in fluorescence associated with activation of force by decreasing ATP concentrations further. The final phase was a slow continuous increase in fluorescence associated with decreasing ATP concentrations to zero while force remained constant or slightly decreased. These results suggest that $cTnC_{IAANS}$ (Cys-84) when incorporated into skinned skeletal muscle fibers detects Ca^{2+} binding to the protein, and different myosin cross-bridge states.

Tu-Pos4

INCORPORATION OF BIOTINYL-TNC INTO TNC-EXTRACTED MYOFIBRILS IS SENSITIVE TO BOTH CALCIUM AND STRONG-BINDING MYOSIN HEADS.

((D.R. Swartz, M.L. Greaser and R.L. Moss)) University of Wisconsin, Madison, WI 53706.

Extraction of TnC from skinned muscle fibers and isolated myofibrils has been used to investigate the role of TnC in thin filament activation; however, the positions of extracted and re-incorporated TnC in the sarcomere are unknown. Experiments have been done to address these questions in myofibrils, and the work is being extended to single skinned fibers. Rabbit skeletal TnC was chemically modified with 3-(N-maleimidyl-propionyl)-biocytin. The ATPase activity of TnC extracted myofibrils at pCa 4.5 showed a dependency on [biotinyl-TnC] (B-TnC) that was similar to unmodified TnC, suggesting that the B-TnC restores normal function. Incorporation of B-TnC into extracted rigor myofibrils was visualized by incubating myofibrils with B-TnC followed by incubation with streptavidin Texas Red and subsequent fluorescence microscopy. Incorportation of B-TnC was Ca^{2+} dependent: greater fluorescence was observed at pCa 4.5 than at pCa 9.0 for all concentrations tested (50μg myofibrils, 10 nM - 100 μM B-TnC). The fluorescence was confined to the region of overlap under these conditions. When saturating levels of myosin S1 were added, fluorescence became greater in the the I-band than the overlap region. This pattern was independent of pCa, but the fluorescence was much greater at pCa 4.5 than at pCa 9.0. These observations suggest that re-incorporation of B-TnC into the TnI-TnT-Tm complex on the actin filament is sensitive to Ca^{2+} and a probable conformational change in this complex induced by rigor or strong-binding myosin heads.

Tu-Pos5

A TIME-RESOLVED FLUORESCENCE STUDY OF TnC SINGLE TRYPTOPHAN MUTANT, F29W.

((I. D. CLARK and A. G. SZABO.)) Institute for Biological Sciences, National Research Council of Canada, Ottawa, Ontario, K1A 0R6.

It was shown that the F29W mutant of TnC prepared by site-directed mutagenesis was useful for spectroscopic studies of metal binding (Pearlstone et al., Biochemistry (1992) 31, 6545-6553). In this study, time-resolved fluorescence measurements were carried out in order to obtain additional information on the protein. After purification, apo F29W was prepared by TCA precipitation and reconstituted in 100mM KCl, 50mM MOPS, pH 7.1. In the apo species, the Trp had three fluorescence lifetime components - 3.82, 1.64 and 0.14ns. Ca^{2+}, Mg^{2+} or Tb^{3+} additions all caused significant changes to the lifetimes and the relative proportions of the pre-exponential terms, and the effect of each metal was unique. The changes upon addition of Mg^{2+}, which binds weakly to sites III and IV in the C-domain, suggested that there was a long range effect on Trp-29, which is adjacent to loop I (30-41) in the N-domain. In the presence of Ca^{2+}, only two fluorescence decay components were observed with decay times of 7.91 and 1.24ns. This indicated that the structure of the N-domain in the presence of Ca^{2+} was significantly different from that of the apo form. When F29W was titrated with Tb^{3+}, the C-domain filled first (Phe112 (site III) or Phe151 (site IV) -> Tb^{3+} energy transfer). There was no significant Trp -> Tb^{3+} energy transfer until Tb^{3+}/F29W ratio was greater than 2. However, at 2:1 the change in Trp fluorescence intensity was approximately 65%, suggesting that Tb^{3+} binding to the C-domain had a long range effect on the N-domain. (The F29W mutant of chicken skeletal TnC used in this study was a kind gift of Dr. L. B. Smillie, Dept. of Biochemistry, University of Alberta, Canada).

Tu-Pos6

ACTIVATION DEPENDENCE OF UNLOADED SHORTENING VELOCITY IN SKINNED SKELETAL MUSCLE FIBERS STUDIED WITH ACTIVATING TROPONIN C.

((D.A. Martyn[1], P.B. Chase[2], and J.D. Hannon[3])) Center for Bioengr.[1], Dept. Radiology[2] and the Dept. Physiol. and Biophys.[3], University of Washington, Seattle, Wa 98195.

The role of Ca^{+2} binding to troponin C (TnC) in the modulation of shortening velocity in skeletal muscle is less understood than its role in the regulation of force. To investigate the effect of Ca^{+2} and thin filament activation on unloaded shortening velocity (V_{us}), we activated single skinned rabbit psoas fibers without Ca^{+2} by replacing endogenous TnC with activating TnC (aTnC; Hannon et al., this volume). For comparison, V_{us} in control fibers with endogenous TnC, had two phases and depended on the level activation, as reported by Moss (J.P. 377, 487-505). Partial activations with aTnC were obtained by either full extraction of endogenous TnC followed by reconstitution with a mixture of aTnC and native cTnC (1:8.5), or partial extraction of endogenous TnC followed by reconstitution with aTnC. Both methods resulted in Ca^{+2}-sensitive and Ca^{+2}-insensitive components of force due to native TnC and aTnC, respectively. When force increased by adding Ca^{+2} or increasing the proportion of aTnC, both phases of V_{us} increased. Endogenous or native cTnC was then selectively extracted, leaving a partial level of activation by only aTnC. The resulting force at pCa 9.2 was 23.4±6.8% of control; the early fast phase of shortening (V_s) was 25.2±6.5% of control and the later slow phase (V_l) was 21.4±4.9%. Corresponding values obtained at pCa 4.0 were 24.1± 7.9% for force, 26.2±7.0 for V_s, and 22.6±5.2% for V_l. Our results indicate that both phases of V_{us} are dependent on the level of thin filament activation in aTnC reconstituted fibers. The results that V_s and V_l are insenstive to calcium in fibers activated with aTnC suggests that Ca^{+2} effects on V_{us} are mediated only through binding to TnC. Supported by grants HL 31962, NS 08384.

Tu-Pos7

CHANGES IN LINEAR DICHROISM OF RHODAMINE PROBES ON TROPONIN-C DURING TENSION DEVELOPMENT OF SKINNED FIBERS ACTIVATED BY PHOTOLYSIS OF CAGED Ca^{2+}

((T.StC. Allen, R.J. Barsotti, G.C.R. Ellis-Davies, J.H. Kaplan, Y.E. Goldman, D.A. Martyn*, and A.M. Gordon*)) U. of Penn., Phila. PA 19104, and *U. of Wa., Seattle, WA 98195

Structural changes in Troponin-C (TnC) induced by Ca^{2+} binding and by cross-bridge attachment were studied in glycerinated single fibers from rabbit psoas muscle. TnC labelled at Cys-98 with tetramethyl rhodamine was exchanged for the native TnC, and the fibers were activated by photolysis of DM-nitrophen, a caged Ca^{2+}. Linear dichroism was measured with a 3 kHz bandwidth (Tanner et al., *J. Mol. Biol.* 223:185-203, 1992). When the fiber was changed from relaxing solution (1 nM free Ca^{2+}; 50 μM free Mg^{2+}) to pre-photolysis solution (0.25 μM free Ca^{2+}; 50 μM free Mg^{2+}), dichroism decreased from 0.013 ± 0.001 (±s.e.m., n=5) to 0.006 ± 0.002, a change attributable to exchange of Ca^{2+} for Mg^{2+} at the high-affinity binding sites. Following photolysis ($[Ca^{2+}]_{free}$ ≈10 μM, absence of phosphate, P_i), dichroism reversed to -0.005 ± 0.002 ($t_{1/2}$<1 ms) and then partially recovered with a time course similar to tension development. In the presence of 20 mM P_i, as well as in fibers stretched to sarcomere lengths of 3.6-4.0 μm, the developed tension and the recovery phase of the dichroism signal were suppressed. Steady state experiments corroborated that P_i enhances the change in dichroism following activation. The early reversal of the dichroism signal is much faster than tension development, and thus the corresponding Ca^{2+}-induced structural change in TnC does not limit the rate of tension development. Supported by the MDA & NIH.

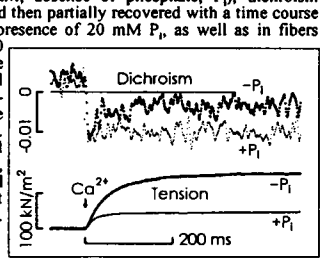

Tu-Pos8

CALCIUM-INDEPENDENT ACTIVATION OF SKELETAL MUSCLE FIBERS BY A MODIFIED FORM OF CARDIAC TROPONIN C.

((J.D. Hannon[1], P.B. Chase[2], D.A. Martyn[3], L.L. Huntsman[3], A.M. Gordon[1] and M.J. Kushmerick[1,2,3])) Dept. Physiol and Biophys.[1], Dept. Radiology[2], and the Center for Bioengr.[3], University of Washington, Seattle, Wa 98195.

We replaced endogenous troponin C (TnC) in single skinned rabbit psoas muscle fibers with modified cardiac TnC (cTnC) which, unlike native cTnC, contains an intramolecular disulfide bond and activates myofibrillar ATPase without Ca^{+2} (Putkey, J.A., D.G. Dotson and P. Mouawad, 1992, Biophys. J. 61: A281). This activating TnC (aTnC) allows force generation and shortening in skinned fibers in the absence of Ca^{+2}. Sarcomere homogeneity and structural integrity were maintained during continuous activation of fibers by aTnC. When fibers were fully extracted and reconstituted with aTnC, force and unloaded shortening velocity (V_{us}) were the same at pCa 9.2 and 4.0. Force with aTnC, as a fraction of that attained with maximal Ca^{+2} activation (pCa 4.0) prior to extraction, was 0.69 ±0.04 (mean± s.d, n=11 fibers) at pCa 9.2 and 0.71±0.04 (n=11) at pCa 4.0. Similarly with aTnC, V_{us} was 1.50±0.26 FL/sec at pCa 9.2 and 1.50±0.22 FL/sec at pCa 4.0, compared to 2.54±0.35 FL/sec for controls (unextracted, pCa 4.0). The ability of aTnC to activate the fiber in the absence of Ca^{+2} is due to an intramolecular disulfide bond because we could reduce (5 mM DTT) isolated aTnC in the presence of urea, renature it and reconstitute it into fibers, thereby restoring Ca^{+2} sensitivity. However, Ca^{+2} sensitivity was not restored by treatment with DTT when aTnC was already incorporated into fibers. Also, aTnC incorporated into fibers was not extracted by standard extraction conditions. These observations indicate that aTnC is a stable model for structural studies of the activating conformation of TnC, as well as a useful tool for studies on the processes underlying Ca^{+2} activation of striated muscle. Supported by grants HL 31962, NS 08384.

Tu-Pos9

PROPERTIES OF ISOLATED RECOMBINANT N AND C DOMAINS OF CHICKEN TROPONIN C. ((Monica X. Li[1], Murali Chandra[1], Joyce R. Pearlstone[1], K. Racher[2], G. Trigo-Gonzalez[2], Thor Borgford[2], Cyril M. Kay[1] and Lawrence B. Smillie[1])) [1]MRC Group in Protein Structure and Function, Dept. of Biochemistry, Univ. of Alberta, Edmonton, Canada T6G 2H7 and [2]Dept. of Chemistry and Inst. of Molecular Biology and Biochemistry, Simon Fraser University, Burnaby, British Columbia, Canada V5A 1S6

Recombinant N(1-90) and C (89-162) domains of chicken troponin C (TnC) containing either F29, W29, F105 or W105 have been characterized. W29 and W105 serve as fluorescent probes for monitoring the Ca^{2+} induced structural transitions of the N- and C-domains, respectively. The Ca^{2+} fluorescence titration results of F29W/N-domain are in excellent agreement with those obtained for F29W/TnC (Pearlstone *et al.*, Biochemistry 31, 6545-6553 (1992)). Ca^{2+} titration of F105W/C-domain shows slightly higher Ca^{2+} affinity when compared with intact F105W/TnC (Trigo-Gonzalez *et al.*, Biochemistry 31, 7009-7015 (1992)). Far UV CD titrations of both domains agree well with the fluorescence results. Summation of the far UV CD spectra of the two domains agrees with those determined for a 1:1 mix of N- and C-domains and for intact F29W/TnC. By these criteria at least, the structural transitions within each domain are cooperative but there is little evidence for effects of the presence or absence of one domain on the other. We have also examined an N-helix deleted N-domain, F29W (12-87) corresponding to the TRIC fragment of rabbit TnC. Unlike previous reports, we observe significant Ca^{2+} induced structural transitions as monitored by both fluorescence and far UV CD. (Supported by MRC of Canada and the Alberta Heritage Foundation for Medical Research.)

Tu-Pos10

PHOSPHORYLATION OF TROPONIN I AND C-PROTEIN DOES NOT EFFECT SHORTENING VELOCITY IN RAT SINGLE SKINNED CARDIAC MYOCYTES. ((Polly A. Hofmann & John H. Lange, III))
University of Tennessee, Dept of Physiology & Biophysics, Memphis TN 38163

Effects of phosphorylation of myofibrillar proteins with purified cAMP-dependent protein kinase (PKA) on maximum velocity of unloaded shortening (Vmax) and isometric tension were studied in enzymatically isolated, adenosine pretreated, tritonized cardiac myocytes. R-phenylisopropyladenosine (10μM) was present during myocyte enzymatic isolation to antagonize nonspecific activation of the β-adrenergic pathway. Control experiments establish that at submaximum [Ca^{2+}] isometric tension, sarcomere length, and Vmax were identical prior to and after immersing the cell in a pCa 9.0 solution for 30 minutes (Table). Exposure of groups of myocytes to PKA (1 unit PKA, Sigma/μl pCa 9.0 soln, 30 min) in the presence of ATP-P^{32} result in phosphorylation of TnI and C-protein. Consistent with previous findings (Hofmann et al, 1991, Biophys J, 59:586a), single cardiac myocytes exposed to PKA have a decreased Ca^{2+} sensitivity of isometric tension (ΔpCa_{50}=0.17). Vmax, at matched levels of isometric tension, was not significantly affected by PKA exposure (Table). This observation supports the hypothesis that neither troponin I or C-protein phosphorylations are involved in the increased rate of myocardial force development observed upon β-adrenergic stimulation. Supported by NIH.

	CONTROL, n=7		PKA, n=9	
	PRE	POST	PRE	POST
Tension (%)	54.0 ± 1.6	50.0 ± 2.6	41.4 ± 2.0	40.0± 2.3
Sarc Lgth (μm)	2.36 ± 0.04	2.40 ± 0.07	2.35 ± 0.03	2.38 ± 0.03
Vmax (ML/s)	1.77 ± 0.10	2.11 ± 0.18	1.91 ± 0.25	2.17 ± 0.15

Values expressed as $\bar{x}$ ± SEM

Tu-Pos11

EFFECTS OF MUTATIONS IN THE INHIBITORY REGION OF SKELETAL MUSCLE TROPONIN I (STnI) ON ITS BIOLOGICAL ACTIVITY. ((Zelin Sheng, Yan Kong, Bo-Sheng Pan, Todd Miller and James D. Potter)), Department of Molecular & Cellular Pharmacology, University of Miami School of Medicine, Miami, Florida 33101.

To investigate the properties of the proposed inhibitory region (residues 96-116) of STnI, we have created two mutants in this region of rabbit STnI by replacing Lys107-Arg108 with Gln107-Gln108 ($TnI_{Q107-Q108}$) and Val114-Arg115 with Thr114-Gln115 ($TnI_{T114-Q115}$), respectively. Based on peptide studies, these residues have been identified as being crucial for inhibitory activity (Van Eyk and Hodges, 1988, ***J. Biol. Chem. 236:1726***). Both mutants, like wildtype TnI (WTnI), bound to a troponin C affinity column and were eluted with 6 M urea and 2 mM EDTA. In addition, the mutants were able to form ternary complexes with TnT and TnC. $TnI_{T114-Q115}$ was as effective as WTnI and RTnI in inhibiting actin-Tm-S1 ATPase activity, while $TnI_{Q107-Q108}$ was less effective. The inhibition by WTnI and both mutants was fully reversed by TnC in the presence of Ca^{2+}. These results indicate that both mutants retain inhibitory actin binding activity as well as Ca^{2} dependent TnC binding. These findings suggest that the inhibitory region of TnI may be more complicated than previously envisioned. Other mutations in the inhibitory region are being studied. (Supported by NIH AR37701 and AR40727)

Tu-Pos12

THE TWO PROLINE RESIDUES IN THE INHIBITORY SEGMENT OF TROPONIN I (P109,P110) ARE NOT ESSENTIAL FOR THE REGULATORY FUNCTION. ((Z. Grabarek, K. Mabuchi, Y. Mabuchi, J. Gergely and T. Tao))
Department of Muscle Research. Boston Biomedical Research Insitute. Boston, MA

Regulation of contraction in skeletal muscle involves Ca^{2+}-dependent changes in the interaction between TnC and TnI. The key segment in TnI appears to be the stretch comprising residues 96-116 (the CN4 peptide), which interacts with actin or with both globular domains of TnC in the absence and presence of Ca^{2+}, respectively. A distinct feature of the CN4 sequence is the presence of two proline residues at position 109 and 110. We have tested the hypothesis that the Pro-Pro sequence has a functional role of restricting the possible conformations of the CN4 region. We have synthesized mutants of TnI in which one or both prolines were replaced with Gly or Ala. All the mutants retained their ability to bind TnC and were able to confer Ca^{2+}-sensitivity on the ATPase activity of the complex containing actin, tropomyosin, troponin T, TnC and myosin-S1. The complexes containing TnI mutants having Gly in place of one or both Pro, thus having increased conformational flexibility in the inhibitory segment, had significantly higher Ca^{2+}-activated ATPase activity. These results indicate that Pro residues at positions 109,110 in skeletal TnI are not essential for the regulatory function and support the idea that the conformational properties of this segment may be an important factor in the regulatory process.

Tu-Pos13

ALTERATION OF CALCIUM RESPONSIVENESS WITH TnI AND TnC ISOFORM SUBSTITUTION IN SKINNED CARDIAC MUSCLE. ((J.D. Strauss, J.E. Van Eyk, C. Zeugner, and J.C. Rüegg.)) II. Physiologisches Institut, Univ. Heidelberg, Germany

By reversibly extracting troponin I (TnI) and troponin C (TnC) in skinned cardiac muscle with vanadate treatment (Strauss et al., FEBS Letters, in press), we were able to substitute exogenously supplied TnI and TnC for the endogenous proteins. Subsequent to incubation with vanadate, the fibers actively contracted in a vanadate-free solution containing low free Ca^{2+} (pCa ≥ 8), achieving 92.3% ± 3.8 (SEM, N =34) of the force attained in response to high free calcium (pCa = 4.5) prior to vanadate treatment. After incubation with different combinations of skeletal and cardiac isoforms of TnI and TnC, calcium-dependent regulation of force was restored. The degree of "recovery" of calcium-dependence was dependent upon the concentration of the various exogenously supplied troponins in the incubation solutions. Regardless of the isoform, TnI concentration correlated with the degree of inhibition of calcium-independent force. The optimum concentration for inhibition was approximately 150 μM, with an EC_{50} of approximately 50 μM for either isoform. Interestingly, the cooperativity of the force-pCa relation (but not pCa_{50}) was dependent upon the concentration of TnI. The "Hill" coeffecient ranged from less than 2 at low TnI concentrations to more than 3 at higher concentrations. In contrast, restoration of maximum calcium-dependent force was independent of TnC concentration between 50 and 210 μM. The calcium sensitivity of the reconstituted fibers, however, correlated with both the isoform of TnC and concentration of TnC in the bathing solutions. Fibers reconstituted with skeletal TnC were more sensitive than those with cardiac TnC, regardless of the TnI isoform (change in pCa_{50} of approximately 0.5 units). We conclude that the concentration dependence demonstrated reflects the number of functional regulatory units reconstituted while the different calcium sensitivities obtained with TnC isoforms reflect characteristics intrinisic to the proteins. Supported by the grants from AvH and NSF-NATO (JDS) and the DFG (JCR).

Tu-Pos14

A SINGLE AMINO ACID SUBSTITUTION IN THE TnI INHIBITORY PEPTIDE (104-115) ALTERS ITS EFFECTS IN PEPTIDE RECONSTITUTED TnI-DEPLETED SKINNED CARDIAC MUSCLE. ((J.E. Van Eyk[a,b], J.D. Strauss[a], R.S. Hodges[b], and J.C. Rüegg[a])) [a]II. Physiologisches Institüt, Univ. Heidelberg, Germany and [b]Dept. of Biochemistry, Univ. of Alberta, Edmonton, Canada T6G 2H7

Using a new method for reversibly extracting TnI and TnC in skinned cardiac muscle (Strauss *et al.*, FEBS Lett. (1992), in press), we found that the synthetic TnI peptide, residues 104-115, is sufficient to substitute for the native TnI protein in the Ca^{2+}-dependent regulation of contraction in Triton X-100 skinned porcine trabecular fibers. Incubation with TnI 104-115 produced a dose dependent inhibition of Ca^{2+}-independent force displayed by the TnI/TnC extracted fibers (maximum inhibition of 75% at 100 μM). Only after subsequent incubation with TnC did the fibers become Ca^{2+}-dependent. The isometric tension cost (ATPase/Force) in these reconstituted fibers was similar to that in control fibers. In contrast, a peptide with a single substitution of Gly for Lys 111 (Gly 111) produced 55% inhibition at 200 μM, indicating a decrease in the potency of the substituted peptide. Unlike TnI 104-115, the effect of the Gly 111 peptide was sensitive to the concentration of Pi, becoming less potent as the Pi concentration was increased. The fibers reconstituted with Gly 111-TnC had a less economical tension cost relationship than fibers reconstituted with TnI 104-115. In addition, the TnC isoform used in the reconstitution modified this relationship. We interpret these data to mean that this single amino acid substitution alters the way in which this region of TnI affects crossbridge kinetics, both alone and in combination with other effectors.

Tu-Pos15

SITE DIRECTED MUTAGENESIS OF CLONED SKELETAL TnI AND SUBSTITUTION FOR NATIVE TnI IN SKINNED CARDIAC MUSCLE.

((J.D. Strauss[a], L. Kluwe[b], J.E. Van Eyk[a], Y. Maéda[b], J.C. Rüegg[a], and R.J. Wiesner[a])) [a]II. Physiologisches Institut, Univ. Heidelberg, Germany and [b]European Molecular Biology Laboratory, Hamburg Outstation, Germany

Rabbit skeletal muscle TnI was cloned and expressed using an M13 phage vector and a high yield pTrc expression plasmid, respectively, in E. coli. We have introduced point mutations by standard methods into the protein sequence of the minimal common TnC/actin binding site (TnI 104-115, -G^{104}-K-F-K-R-P-P-L-R-R-V-R^{115}-). Four mutant TnI's were produced by substitution of: T for P^{110}, G for P^{110}, G for L^{111}, and G for K^{105}. The mutations chosen were based on previous work using small synthetic polypeptides which demonstrated that single amino acid substitution can profoundly influence the activities of these peptides in inhibiting ATPase activity in acto-S1 preparations and contraction in skinned fibers. After extensive sonication and Triton X-100 extraction of bacterial pellets from 1 liter cultures, the precipitate was dissolved in a buffer containing 6 M guanidine thiocyanate, pH 8.5. Dialysis against 20 mM Tris (pH 7.4) and 100 mM NaCl yielded a soluble protein fraction (100-150 mg) which was ≥85% TnI (identified by immunoblots) as determined by densitometry of coomassie blue-stained polyacrylamide gels. The wild type, E. coli-expressed TnI substituted for endogenous TnI in cardiac fibers from which TnI and TnC had been extracted (and thus were made Ca^{2+}-independent) by vanadate treatment. At pCa ≥ 8, tension was inhibited by an average of 57.7% ± 7.0 (± SEM, n=7) by the wild type protein at a bathing concentration of approximately 75 μM, comparable with the inhibition achieved with native rabbit skeletal TnI (69.6% ± 4.8, n=8) or with bovine cardiac TnI (64.2% ± 2.1%, n=8) at similar concentrations (50-100 μM). When used in combination with purified TnC, calcium-dependence of the fiber was restored, demonstrating a functional reconstitution of the calcium regulatory system. The mutated TnI's were also able to substitute in the troponin regulatory complex, but to differing degrees of potency and effectiveness. Supported in part by grants from the NSF-NATO (JDS), DFG (JCR, RJW), and AvH (LK).

Tu-Pos16

THE TNC BINDING SITE DOES NOT COINCIDE WITH THE ACTIN BINDING SITE IN THE INHIBITORY SEGMENT OF TNI (RESIDUES 96-116).

((Z. Grabarek, E. Gowell, J. Gergely and P.C. Leavis)) Dept. Muscle Res., Boston Biomed. Res. Inst., Boston, MA 02114.

A cyanogen bromide peptide derived from residues 96-116 of skeletal muscle troponin I (CN4) binds to both troponin C (TnC) and actin (Syska et al *Biochem. J.*, 153; 375, 1976). Talbot & Hodges, (*J. Biol. Chem.* 256; 2798, 1981) showed that residues 104-116 represent the shortest segment of CN4 capable of binding to actin. ^{1}H-NMR studies (Grand et al *Biochem J.*, 203; 61, 1982) revealed perturbations of specific residues in the N-terminal portion of CN4 on TnC binding and in the C-terminal portion on actin binding. In order to further investigate the localization of TnC binding, we have synthesized peptide analogs of residues 96-108. To facilitate monitoring the interaction with TnC, Trp was substituted for Phe at either position 100 or 106. Titrations of these peptides with TnC, monitored by changes in the Trp fluorescence, yielded binding constants of ~2 x 10^6 M^{-1}, similar to that of CN4. The effects of the peptides on actomyosin ATPase activity was determined by adding increasing amounts of peptide to a system containing myosin S1, actin and tropomyosin. There was >60% inhibition of the activity with with either TnI or CN4 at a ratio of 0.5 to actin but no inhibition was seen with the synthetic peptides even at considerably higher ratios, suggesting that they do not interact with actin-tropomyosin. These results imply a compartmentalization of function in CN4 in which the TnC and actin binding regions are different. This, in turn, suggests that a mechanism other than simple competition between TnC and actin for the same binding region on TnI might be involved in regulating contraction.

Tu-Pos17

A DIRECT REGULATORY ROLE FOR TROPONIN T IN THE Ca^{2+} REGULATION OF MUSCLE CONTRACTION.

((James D. Potter, Zelin Sheng and Bo-Sheng Pan)). University of Miami School of Medicine, Department of Molecular & Cellular Pharmacology, Miami, Florida 33101.

Troponin T (TnT) is a key component in conferring Ca^{2+} sensitivity to actomyosin ATPase activity. Since TnT can interact with both TnI and possibly TnC, an important question arises about whether TnT exerts this role through a direct interaction with TnC or indirectly through its interaction with TnI. To answer this question, we have studied a deletion mutant (deletion of residues 1-57) of TnI ($TnI_{\Delta 57}$). Two different methods showed that $TnI_{\Delta 57}$ lost the ability to interact with TnT. However, in the presence of Ca^{2+}, $TnI_{\Delta 57}$ was still able to form a ternary complex, presumably through TnC. Both wild type (TnI·TnC·TnT) and mutant ($TnI_{\Delta 57}$·TnC·TnT) equally regulated actomyosin-S1 ATPase activity. Furthermore, they share the same Ca^{2+} dependence of ATPase activation (pCa_{50} ~ 6.5 and Hill coefficient n ~ 1.1), indicating that the sensitivity and cooperativity of the Ca^{2+} regulation of the ATPase activity was not affected by the lack of interaction between TnT and TnI. Therefore, since $TnI_{\Delta 57}$ does not interact with TnT, TnT probably reconstitutes native Ca^{2+} sensitivity to Tn via direct interaction with TnC. In addition, whereas Ca^{2+} binding to TnC relieves TnI inhibition, it is clear from these studies that the Ca^{2+} dependent interaction of TnC with TnT is responsible for conferring activation of the ATPase. (Supported by NIH AR37701 and NIH AR40727).

Tu-Pos18

TWO RECOMBINANT TROPONIN T FRAGMENTS REPRESENTING α AND β ISOFORMS EXHIBIT STRUCTURAL AND FUNCTIONAL DIFFERENCES.

((B. Pan, D. Meinholtz and J. D. Potter)), Dept. of Molecular & Cellular Pharmacology, University of Miami School of Medicine, Miami, Florida 33101.

We showed previously that T2p-α and T2p-β, two recombinant peptides containing respectively the carboxyl 2/5 of the α and β isoforms of troponin T (TnT), differ in affinity for troponin C (TnC). We have further characterized the structural and functional properties of the peptides. Analyses of circular dichroism spectra suggested that T2p-α and β had essentially the same degree of helix and turn (38% and 31% respectively, for T2p-α and 40% and 34% for T2p-β). However, T2p-β had significantly more disordered structure than did T2p-α (24% for T2p-α vs. 31% for T2p-β). An overall difference in the content of β-sheet was also indicated, although this should be interpreted with some caution. In addition, we studied Ca^{2+} binding to fluorescently labeled TnC complexed to either T2p-α or T2p-β. The Ca^{2+} affinity of the low affinity, regulatory sites in TnC·T2p-β were about 3-fold lower than in TnC·T2p-α, while the Ca^{2+} binding properties of the high affinity sites did not differ between the two complexes. The data imply that the sequence of the COOH-terminal variable region of TnT is a determinant of the Ca^{2+} sensitivity of the contractile machinery. (Supported by NIH AR37701 and NIH AR40727).

Tu-Pos19

IDENTIFICATION OF THE ALTERNATIVE SPLICING PATTERNS OF FETAL AND ADULT FAST TROPONIN T ISOFORMS.

((M.M. Briggs, P.W.Brandt,* and F. Schachat)) Departments of Cell Biology, Duke University Medical Center, Durham, NC 27710, and *College of Physicians and Surgeons, Columbia University, New York, NY 10032.

Multiple isoforms of fast TnT are generated by alternative splicing of several 5' exons in the rat fast TnT gene (Breitbart et al., (1985) *Cell* 41, 67). To define the alternative splicing events that actually occur, we have used reverse transcription coupled to PCR to produce cDNAs representative of the mRNAs present in fetal and adult rabbit skeletal muscles. The fetal TnTs are of particular interest because their properties are not explained by any combination of the known exons (Briggs et al., (1990) *Dev. Biol.* 140, 253). Sequencing of the cDNAs from fetal muscle revealed the presence of a new fetal exon (F) in the 5' alternatively spliced region. Parallel studies with rat RNA confirmed that this exon is also present in the rat TnT gene. In adult muscles, the three most abundant cDNAs correspond to our N-terminal protein sequences of TnT_{1f}, TnT_{2f}, and TnT_{3f}. These species comprise more than 90% of the TnT in rabbit fast muscles, and modulate the Ca^{+2} responsiveness in single muscle fibers. Three less abundant cDNAs correspond to minor TnTs that were observed previously: TnT_{2fa}, $TnT_{2.5f}$, and TnT_{4f}, which make up 1-15% of the TnT in certain muscles. The adult and fetal isoforms derive from alternative splicing of exons 4, 6, 7; the fetal isoforms also include the newly identified fetal exon F. These studies show that a limited number of splicing events occurs and that there is a direct correspondence between the observed cDNAs and the TnT isoforms expressed in rabbit skeletal muscles.

Tu-Pos20

CHARACTERIZATION OF CHICKEN STRIATED MUSCLE α-TROPOMYOSIN EXPRESSED IN INSECT CELLS USING BACULOVIRUS.

((M. Urbancikova and S. E. Hitchcock-DeGregori)) Dept. of Neuroscience and Cell Biol., UMDNJ-Robert Wood Johnson Med. Sch., Piscataway, NJ 08854 (Spon. by F. Matsumura)

Tropomyosin (TM) expressed in *E. coli* polymerizes poorly and has a much lower affinity for actin than muscle α-TM presumably because the N-terminal Met is unacetylated[1]. To obtain acetylated TM we have expressed a chicken striated muscle α-TM cDNA in *Spodoptera frugiperda* Sf9 insect cells using a baculovirus expression vector system (BEVS). We cloned muscle TM cDNA (gift of S. MacLeod) into the NheI site of the baculovirus transfer vector pBlueBac (Invitrogen). There was good expression of the protein in Sf9 cells cotransfected with wild type baculovirus DNA and pBlueBac/TM cDNA. The yield of the purified recombinant protein (BEVS-TM) is about 12 mg/L of cell suspension. BEVS-TM is soluble after cell lysis and is heat stable. A 35%-70% $(NH_4)_2SO_4$ saturation precipitate was further purified using DE-52 and hydroxylapatite column chromatography. The BEVS-TM crossreacts with goat anti-chicken striated muscle α-TM. The BEVS-TM affinity for actin is much greater than the bacterial TM and is similar to muscle TM. Polymerization of BEVS-TM is weak and comparable to bacterial TM. [1]Hitchcock-DeGregori and Heald, 1987, J. Biol. Chem., 262, 9730-9735. Supported by MDA and NIH.

Tu-Pos21

ANALYSIS OF TROPOMYOSIN'S PERIODIC ACTIN BINDING SITES

((Y.M. An and S.E. Hitchcock-DeGregori)) Dept. of Neuroscience and Cell Biology, Robert Wood Johnson Medical School, Piscataway, NJ 08854.

We have been investigating tropomyosin's (TM) periodic actin binding sites. The actin affinity of unacetylated chicken striated α-TM expressed in E. coli was measured by cosedimentation in the presence of Tn (+Ca^{2+}) since unacetylated TM alone binds poorly to actin. To learn the contribution of individual sites, we deleted the 3rd actin binding site (res. 86-127) and compared the mutant to one in which the 2nd site was deleted (res. 47-88)[1]. Deletion of site 3 reduced the actin affinity 20-fold (2.2 x 10^6 M^{-1}) compared to wildtype (5.0 x 10^7M^{-1}), much more than deletion of site 2 (1.3 x 10^7M^{-1}). Therefore, actin binding sites are not equivalent in their contribution to the overall affinity. The affinities of all 4 TMs to actin with Tn in the absence of Ca^{2+} were similar, consistent with previous results.[1] We have begun to investigate the sequence requirements of actin binding sites. Substitution of res. 47-60 with 14 res. of the GCN4 leucine zipper[2], which changes 13 of 14 res. in the first part of site 2, reduced actin affinity to the same extent as deletion of the 2nd site. We suggest that the periodic sites are bona fide sites and do not function merely as spacers on the thin filament. 1. Hitchcock-DeGregori & Varnell (1990) J. Mol. Biol. 241, 885-896. 2. Landshulz et al. 1988. Science 240, 1759. Supported by NIH.

Tu-Pos22

NOVEL PROPERTIES OF CARBOXYPEPTIDASE-TREATED UNACETYLATED TROPOMYOSIN.

((C.A. Butters, K.W. Willadsen, and L.S. Tobacman)) Department of Internal Medicine, University of Iowa, Iowa City IA 52242.

Carboxypeptidase A removes 11 residues from tropomyosin, producing a molecule (cpTm) that does not polymerize and does not bind to actin unless troponin is present. These functional deficiencies resemble those of bacterially expressed recombinant tropomyosin, which differs from muscle tropomyosin by the absence of N-terminal acetylation. We used a linear lattice model for thin filament assembly to analyze the defective actin binding exhibited by each of these altered tropomyosins, one altered at the N-terminus and the other altered at the C-terminus. Either of the alterations greatly diminished (at least 20- to 40-fold) the affinity of tropomyosin or troponin-tropomyosin for an isolated site on the actin filament. Neither N- nor C- terminal defects had a large effect on cooperative interactions between adjacent tropomyosins. Unexpectedly, the effects of N- and C-terminal structural changes were not additive; loss of N-terminal acetylation had no effect on the actin binding of cpTm. The data can be rationalized according to the previous suggestion that tropomyosin has two quasi-equivalent sets of actin binding sites along its length. We additionally propose that the ends of tropomyosin are important for binding when one set of sites is used and are unimportant when the alternative set of sites is used.

Tu-Pos23

TROPONIN-TROPOMYOSIN REGULATES THE BINDING OF NUCLEOTIDES TO MYOSIN SUBFRAGMENT 1 AND HMM.

((A.M. Resetar & J.M. Chalovich)) East Carolina University School of Medicine, Greenville, NC 27858-4354, USA.

Since troponin-tropomyosin inhibits the maximum rate of ATP hydrolysis with little effect on the degree of binding of myosin-ATP to actin, it has been suggested that the regulated transition in ATP hydrolysis could be a step associated with the release of P_i from the acto-S1-ADP-P_i complex (Chalovich et al. JBC 256: 575, 1981). Rosenfeld & Taylor (JBC 262: 9984, 1987) have observed that the rate of release of nucleotides and products from regulated acto-S1 is inhibited in the absence of Ca^{2+}. We now report that this change in the rate of dissociation of nucleotides is accompanied by a change in the affinity of nucleotides to regulated acto-S1 and acto-HMM. The binding of ATP in the presence and absence of Ca^{2+} was estimated from the apparent Michaelis-Menten constant and the binding of ATPγS was estimated by the method of Biosca et al., (JBC 261: 9793, 1986) with ATPγS as a competitive inhibitor of the ATPase activity. Experiments were done at low ionic strength and with covalently crosslinked acto-S1 or with high concentrations of actin-troponin-tropomyosin to insure that most of the S1 or HMM was bound to actin. The apparent binding of both ATP and ATPγS was 5-10 fold stronger in the absence of Ca^{2+}. Thus Ca^{2+} accelerates the rate of release of nucleotides and this is associated with a weakening of the association constant of nucleotides to the acto-S1 complex.

Tu-Pos24

REDUCED WING BEAT FREQUENCY AND FLIGHT MUSCLE STIFFNESS IN TWO TROPOMYOSIN I MUTANTS OF *DROSOPHILA*

((A. Kreuz, J. Molloy*, R. Schaaf*, A. Simcox and D. Maughan*)) Dept. Mol. Genetics, Ohio State U., Columbus, OH 43210 and *Dept. Physiology/Biophysics, U. Vermont, Burlington, VT 05405.

We have studied the structure and function of indirect flight muscle fibers (IFMs) that are mutant for tropomyosin. Flies from two separate lines that carry different mutations in the Tropomyosin I (TmI) gene were analyzed. One line, *Ifm(3)3*, is an insertional mutation that reduces the expression of the IFM-specific TmI isoform, and the second, *S2*, is an AT > GC transition, substituting Asn (residue #121) for Asp. Both mutations, however, give similar results. Wingbeat frequency and flight ability is reduced in *S2/+* and *Ifm(3)3/+* flies to about the same extent compared to wild-type (+/+), and IFM fibers from both mutants show similar patterns of disruption in the periphery of myofibrils. Additional results from isolated, skinned IFMs of *+/+*, *Ifm(3)3/+*, *Ifm(3)3/Ifm(3)*3, and *Ifm(3)3* transformed with one or two copies of the wild type TmI gene suggest a correlation between active stiffness, number of myofibrils in the organized myofibrillar lattice, and number of wild type copies of the TmI gene. The kinetics of the process underlying generation of force during stretch appear unaltered. The results from *S2* suggest that the charge difference between the mutant Asn residue and the wild-type Asp disrupts myofibril assembly in the IFM, leading to reduced active muscle stiffness and lower wing beat frequency. Supported by NIH AR40234.

Tu-Pos25

MAPPING THE CALDESMON MOLECULE: FRAGMENT EFFECTS ON MUSCLE MECHANICS

((J. Heubach+, B. Brenner+ and J. M. Chalovich*)) +University of Ulm, Germany; *East Carolina University, NC

Various solution studies have implicated regions of the C-terminus of caldesmon in the regulation of the actomyosin interaction. The observation that several polypeptides from the C-terminal region have actin binding activity have lead to the Mosaic-Multiple Binding model of inhibition (Chen & Chalovich, Biophys. J. in press). This model predicts that some regions of the C-terminal region of caldesmon bind to actin and strongly compete with the binding of myosin while other regions may bind to actin with little competition of myosin binding. Mechanical experiments, with single skinned rabbit psoas fibres, allow us to monitor the ability of various fragments to inhibit stiffness (a measure of crossbridge binding to actin) and Ca^{2+}-activated tension (a measure of activity). The advantage of this technique is that the geometry of the actin-myosin interaction is preserved. Three C-terminal chymotryptic fragments of caldesmon were compared. The 35 kDa and 20 Kda fragments inhibited stiffness and Ca^{2+}-activated tension over a concentration range similar to that of intact caldesmon. The 7.3 Kda fragment (Velaz et al., J. Biol. Chem. 1992) also inhibited both stiffness and tension but at much higher (50 x) molar concentrations. The maximum observable effect also decreases with the smaller fragments. Both the 35 and 20 Kda fragments contain the 7.3 Kda region. Other fragments, which bind to actin in solution, but which do not contain the 7.3 Kda region do not inhibit stiffness and tension. These results support the Multiple-Mosaic model and suggest that the 7.3 Kda fragment of caldesmon is a key regulatory site.

Tu-Pos26

THIADIAZINONES INCREASE ACTOMYOSIN ATPASE ACTIVITY BY A MECHANISM DEPENDENT ON THIN FILAMENT ISOFORM POPULATION.

((M.V. Westfall, K.L. Ball, M.R. Keller, R.J. Solaro)) Dept. of Physiology & Biophysics, Univ. of Illinois, Chicago, IL 60680.

EMD-53998 sensitizes the myofilament to Ca^{2+} but does not alter Ca^{2+}-binding to myofibrillar troponin C (TnC;J. Mol. Cell. Card. 24(3):S41,1992). We investigated other possible sites of EMD-53998 action by measuring actomyosin ATPase activity in adult rabbit cardiac and soleus muscle myofibrils which have the same TnC isoform but vary in other troponin (Tn) and myosin isoforms. EMD-53998 decreased cooperativity but increased Ca^{2+} sensitivity and maximum myofibrillar ATPase activity in both preparations. The EC_{50} for the active enantiomer, EMD-57033 also was similar for cardiac and soleus myofibrils. EMD-57033 had no effect on cardiac myosin ATPase activity and EMD-53998 had the same effect on adult and senescent rat heart myofibrils which contain different myosin isoforms. The rabbit cardiac myofibrillar response to EMD-57033 was 3-5x higher than the soleus muscle response at all [Ca^{2+}]s. Soleus and cardiac muscle contain different TnT and TnI isoforms. Moreover, EMD-53998 increased myofibrillar ATPase activity more in adult than neonatal rabbit cardiac myofibrils, which also have different TnT and TnI isoforms. Our results suggest that the response to these thiadiazinones may depend on the TnT and/or TnI isoform population. Studies are underway to determine whether thiadiazinones cause similar changes in force using detergent skinned soleus and cardiac preparations. Support: NIH T32-HL-07692, HL-22231 & AHA Student Fellowship.

Tu-Pos27

CARDIAC THIN FILAMENT PROTEINS AND THEIR EXPRESSION IN CARDIOMYOPATHY.

((A. Malhotra, A. Nakouzi, A.M. Murphy, S. Schiaffino, and P. Buttrick)) Montefiore Medical Center and Albert Einstein College of Medicine, Bronx, NY 10467.

We have demonstrated that alterations in the regulatory complex, troponin-tropomyosin (TnTm), can account for changes in myofibrillar ATPase in hamster cardiomyopathy. To study the role of the troponin-I (TnI) subunit in cardiomyopathy, cardiac myofibrils (Mf) were purified from control (C) and 7-8 mo old TO2 myopathic (M) hamsters. Cardiac myofibrils were subjected to immunoelectrophoresis. Western blots using a monoclonal antibody for TnI appeared to show changes in cardiac TnI isoensyme in M hamsters. To address whether the changes in cardiac TnI reflected changes in mRNA, RNA was prepared from C and M ventricular muscle from 11-12 mo old animals and was size fractionated, transferred and probed with a gene specific cDNA probe for TnI. Relative to 18s and GAD, cardiac TnI mRNA is weakly expressed in M when compared to C. These data suggest that TnI plays an important role in understanding the abnormal regulation of contractile protein ATPase in hamster cardiomyopathy.

Tu-Pos28

CALPAIN II DIGESTS TROPONIN I AND TROPONIN T BUT NOT TROPONIN C IN RABBIT VENTRICLE MYOFIBRILS.

((D. Kenigsberg, B.S.Pan, N.R. Brandt and J.D. Potter)), Department of Molecular & Cellular Pharmacology, University of Miami School of Medicine, Miami, FL 33101.

Calpains are endogenous cytoplasmic Ca^{2+} activated neutral proteases that have been shown to disrupt skeletal muscle fibres. This is in part due to the removal of the 40nm periodicity in the I band containing the troponin (Tn) complex (Dayton et al., Biochem. 15:2159, 1976). It has also been shown to degrade TnI but not TnC in mixtures of the pure skeletal Tn subunits (Wang et al., Biochem. J. 262:693, 1989). We now report that exogenous calpain II attacks both cardiac TnI and TnT but not TnC when added to rabbit ventricular muscle myofibrils. Western blot analysis of the proteolysis products with polyclonal antibodies against TnI and TnT showed sequential loss of the intact protein and the appearance of a new band of lower M_r. TnC was not degraded. These observations were confirmed with the pure Tn subunits alone, in mixtures and in the Tn complex. Interestingly, cleavage of TnI and TnT does not appear to grossly affect the Ca^{2+} regulation of Triton skinned ventricular muscle fibres. (Supported by NIH and AHA (FL Affil.) grants).

Tu-Pos29

EFFECTS OF CAFFEINE ON Ca^{2+} REGULATION IN BOVINE MYOCARDIUM.

Ronglih Liao and Judith K. Gwathmey, Cardiovascular Division, Beth Israel Hospital, Boston, MA 02215.

We have recently studied the interactions of caffeine with isolated troponin C (TnC) and its complex with troponin I (TnI) and troponin T (TnT) from bovine myocardium with fluorescence measurements. Cardiac TnC labeled with a fluorescent probe IAANS (2-(4'-iodoacetamidoanilino)naphthalene-6-sulfonic acid) was excited at 325 nm and the changes in fluorescence intensity in the presence and absence of caffeine as a function of $[Ca^{2+}]$ were monitored at 450 nm. In isolated TnC a biphasic curve induced by Ca^{2+}-binding was observed both in the presence and absence of caffeine. There is a small decrease in fluorescence as Ca^{2+} binds to the two high affinity sites and a large increase in fluorescence when Ca^{2+} subsequently occupies the low affinity site. The data showed that caffeine had no effect on the binding of Ca^{2+} to the high affinity sites, but induced a shift of the pCa-fluorescence curve toward higher free Ca^{2+} concentrations suggesting a decrease in the affinity of TnC for Ca^{2+} at the low affinity site. In the reconstituted binary (TnC•TnI) and ternary (TnC•TnI•TnT) complex titration with Ca^{2+} led to a monophasic decrease in fluorescence. In the binary complex caffeine shifted the pCa-fluorescence curve toward higher Ca^{2+} concentrations by 0.4 unit at the pCa_{50S}. However, in the ternary complex caffeine was able to shift the pCa-fluorescence curve toward lower Ca^{2+} concentrations by 0.2 unit at the pCa_{50S}. In summary, caffeine acts as a calcium sensitizer in the integrated contractile apparatus of myocardium. Also troponin T plays an important role in relaying the Ca^{2+} sensitizing effect of caffeine on myocardial contractility.

Tu-Pos30

EFFECT OF LOW pH ON TENSION-pCa RELATIONSHIP IN RAT CARDIAC TRABECULAE AND SOLEUS FIBERS

J. Wattanapermpool, R.J. Solaro, P.J. Reiser. Dept. Physiology & Biophysics, Univ. of Illinois, Chicago, IL 60680.

Changes in pH sensitivity of tension generation in developing heart were proposed to be due to troponin-I (TnI) isoform switching (Solaro et al. Circ. Res.58:721, 1986). Rat trabeculae, containing cardiac TnI and TnC, and soleus fibers, with slow skeletal TnI and cardiac TnC, were chosen to test the effect of low pH on the tension-pCa relation. Tension was measured at pH 7.0 and 6.2 in skinned trabeculae and soleus fibers at several sarcomere lengths (SL). Maximum tension is more suppressed in trabeculae (45%) than in soleus fibers (20-30%) and a larger rightward pCa_{50} shift was detected in trabeculae than in soleus fibers at pH 6.2. SL did not affect the pH-induced shift in pCa_{50} in soleus fibers. Therefore, it is possible that the pH effects on tension generation and Ca-sensitivity are due to the different TnI isoforms in soleus fibers and trabeculae. Supported by AHA of Chicago and NIH.

Fiber	SL (μm)	pH	pCa_{50}	Hill Coeff	P_o/CSA (kN/m²)
Trabeculae	2.02±0.02	7.0	5.74±0.03	3.54±0.43	17.06±2.01
		6.2	4.49±0.02*	5.02±0.22*	9.80±1.54
Short SL Soleus	2.06±0.02	7.0	6.14±0.01†	2.51±0.05†	79.46±7.98
		6.2	5.35±0.03*†	4.00±0.55*†	62.41±5.59
Optimal SL Soleus	2.33±0.01	7.0	6.25±0.01†	1.78±0.04†	100.25±4.64
		6.2	5.37±0.02*†	2.91±0.18†	73.23±5.40
Long SL Soleus	2.57±0.02	7.0	6.24±0.02†	1.83±0.11†	105.16±6.7
		6.2	5.39±0.02*†	3.40±0.40*†	80.7±3.9

Data are presented as mean ± SEM (N=8), CSA = cross-sectional area, * sig. diff. from pH 7.0, † sig. diff. from trabeculae at the same pH.

Tu-Pos31

Ca^{+2}-INDUCED FOLDING OF CALSEQUESTRIN FROM SKELETAL MUSCLE SARCOPLASMIC RETICULUM IS INHIBITED BY MELITTIN AND TRIFLUOPERAZINE

((Z. He, A. K. Dunker‡ & W. Trumble)) Dept. of Bact & Biochem., U. of Idaho, Moscow, ID 83843; Dept. of Biochem/Biophys., Washington State U., Pullman, WA 99164 ‡.

Calsequestrin (Cs) is a low affinity, high capacity Ca^{+2}-binding protein found in the lumen of the sarcoplasmic reticulum. Upon Ca^{+2} binding, Cs undergoes a conformational change, folding into a more compact structure that is trypsin resistant, and burying a hydrophobic site for the drug trifluoperazine (TFP), a site shared by the calmodulin family. The structural and functional roles of the TFP binding site in the Ca^{+2}-induced folding of Cs were studied using the calmodulin antagonists TFP and melittin. If TFP or melittin is added to Cs prior to Ca^{+2} addition, then Ca^{+2}-induced folding is inhibited as determined by circular dichroism (CD) and the blockage of trypsin resitance. If, however, Ca^{+2} is added prior to TFP or melittin, the conformational change leading to trypsin resistance is not blocked. Cs crystals that exhibit high Ca^{+2} binding capacity have previously been shown to occur at high Ca^{+2} and Cs concentrations. By preventing a prerequisite folding step, TFP and melittin prevent Ca^{+2}-induced crystal formation, and decrease the maximal Ca^{+2} binding. These data suggest that the TFP binding site is critically involved in a Ca^{+2}-induced intramolecular folding step required for the intermolecular interactions leading to high capacity Ca^{+2}-binding.

Tu-Pos32

REDUCED pH SLOWS THE RATE OF RELAXATION OF BARNACLE MYOFIBRILLAR BUNDLES UPON PHOTOLYSIS OF DIAZO-2.

((R.E. Palmer, J.D. Potter* and C.C. Ashley)) University Laboratory of Physiology, Parks Road, Oxford, OX1 3PT, U.K.; * Dept. Molecular and Cellular Pharmacology, Univ. Miami Medical School. (spon. by P.J. Griffiths)

Mechanically skinned myofibrillar bundles of the giant barnacle, *Balanus nubilus*, were bathed in a 2 mM solution of the caged Ca^{2+} chelator, diazo-2. Laser photolysis of the preparation led to a rapid uptake of free Ca^{2+} and a rapid relaxation of force. At pH 7.2 the bundles relaxed with a mean half-time of 167.9 ± 7.9 (s.e.m.) ms (n=30, 12 °C), which is slightly faster than observed relaxations in intact fibres. Reducing the pH from the control value of pH 7.2 to pH 6.7 led to a slight slowing of the rate of relaxation, as shown in the figure. Photolysis of diazo-2 occurred at time zero. The slowing of relaxation is due to either a direct action upon the crossbridges, or upon thin filament regulation. The effect was considerably smaller than the effect of reduced pH upon skinned single frog fibres. Studies with the skinned adductor muscle suggest it to be TnC regulated and it's relaxation rate to be similar to intact depressor fibres. Support from SERC, MDA and NIH.

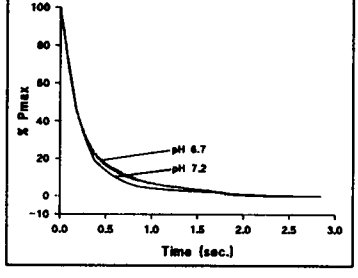

Tu-Pos33

ASYMMETRIC DISTRIBUTION OF A SARCOPLASMIC CALCIUM BINDING PROTEIN IN LOBSTER CLAW MUSCLE ((Mark Snyder & Tim Otter)) University of Vermont, Burlington, VT 05405-0086

To understand the biochemical basis for the difference in contraction speed between a lobster's cutter claw muscle (Cu; >90% fast twitch) and its crusher claw muscle (Cr;≈70% slow/30% fast), we have begun to investigate the possibility that the fast twitch properties of the cutter involve sarcoplasmic Ca^{2+}-binding proteins (SCP's) that may function in a manner similar to that proposed for parvalbumin (pVa) in vertebrate skeletal muscle. By devising purification procedures based on methods published for purification of pVa, we have partially purified from cutter claw muscle a soluble, heat-stable protein of pI≈4.9, M_r≈22kd, with a strong UV absorption maximum at 278nm. This protein stains intensely with Commassie Blue R-250, but not with silver (BioRad) and has Ca^{2+}-dependent mobility in gels. These properties are peculiar features of many EF hand proteins. Consistent with its proposed role in cutter muscle, minute quantities of this protein are present in the crusher muscle, even though the crusher comprises ≈30% fast fibers. Based on its biochemical properties, asymmetric distribution, proposed function, and similarities with SCP's in lobster and crayfish tail muscle, the name we propose for this protein is **snappin** and we tentatively assign it to the E-F hand superfamily of calcium binding proteins. We are currently examining amino acid composition and *in vitro* Ca^{2+}-binding properties of isolated snappin.

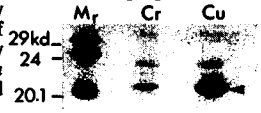

Tu-Pos34

PROBING THE SUBSTRATE BINDING SITE OF MYOSIN LIGHT CHAIN KINASE WITH A PEPTIDE-BASED PHOTOAFFINITY LABEL. ((Gao, Z.-H., and Stull, J.T.)) Department of Physiology, UT Southwestern, Dallas, TX 75235.

Myosin light chain kinase (MLCK) from skeletal muscle catalyzes the Ca^{2+}/ calmodulin (CaM)-dependent phosphorylation of the regulatory light chain of myosin. A photoreactive amino acid p-benzoyl-L-phenylalanine (Bpa) was incorporated into a peptide substrate to produce BpaKKRAARATSNVFA which was then radiolabeled (^3H) by acetylation at the N-terminus. The kinetic properties for phosphorylation of peptide I by skeletal muscle MLCK were similar to the peptide without Bpa. Upon photolysis peptide I was cross-linked stoichiometrically to MLCK in a CaM-dependent manner. Covalent modification of MLCK resulted in loss of kinase activity towards light chain and slowed the rate of intramolecular autophosphorylation. Peptide I cross-linked to MLCK was phosphorylated in the presence of EGTA and the rate was increased in the presence of CaM. After CNBr digestion peptides of MLCK cross-linked with peptide I were purified by HPLC, and a common sequence from Trp 477 to Tyr 484 was found. Based upon the structure of MLCK modelled to cAMP-dependent protein kinase, this sequence corresponds to the F α-helix in the lower lobe of the catalytic core.

Tu-Pos35

SUBCELLULAR LOCALIZATION OF MYOSIN LIGHT CHAIN KINASE IN VERTEBRATE SKELETAL MUSCLE. ((K. Trombitás†, C. L. Roush‡, and G. H. Pollack†)) †Center for Bioengineering, WD-12 University of Washington, Seattle, WA 98195, and ‡Department of Microbiology, SC-42 University of Washington, Seattle, WA 98195.

Immunoelectron microscopy was used to determine the localization of myosin-light-chain kinase in intact sarcomeres of rabbit psoas muscle. Although the kinase is broadly assumed to be soluble, the typical yield of enzyme in the supernatant of crude muscle homogenates is extremely low, implying a major bound fraction. We used three methods to investigate the possibility of localized enzyme: (1) standard immunolocalization methods; (2) immunolocalization in frozen dehydrated muscles; and (3) the freeze-break method. In the latter, freshly prepared small bundles of fibers were quickly frozen and broken into small pieces under liquid nitrogen. The still-frozen specimens were thawed in the presence of fixative. The exposed, transverse surfaces allowed easy access of antibody solution to the myofilament lattice. Results with all three methods were similar. Polyclonal antibody deposits showed that like creatine kinase, myosin-light-chain kinase is bound to the M-line. Labelling was intense. The bridged region of the A-band was also labelled, implying possible co-localization of enzyme and light chain. Contrary to the widely held view, therefore, at least some of the kinase enzyme is bound to the cell's proteins—a finding that may have implications for kinase-enzyme function.

Tu-Pos36

CONFORMATIONAL COUPLING IN CALMODULIN. ((Z. Grabarek and J. Head)) Dept. of Muscle Research, Boston Biomed. Res. Inst. and Dept. of Physiol., Boston Univ. School of Medicine, Boston MA.

Based on our studies on the disulfide crosslinked CaM mutants (Grabarek et al. Biophys. J. 59,23a,1991) we have concluded that the Ca^{2+}-induced conformational transitions in CaM are similar to those proposed by Herzberg et al. (J. Biol. Chem. 261,2638,1986) for the N-terminal domain of troponin C and involve a change in the interhelical dihedral angles in both domains of CaM. In search of the structural elements that may be responsible for coupling between Ca^{2+}-binding at the ligand-providing loop and the resulting transitions we have replaced Phe92, the residue preceding the first Ca^{2+}-binding ligand of site III with Ala. The mutant (CaM-F92A) has increased affinity for Ca^{2+} at sites III and IV reflected by a 0.4 pCa shift in tyrosine fluorescence titration curve but its ability to activate phosphodiesterase is decreased by 80% as compared with the wild type CaM. A plausible interpretation is that Phe92 is indeed involved in the coupling mechanism. To gain further insights we have crystallized CaM-F92A and CaM41/75 - the mutant containing a disulfide bond in the N-terminal domain. CaM-F92A crystallizes in triclinic form P1 - the form of the wild type CaM - but one of the unit cell dimensions is shorter. CaM41/75 gives tetragonal crystals, of the space group $P4_12_12$. The crystals diffract to 2.1 Å and 2.5 Å for the CaM-F92A and CaM41/75, respectively. The work on the atomic structure of these mutants is in progress.

Tu-Pos37

CALMODULIN-LIKE MIMICRY OF A TnC DERIVATIVE ((Arvind Babu and Jagdish Gulati)) Albert Einstein College of Medicine, Bronx, NY 10461.

Calmodulin and TnC are highly homologous (~50% sequence identity) EF-hand proteins. They putatively shared the same evolutionary precursors, but their present functions are manifestly different. Two preeminent disparities between their atomic structures are: (1) CaM lacks the 3½-turn α-helix in the N-terminal overhang. (2) It also lacks a ^{88}KGK^{90} cluster in the central helix. Consequently, we investigated the effects of deleting these domains. A rabbit skeletal muscle TnC-encoding synthetic gene with multiple restriction sites was mutagenized, deleting: (1) the nucleotides encoding 10 residues of the N-terminal overhang (-N_t◆TnC), (2) only the KGK cluster (-KGK◆TnC), and (3) both the N_t and the KGK cluster (-N_t-KGK◆TnC). The proteins were expressed in E. coli, purified, and tested in skinned guinea-pig taenia coli, normally activated with pCa4 and 0.5μM CaM. Compared with CaM (100%P_0), neither the wild type TnC (3±2%P_0), the -N_t◆TnC (5±2%P_0), nor the -KGK◆TnC (4±2%P_0) was effective. In contrast, the -N_t-KGK◆TnC (90±1%P_0) derivative closely mimicked the CaM response. All derivatives denoted the same level of Ca-binding (4/mole protein). The results indicate that interaction between the N-terminal α-helical overhang and the central helix is dominant in TnC and the lack of this interaction, moreover, contributes significantly towards the functional distinctions of CaM. (NIH & NY Heart funded)

Tu-Pos38

RESOLUTION OF STRUCTURAL CHANGES ASSOCIATED WITH CALCIUM ACTIVATION OF CALMODULIN USING FREQUENCY-DOMAIN FLUORESCENCE SPECTROSCOPY. Yihong Yao and Thomas C. Squier. University of Kansas, Lawrence, KS 66045-2106.

We have specifically labeled the unique cysteine group (Cys_{27}) available in wheat germ calmodulin with a variety of sulfhydryl group directed fluorescent probes that can function as energy transfer donors. Likewise, we are able to selectively modify the single tyrosine (Tyr_{139}) in the opposite domain of the dumbbell shaped calmodulin (relative to Cys_{27}) with tetranitromethane. Nitrotyrosine has a significant absorption coefficient in the blue-green and can function as an energy transfer acceptor, permitting direct measurements of time-dependent changes in the separation between the globular domains of calmodulin. Upon calcium binding we resolve a large decrease in both the average donor-acceptor separation and conformational flexibilty of calmodulin (see figure). Our results are consistent with previous models that suggest calcium binding disrupts the central helix, resulting in a closer interaction between the two globular domains.

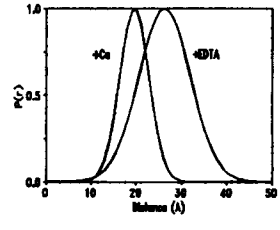

Tu-Pos39

THE AMINO ACID SEQUENCE OF CARDIAC MYOSIN LC1 AND LC2 FROM CONTROL AND DILATED CARDIOMYOPATHIC HUMAN HEARTS. ((S.S. Margossian, J.C. Holt, J.B. Caulfield and P. Norton)) Montefiore Medical Center, Bronx, NY 10467; Rorer Biotechnology Inc., King of Prussia, PA 19406 and Univ. Alabama, Birmingham, AL 35294.

Cardiac myosin LC1 and LC2 from human hearts obtained at transplant were purified by reverse phase HPLC on a C-4 column in 0.1% trifluoroacetic acid and eluted with an acetonitrile gradient. LC1 in 5M guanidine hydrochloride was reduced with 3M DTT under argon and S-pyridylethylated (S-PE) with vinyl pyridine. CNBr peptides were prepared from alkylated LC1 and untreated LC2. Fragments which were obtained by proteolysis of LC1 and LC2 using endoproteinase Asp-N, endoproteinase Lys-C and V8 protease were separated by reverse phase HPLC. Sequence analysis identified the blocked N-terminal residues in both LC1 and LC2 to be trimethyl alanine. Sequences of both light chains revealed about 97% identity with those obtained from cDNA clones. When the sequences were determined for LC1 and LC2 purified from human heart myosin with idiopathic dilated cardiomyopathy, no differences could be detected between the controls and the dilated cardiomyopathic. These results suggest that the functional alterations observed in dilated cardiomyopathic myosin were induced by factors other than a change in the primary structure of the essential or the regulatory light chains.

Tu-Pos40

OBSERVATION AND IDENTIFICATION OF MULTIPLE MYOSIN SUBFRAGMENT-1:ADP:FLUOROBERYLLATE COMPLEXES USING ^{19}F NMR SPECTROSCOPY.

((Gillian D. Henry*, Shinsaku Maruta**, Mitsuo Ikebe*** and Brian D. Sykes*)) *Department of Biochemistry, University of Alberta, Edmonton, Alberta, CANADA; **Department of Bioengineering, Soka University, Hachioji, JAPAN; ***Department of Physiology and Biophysics, Case Western Reserve University, Cleveland, Ohio 44106.

Fluoroaluminate and fluoroberyllate are potent inhibitors of the ATPase activity of myosin. Inhibition requires the presence of ADP, and much evidence has accumulated to suggest that the tetrahedral fluoroaluminate and fluoroberyllate anions act as phosphate analogues, binding with high affinity at the active site in the position normally occupied by the terminal phosphate of ATP. Both the S1:ADP:fluoroaluminate and S1:ADP:fluoroberyllate species resemble kinetic intermediates in the actomyosin ATPase cycle. Characterisation of S1-bound fluoroaluminate by ^{19}F NMR is straightforward; a single resonance identified AlF_4^- is observed readily. Bound fluoroberyllate, by contrast, gives rise to four separate peaks: a downfield pair at -80.1 ppm and -83.5 ppm and an upfield pair at 101.3 ppm and 102.8 ppm, demonstrating the coexistance of four distinct S1:ADP:fluoroberyllate species. The relative intensities of the bound resonances can be altered by changing the F:Be ratio during complex formation. Integration of a spectrum acquired in the presence of the ^{19}F-labelled nucleotide derivative, 4-fluorobenzoic-ADP yielded a bound fluoride to nucleotide ratio of only 1.7 to 1. It is suggested that the bound resonances correspond to the neutral species $BeF_2(H_2O)_2$ and $BeFOH(H_2O)_2$, and the negatively charged species $[BeF_2OH(H_2O)]^-$ and $[BeF_3(H_2O)]^-$.

Tu-Pos41

MYOSIN-ADP-FLUOROALUMINATE AND MYOSIN-ADP-FLUOROBERYLLATE TERNARY COMPLEX AS TRANSITION STATE ANALOGUE.

((S. Maruta, G.D. Henry#, B.D. Sykes# and M. Ikebe*)) Department of Bioengineering, Soka University, Hachioji, Tokyo 192 JAPAN. #Department of Biochemistry, University of Alberta, Edmonton, Alberta, T6G 2H7, CANADA. *Department of Physiology & Biophysics, Case Western Reserve University, Cleveland, Ohio 44106

Myosin formes a stable ternary complex with ADP and fluoroaluminate or fluoroberyllate which are thought to be phosphate analogue[1]. We studied the properties of these two ternary complexes which are thought to be the transition state analogue of myosin ATPase.

To study the nature of the binding state between the ternary complexes and actin, the dissociation of acto-S1 induced by ADP and either fluoroaluminate or fluoroberyllate was examined by measuring the change in the acto-S1 turbidity. Acto-S1 dissociated rapidly after addition of ADP/fluoroberyllate, slowly after addition of ADP/Vi wherease it did not dissociate by addition of ADP/fluoroaluminate. These results suggested that myosin/ADP/fluoroberyllate is a weak binding state, while myosin/ADP/fluoroaluminate is a strong binding state. Effects of actin on the stability of the ternary complexes were also studied . The bound ADP in the S1/ADP/fluoroberyllate complex was rapidly released by addition of actin while the bound ADP was not released by addition of actin from the S1/ADP/fluoroaluminate complex. These results also suggest that the two ternary complexes represent the distinct states along myosin ATPase kinetic pathway. To further study the active site conformation of myosin in these ternary complexes, we employed fluorine labelled ADP analogues as probe and the conformation was monitored by ^{19}F-NMR. ATP analogue, 2-[(4-trifluoromethyl-2-nitrophenyl)amino]ethyl triphosphate and 3'(2')-O-(4-fluorobenzoic)-ATP were synthesized. These analogues were hydrolyzed by myosin similar to ATP and bound to myosin stably in the presence of either fluoroaluminate or fluoroberyllate. The ^{19}F signal of ATP analogues bound to myosin were distinguished from that of free compounds. The ^{19}F signal of the bound analogues in the ternary complexes were analyzed by ^{19}F-NMR. (Supported by grants from NIH, AHA and The Japan Science Society) 1) Maruta, S. et. al (1991) Biophys. J. 59, 436a.

Tu-Pos42

NUCLEOTIDE INDUCED INTERNAL MOTIONS IN MYOSIN S1: A CROSS-LINKING STUDY.

((Edna Blotnick and Andras Muhlrad)) Hebrew University Hadassah School of Dental Medicine, Jerusalem 91010, Israel.

The heavy chain of myosin S1 is cleaved by limited trypsinolysis into three fragments , 27K, 50K and 20K-- aligned in this order from the N-terminus. The spatial relation between the fragments in the molecular structure and nucleotide induced motions were studied by N-ethoxycarbonyl-2-ethoxy-1,2-dihydroquinoline (EEDQ), 1-ethyl-3-(3 dimethyl aminopropyl) carbodiimide, phenyldiglyoxal and glutaraldehide cross-linkers. The cross-link formation was analyzed by SDS-PAGE with the help of fluorescence probes, 9-anthroylnitrile and IAEDANS, which specifically label the 27K and 20K fragments, respectively. The reaction with all the four cross-linkers leads to the formation of cross-links between the 27K and 20K fragments showing that regions of these fragments are proximal in the spatial structure in spite that they are far away from each other in the amino acid sequence. Cross-links were also formed between the 27K and 50K and between the 50K and 20K fragments, which are proximal in the primary structure. Two distinct cross-linked products, with different electrophoretic mobilities, were formed between the 50K and 20K fragments. In the presence of MgATP or MgADP the formation of the higher electrophoretic mobility 50K-20K product dramatically increased when EEDQ cross-linker was used. This indicates that nucleotide induced internal motions lead to distance changes between specific regions in the S1 segment of the myosin.

Tu-Pos43

RESONANCE ENERGY TRANSFER BETWEEN RESIDUES 2 AND 155 IN A MUTANT CHICKEN SKELETAL MYOSIN LIGHT CHAIN 2

((V.Wolff, T. Tao, and S. Lowey)) Rosenstiel Research Center, Brandeis University, Waltham, MA 02254 and Dept. of Muscle Research, Boston Biomedical Research Institute, Boston, MA 02114.

Disulfide crosslinking studies on a mutant chicken skeletal muscle myosin light chain 2 (LC2) containing an engineered cysteine at residue 2 and an endogenous cysteine at residue 155, have shown that the N- and C-terminal regions can come into close proximity (Wolff et al. J. Cell Biol. 1991, 115:184a). Here, the same mutant, C2/C155, as well as the single cysteine mutants, C2 and C155, were used to probe the free and bound conformations of LC2 by fluorescence spectroscopy. C2 labeled with 1,5-IAEDANS, yielded a fluorescence lifetime of 14.9 ns, which increased to 16.7 ns upon binding to myosin heavy chain (MHC), indicating a more hydrophobic environment at the N-terminus of LC2. C155 labeled with 1,5-IAEDANS yielded a lifetime of 16.7 ns which did not change in the presence of MHC, suggesting that residue 155 may be shielded within the LC2 structure. Because Cys2 is several-fold more reactive than Cys155, C2/C155 could be first labeled with the donor, 1,5-IAEDANS, at Cys2 and subsequently reacted with the acceptor, DDPM, at Cys 155. The transfer efficiency was measured to be 17%, corresponding to a distance of 35Å for free C2/C155. For MHC-bound C2/C155, the transfer efficiency increased to 39%, corresponding to a distance of 29Å, indicating that the distance between residues 2 at the N-terminus and 155 at the C-terminus decreases by ~6Å when C2/C155 binds to MHC. Thus, both the disulfide crosslinking and the energy transfer studies described here suggest that LC2 adopts a compact structure in the MHC-bound state.

Tu-Pos44

VANADATE-MEDIATED PHOTOMODIFICATION OF SCALLOP MYOSIN: IMPLICATION OF SER-179 OF THE HEAVY CHAIN IN CALCIUM REGULATION. ((Bruce A. Kerwin, Julia Douthart and Ralph G. Yount)) Department of Biochemistry and Biophysics, Washington State University, Pullman, WA 99164-4660.

Vanadate(V_i)-mediated photooxidation of myosin has previously been used to modify Ser-180 of skeletal (Cremo et al., (1989) *J. Biol. Chem.* 264:6608) and Ser-179 of gizzard (Cole and Yount (1992) *Biochemistry* 31:6186) myosin. Here, we have used this procedure to photomodify scallop myosin and determine the effect on calcium regulation. After a 4 min photolysis of the scallop myosin•MgADP•V_i complex, V_i was stoichiometrically released from the active site accompanied by a 40% increase and an 85% decrease in the CaATPase and K^+-EDTA ATPase activities, respectively. The Ca^{2+}-activated actomyosin ATPase activity was activated only two-fold in the presence of Ca^{2+} compared to a twelve-fold activation for the control. Because vanadate photomodification reportedly oxidizes a Ser to a serine aldehyde, we reduced the photomodified scallop myosin with $[^3H]NaBH_4$ to localize the oxidized residue(s). Following tryptic digestion of the reduced myosin a [^{3}H]peptide was purified by HPLC and sequenced by automated Edman degradation. The sequence of the [^{3}H]peptide was E-N-Q-S-C-L-I-T-G-E-[^{3}H]S-G-A-G-K corresponding to residues 169-182 of the heavy chain (Nyitray et al., (1991) *J. Biol. Chem.* 266:18469). These data suggest that Ser-179 is near the γ-phosphate of ATP when it occupies the active site and that Ser-179 is an important part of the Ca^{2+}-mediated regulatory pathway of scallop myosin. (Supported by NIH grant DK 05195 and a MDA postdoctoral fellowship to BK).

Tu-Pos45

CHARACTERIZATION OF THE CLEAVAGE PRODUCTS FORMED BY VANADATE PHOTOCLEAVAGE OF MYOSIN SUBFRAGMENT 1 (S1). ((Jean C. Grammer and Ralph G. Yount)), Dept. of Biochem. and Biophys., Washington State University, Pullman, WA, 99164-4660.

S1 has been shown to undergo photomodification of Ser-180 upon irradiation of the S1·MgADPVi complex (Grammer *et al.*, (1988), *Biochemistry* 27, 8408; Cremo *et al.*, (1988), *Biochemistry* , 27, 8415, and (1989) *J. Biol. Chem.* 264, 6608). The photomodified S1 (pmS1) can retrap MgADP Vi and upon irradiation of the pmS1·MgADPVi complex, the S1 heavy chain is cleaved into 21 kDa N terminal and 74 kDa C terminal fragments. To show that Ser-180 is the site of cleavage, peptides containing either the new N terminus or C terminus generated by photocleavage were isolated. CNBr treatment of the N terminal 21 kDa fragment followed by peptide separation on HPLC was used to isolate the new C terminal peptide. Several methods including mass spectrometry and capillary electrophoresis were used to show the C terminal blocking group was an amide on Glu-179 with the amide NH_2 arising from the amino group of Ser-180. The N terminus of the 74 kDa fragment was isolated by preparative electrophoresis using a BioRad Prep Cell followed by tryptic digestion after blocking lysines with either succinic anhydride or ethyl thioltrifluoroacetate. The peptides were separated by HPLC and the blocked N terminal peptide was found by use of trinitrobenzenesulfonate to detect free N termini. The amino acid composition of the blocked peptide was consistent with the N terminal amino acid being Gly-181. The nature of the blocking group is being examined by mass spectrometry and NMR. Supported by NIH (DK-05195) and MDA.

Tu-Pos46

MYOSIN-ATP CHEMOMECHANICS. ((S. Highsmith and D. Eden))Dept. Biochem., UOP, S.F., CA, 94115 and Dept. Chem., SFSU, S.F., CA, 94132

The rate of rotational Brownian motion of skeletal muscle myosin S1 in the presence of ATP was measured in solution by transient electric birefringence techniques. A 6 us, 3000 v/cm electric field was used to partially align the S1.MgADP,Pi and the decay of its birefringence signal was fitted by a single exponentional function. At 3.5°C, the decay time was 259 ns after ATP was added and increased to 271 ns, as ATP was hydrolyzed to ADP. The time dependence of the observed increase in hydrodynamic size as S1 changes from being predominately S1.MgADP,Pi to being S1.MgADP is predicted accurately from known values of S1 activity, the Km for ATP and the Ki for ADP. This indicates that the change in hydrodynamic size is ATP-induced. We propose that S1.MgADP,Pi is rotating faster than S1.MgADP because the former has been made more compact by MgATP binding and that this compact structure has stored mechanical energy that is released as the less compact S1.MgADP is formed. Simple structural models of S1 indicate that an elongation of 5 nm is consistent with the observed increase in rotational decay time caused by Pi dissociation. (supported by NIH AR37499 and GM31083)

Tu-Pos47

HEAVY MEROMYOSIN HEADS ARE INVOLVED IN THERMALLY DEPENDENT SELF-ASSOCIATION. ((U. Ghodke and P. Dreizen)) Physiology and Biophysics, SUNY Health Science Center at Brooklyn, NY 11203.

Ueno et al (1983) reported self-association of heavy meromyosin (HMM) at 5-24°C, attributed to S2 interactions related to Mg^{2+}/Ca^{2+} binding at low-affinity sites on S2. We have further explored the thermal dependence of HMM self-association. There are 2 distinct processes involving HMM head region in some way. (1) At 34-40°C in 1mM EDTA-EGTA, HMM exhibits self-association in absence of Mg^{2+} or Ca^{2+}. Turbidity kinetics show exponential rise with $T_{1/2} \approx 5$ min. Self-association is inhibited by Mg^{++}/Ca^{++} ($K_i \approx 150\mu M$), presumably due to binding at high-affinity sites on LC2, and also by MgATP, MgADP, and MgAMP-PNP ($K_i \approx$ 40-100μM), presumably due to saturation of S1 nucleotide binding site. (2) HMM also undergoes reversible self-association at Mg^{++}/Ca^{++} > 1mM at 34-40°C at low ionic strength. The time course of turbidity rise is sigmoidal, consistent with cooperativity, as previously described. The process is highly sensitive to nucleotide at concentrations which saturate the S1 catalytic site. In the nucleation phase, HMM self-association is inhibited by nucleotides with representative $K_i \approx 5\mu M$ for AMP-PNP. In the growth phase, K_i values are 5μM for AMP-PNP, <100μM for ATP, and ~500μM for ADP. Under usual ligand conditions for the ATP cross-bridge cycle, HMM self-association is greatest in the absence of nucleotides, somewhat less with ADP, and negligible or absent with ATP and AMP-PNP. The findings are consistent with state-specific head interactions during the cross-bridge cycle.

Tu-Pos48

ELECTRON PARAMAGNETIC RESONANCE OF SPIN-LABELED SINGLE CRYSTALS OF CHICKEN MYOSIN S-1. ((Edmund C. Howard, Ivan Rayment, and David D. Thomas)) University of Minnesota Medical School, Minneapolis, MN 55455 and University of Wisconsin-Madison, Madison, WI 53706.

We have labelled single crystals of chicken S-1 with both 4-(2-iodoacetamido)-TEMPO and 4-maleimido-TEMPO, and obtained EPR spectra using a loop-gap resonator fitted with a programmable goniometer with better than 1° resolution. These spectra show most of the probes to be well ordered and immobilized, although analysis of powder spectra shows a smaller population of moderately immobilized probes. This approach yields probe orientations on the myosin head, and can be used to determine the orientation between actin and myosin, as well as between myosin and the muscle fiber.

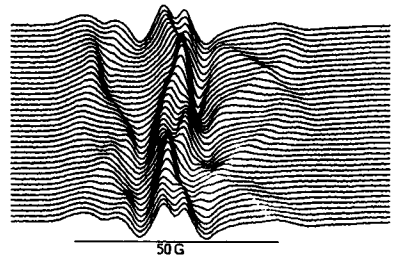

Spectra of S-1 crystals labelled with IASL, recorded every 5°. Rotation axis was near the crystal *b* axis.

SMOOTH MUSCLE MYOSIN

Tu-Pos49

MUTAGENESIS OF THE PHOSPHORYLATION SITE (SER 19) OF THE REGULATORY LIGHT CHAIN AND ITS EFFECTS ON SMOOTH MUSCLE MYOSIN FUNCTION.

H. Kamisoyama, Y.Araki and M.Ikebe Dept. of Physiolgy & Biophysics, Case Western Reserve Univ. Cleveland, OH 44106

Smooth muscle actomyosin ATPase activity is regulated by the phosphorylation of the regulatory light chain of myosin at Ser 19. However, the molecular mechanism by which the phosphorylation regulates the ATPase activity is still obscure. In the present study, we produced two mutant regulatory light chains whose Ser 19 is substituted for either alanine or aspartic acid. A cDNA which covers the entire open reading frame of the regulatory light chain was inserted into pT7 expression vector and the recombinant proteins were expressed in E. coli. The recombinant light chain was extracted from E. coli cells and purified by DEAE Sephacel to homogeneity. Approximately 20mg of light chains were prepared from 1 liter of liquid culture. The recombinant light chains were exchanged with smooth muscle heavy meromyosin[1)] and actin activated ATPase activity was determined. The alanine mutant showed activity similar to the dephosphorylated wild type light chain. On the other hand, the aspartic acid mutant showed a few times higher activity than the dephosphorylated wild type light chain although the activity was less than the phosphorylated light chain. These results suggest that 1) the negative charge on the 19 position is important for the activation of ATPase activity; 2) the specific configuration of the acidic moiety, however, may be necessary to achieve the effective activation; 3) the serine side chain is not responsible for the inhibition of the ATPase activity. (Supported by NIH and AHA)

1) Morita et al. (1991) Biochemistry, 30, 9539-9545

Tu-Pos50

MYOSIN HEADS MOVING OUT: MYOSIN PHOSPHORYLATION IN MAMMALIAN STRIATED MUSCLE. ((R.J.C. Levine[1], H.L. Sweeney[2], R.W. Kensler[3] and Z. Yang[2])) [1]Medical College of Pennsylvania, Philadelphia, PA 19129, [2]University of Pennsylvania, Philadelphia, PA 19104 and [3]University of Missouri, Kansas City, MO 64108.

Phosphorylation of myosin regulatory light chains (MRLCs) potentiates tension development of skinned rabbit psoas fibers at low Ca^{2+} and optimal overlap of thin and thick filaments. Since decreasing lattice spacing by increasing either sarcomere length or osmotic pressure lessens this effect[1], we suggested that S1s with phosphorylated MRLCs are closer to thin filaments than in the unphosphorylated state. This hypothesis is supported by the results of structural studies on thick filaments separated from rabbit psoas fibers, all performed at 23° C. Negatively-stained filaments, exposed only to relaxing solution, show an ordered array of surface myosin and produce Fourier transforms consistent with their demonstrated structure[2]. Incubation on Ca^{2+}-dependent myosin light chain kinase (+ calmodulin and Ca^{2+}) or Ca^{2+}-independent kinase all cause outward movement of S1s, and disorder of the surface lattice. After all control incubations: Ca^{2+}-dependent kinase without Ca^{2+} and calmodulin; BSA; Ca^{2+} (pCa 5.0) in relaxing solution, thick filaments, well-separated from thins, retain an ordered array of surface myosin, apparent on micrographs and transforms obtained from them. In the Ca^{2+} controls, thin filaments are de-repressed and in areas where they are close to the thicks, clumps and rafts of interacting filaments occur. We conclude that MRLC phosphorylation potentiates tension development at low Ca^{2+} by moving myosin heads into positions where they can more easily bind to actin on thin filaments.

[1]Yang et al.'92 Biophys. J. 61:A267,. [2]Kensler & Stewart. *ibid.* A301.

Tu-Pos51

PROBING THE N-TERMINUS OF THE SMOOTH MUSCLE MYOSIN REGULATORY LIGHT CHAIN. ((Zhaohui Yang, G. Zhi, James T. Stull, Kathy M. Trybus, and H. Lee Sweeney)) Univ. of Pennsylvania School of Medicine, Philadelphia, PA 19104-6085; U.T. Southwestern Medical School, Dallas, TX 75235; and Brandeis Univ., Waltham, MA 02254.

The simplest hypothesis for the mechanism of myosin regulatory light chain (RLC) phosphorylation is that phosphorylation changes the net charge in a critical region of the N-terminus of the RLC. This alteration in charge would in turn alter interactions between the RLC and myosin heavy chain. To assess this hypothesis, a series of mutant RLCs have been engineered and expressed in *E. coli*. These include mutants in which positively charged amino acids near the phosphorylatable serine (S19) of the human smooth muscle RLC have been replaced by alanines, and mutants where S19 has been replaced with glutamate or T18 and S19 have been replaced with glutamates. These mutants have been evaluated for their ability to mimic the phosphorylated form of the wild type RLC when reconstituted into scallop striated muscle bundles (for force measurements) or into isolated gizzard myosin (for folding, ATPase and motility measurements). The results indicate that net charge in the region from R13 to S19 can account for the ability of RLC phosphorylation to potentiate force in scallop striated muscle and unfold smooth muscle myosin. Thus the effect of RLC phosphorylation in striated muscle may be due to alteration of net charge at the N-terminus of the light chain. The ability of RLC phosphorylation to convert the folded form (6S) of smooth muscle myosin to unfolded (10S) may be the smooth muscle equivalent of the phosphorylation effect in striated muscle. The ability of phosphorylation to turn on ATPase activity and motility in smooth muscle myosin involves a more complex mechanism.

Tu-Pos52

IS THE ESSENTIAL LIGHT CHAIN (LC17) AT THE ACTIVE SITE OF GIZZARD MYOSIN? A REINVESTIGATION. ((Jean C. Grammer and Ralph G. Yount)), Dept. of Biochem. and Biophys., Washington State University, Pullman, WA, 99164-4660.

Previously, we have reported that both LC17 and the heavy chain (HC) of gizzard myosin were photolabeled by the ADP analog, NANDP (Okamoto *et al.*, (1988) *Nature* 324, 78.) We were confident of this unusual result because prior to irradiation, NANDP was trapped at the active site with vanadate and the complex purified by gel filtration. However, in extensive experiments since that time we have observed variable labeling of both the HC and LC17. Of a total incorporation of 11-16%, only about 20% was on LC17. This meant only 2-3% of LC17 was photolabeled. Even so, it was possible to isolate two labeled tryptic peptides which by compositional analysis and their inability to be sequenced identified them as coming from the blocked NH_2-terminus of LC17. However, the variable and very low incorporation led us as a control to block the active site with the photostable Co(II)ADP vanadate complex and add concentrations of 1, 2.5, 5, 10 and 20% of [^{32}P]NANDP per active site. Over 50% of this adventitious analog was photoincorporated with 90% of it labeling LC17. No protection was afforded by additions of ADP, ATP or PPi. These results suggest that photolabeling of LC17 is not active site related and occurs with the trace amounts of [^{32}P]NANDP which were not removed by gel filtration. The NH_2-terminus of LC17 appears to be unusually reactive to photolabeling by aryl nitrenes. Thus the active site of gizzard myosin is made up solely of the heavy chain as has been observed in labeling studies of other myosins. Supported by NIH (DK-05195) and MDA.

Tu-Pos53

CONFORMATION DEPENDENT PHOTO-CROSSLINKING IN GIZZARD MYOSIN WITH SPECIFICALLY LABELED REGULATORY LIGHT CHAINS. ((Jennifer J. Olney, Derek J. Pouchnik, Mark R. Tibeau and Christine R. Cremo.)) Biochemistry/Biophysics Program, Washington State University, Pullman, WA. 99164-4660.

Conformation dependent photocrosslinking of chicken gizzard myosin subunits has been examined by covalently labeling the regulatory light chain (RLC20) at two distinct sites with a photoreactive probe. Purified regulatory light chains (RLC20) were labeled on Ser-19 with benzophenone-4-iodoacetamide (BPIA), by use of the method of Facemyer & Cremo (1992) *Bioconjugate Chem.* 3, 408 - 413. Alternatively, Cys-108 was labeled with the same probe. Labeled RLC20 was exchanged onto whole myosin using a method given to us by Dr. K. Trybus (unpublished data). We typically achieve an efficiency of 50-90%, and the exchange procedure does not affect the myosin ATPase activity or the ability of the protein to undergo the 6S-10S transition. We used polyacrylamide gel electrophoresis to examine the pattern and extent of photocrosslinking after UV irradiation under conditions which favor various conformations of the myosin.

Cys-108 BPIA labeled RLC20 crosslinked to the heavy chain (HC) in a conformation dependent manner. This RLC-HC link is observed in the 10S form and the filamentous form, but does not occur in the 6S form. The same pattern of crosslinking occurs for Ser-19 BPIA RLC20 although the extent of RLC-HC crosslinking is less than that observed for the Cys-108 label. Ser-19 BPIA RLC20 also crosslinks to either the other RLC20 or to the essential light chain (LC17) in all myosin conformations with less efficient crosslinking apparent in the 10S form. Preliminary evidence with Cys-108 BPIA labeled RLC20 also shows intramolecular (within the RLC20) crosslinking which is not conformation dependent.

Tu-Pos54

CLEAVAGE OF SMOOTH MYOSIN AT 68 KD FROM N-TEMINUS ALTERS THE AFFINITY OF MYOSIN FOR ACTIN IN ATP.

M. Ikebe, S. Mitra and D. J. Hartshorne*, Dept. of Physiology and Biophysics, Case Western Reserve Univ., Cleveland, OH 44106 and * Dept. of Animal Science, Univ. of Arizona, Tucson, AZ 85721.

It is assumed that light chain phosphorylation ultimately changes the conformation of the ATPase site and actin binding site of smooth myosin, however, the mechanism is still obscure. It has been found that smooth muscle myosin forms 10S-6S myosins. We have proposed that part of the 10S-6S transition is involved in regulation and that the change in the conformation at the two sites is involved during the 10S-6S transition. One(B site) is at the head-neck junction and the other(A site) is located about 68kd from the N-terminus of the heavy chain. In this study, we investigated the significance of the A site on actin activated ATPase activity. S. aureus protease(SAP) produces S1 whose heavy chain is cleaved at the A site and it was found that acto S1 ATPase activity of SAP-S1 was markedly lower than that of papain S1. Subsequent digestion of SAP S1 by papain significantly activated the acto S1 ATPase activity. During the course of this activation, the regulatory light chain was degraded and a new 94 kd peptide from 68 kd and 26 kd was formed. The exchange of the undigested regulatory light chain to the papain digested S-1 did not decrease the ATPase activity and therefore it was concluded that the activation of ATPase was due to the formation of the 94kd peptide. The kinetic analysis revealed that the activation is due to the decrease in Kactin but not Vmax. The A site was identified as Glu 642-Ser 643 according to the sequence analysis. These results suggest that the A site is involved in the actin binding site of smooth muscle myosin during the ATPase cycle(supported by NIH and AHA).

Tu-Pos55

STRUCTURAL REQUIREMENTS FOR PHOSPHORYLATION OF MYOSIN REGULATORY LIGHT CHAIN FROM SMOOTH MUSCLE. ((Zhi, G., and Stull, J.T.)) Department of Physiology, UT Southwestern at Dallas, TX 75235

Synthetic peptide substrates of myosin regulatory light chains (RLCs) have been used to identify residues in the N-terminal domain important for phosphorylation by Ca^{2+}/calmodulin-dependent myosin light chain kinases (MLCK). However, these short peptides have altered phosphorylation properties with V_{max} values that are 10% or less of the homologous RLC. Therefore, site-directed mutagenesis has been used with human smooth muscle RLC to identify residues around Ser 19 that are important for phosphorylation by smooth muscle MLCK. Substitutions in the N-terminus (K11A, K12A, R13A, R16A and R13,16A) increased K_m values 4-8 fold with little or no change in V_{max} values. Deletion of N20, V21 and F22 individually or together increased K_m values 4-10 fold and decreased V_{max} values 6 fold. Interestingly, the exchange of N20 and F22 had no effect on the catalytic properties. Likewise, the addition of 3 A between A23 and M24 had no effect. Substitution of S19 with E resulted in a 17-fold increase and a 10-fold decrease in the K_m and V_{max} values respectively, presumably reflecting the phosphorylation properties of T18. These results support the hypothesis that basic and hydrophobic residues N- and C-terminal of S19, respectively, bind to the catalytic core of MLCK. However, because the changes in the relative specificity (V_{max}/K_m) of mutated RLCs are an order of magnitude less than changes reported for homologous synthetic peptides, structural determinants affecting phosphorylation properties appear to reside in other RLC domains.

Tu-Pos56

TIME-RESOLVED FLUORESCENCE STUDIES OF STABLE SMOOTH MUSCLE MYOSIN COMPLEXES WITH AlF_4^-, BeF_3^- AND Vi. ((R.Takashi, M. Ikebe and S.Maruta)) BRI, Baylor Univ. Med. Ctr., Dallas, TX 75226, Dept. of Physiol. and Biophys., Case Western Reserve Univ., Cleveland, Ohio 44106 and Dept. of Bioengineering, Soka Univ., Hachioji, Tokyo, Japan.

Maruta et al. (Biophys. J. 59:436a, 1991) reported that smooth muscle myosin in the presence of Mg.ADP forms the stable complexes with two phosphate analogues, AlF_4^- and BeF_3^-, which mimic the transient state of the ATP hydrolysis. We have performed a comparative study of the structure of the stable myosin.Mg.ADP complexes containing BeF_3^-, AlF_4^-, or Vi using time-resolved fluorescence spectroscopy. Two kinds of fluorescent analogues of ADP, 2'(3')-O-(N-methylanthraniloyl)adenosine diphosphate(Mant-ADP) and 1,N^6-ethenoadenosine diphosphate(εADP), were used to monitor changes in local environment near the ribose or adenine binding site of the stable complex. The fluorescence lifetime (τ) of Mant-ADP in solution is 4.3 ns at 10°C and this increases markedly upon the formation of the complex with the phosphate analogue at the active site of myosin, yielding 9.8 ns (Mg.Mant-ADP.BeF_3^-), 9.5 ns (Mg.Mant-ADP.AlF_4^-) and 9.1 ns (Mg.Mant-ADP.Vi), respectively. There is a small but reproducible decrease in τ of the Mant-ADP by the light chain phosphorylation or the conformational transition from 10S to 6S. The fluorescence lifetime of εADP free in solution is 26.7 ns and increases to 30.5 ns upon trapping on dephosphorylated myosin by AlF_4^- or BeF_3^- while that of εADP decreases to 16.7 ns when trapped at the active site by Vi. A small decrease in τ is also observed with myosin.Mg.εADP containing AlF_4^- or BeF_3^- upon phosphorylation or the 10S-6S transition whereas no differences in τ could be detected between dephosphorylated and phosphorylated myosin.Mg.εADP.Vi complexes or between 10S and 6S myosin. The results suggest that the conformation of the stable complexes is distinct from each other. Supported by Grants from BRI, NIH, AHA and Soka University.

Tu-Pos57
SMOOTH MUSCLE MYOSIN IS ACTIVATED BY POLYLYSINE VIA BINDING TO REGULATORY DOMAINS. ((P.T. Szymanski & R.J. Paul)). Dept. Physiol. & Biophys. Univ. of Cincinnati, Col. of. Med. Cincinnati, OH 45267-0567 (Spon. by S. Lehrer).

Polylysine (10-13 kDa) activates smooth muscle myosin ATPase activity by promoting a 10S to 6S transition. The effects of polylysine are neither simply attributable to ionic strength nor connected with phosphorylation/ dephosphorylation. However, its overall effect on the stabilization of unfolded form of myosin is similar to that of myosin light chain (MLC) phosphorylation, high salt or magnesium ions. To obtain further information on the mechanism of polylysine activation of smooth muscle myosin, we tested the hypothesis that the effects of polylysine were associated with binding, rather than indirect solution effects of polylysine. Our light-scattering evidence supports the direct binding hypothesis. We determined which subfragments of myosin were involved and thus differentiated between mechanisms involving regulatory site(s) and/or direct activation at the catalytic site for ATP hydrolysis. Our results indicate that polylysine has a similar effect to MLC phosphorylation in that they both stimulate ATPase activity in native myosin, tailless myosin, and HMM but do not activate the S1 subfragment. As such, polylysine may be a useful probe for identification of the regulatory domain(s) in smooth muscle myosin which play a critical role in its regulation. Supported by NIH HL22619 and AHA-F943.

Tu-Pos58
CLONING OF MOUSE SMOOTH MUSCLE MYOSIN ALKALINE LIGHT CHAIN GENE. ((T.E. Chang, Q. Wu, and D.R. Hathaway)) Krannert Institute of Cardiology, Department of Medicine, Indiana University, Indianapolis, IN 46202.

The mammalian smooth muscle myosin molecule consists of two heavy chains of 200 or 204 kD each, two 20 kD regulatory light chains and two 17 kD alkaline light chains (LC_{17}). Alternative splicing of the 3'-end of the LC_{17} gene produces two isoforms: LC_{17}a (pI=4.13) and LC_{17}b (pI=4.19), which differ by 9 amino acids at their carboxyl terminus. We have cloned the LC_{17} gene from mouse in order to study the functional significance of the LC_{17} isoforms in a transgenic animal model. The clone was identified by a 0.7 kb probe corresponding to the last intron of the LC_{17} gene from a mouse genomic library. This probe was made by PCR amplification using primers based on the sequence of exons 6 and 7 flanking the last intron. The positive clone was further subcloned into a plasmid as a 7 kb BamH I fragment that was used for sequencing and restriction mapping analyses. DNA sequencing shows that there are 2.7 kb from the first to the last exon. We have also obtained 1.5 kb and 0.46 kb at the 5' and 3'-end flanking regions, respectively. Comparison of the mouse and human genes revealed identical coding sequences. In general, corresponding introns were homologous, the least being intron E (68.7%) and the highest being intron F (80.9%). Computer analysis identified several potential eukaryotic promoter elements including CREB, MEF-1, and SP-1.

NONMUSCLE MYOSIN

Tu-Pos59
EXPRESSION OF A TRUNCATED FORM OF CHICKEN BRAIN MYOSIN THAT BINDS TO ACTIN IN AN ATP-DEPENDENT MANNER USING THE BACULOVIRUS EXPRESSION SYSTEM. ((M.D. Pato, Y.A. Preston, J.R. Sellers and R.S. Adelstein)) NHLBI, NIH, Bethesda, MD 20892.

Recently, our laboratory completed cloning cDNA encoding a chicken brain myosin heavy chain (MHC-B), in which some of the MHCs were found to contain inserted amino acids at the 25-50 and 50-20 junctions (Takahashi et al., J. Biol. Chem. 267: 17,864, 1992). We, therefore, initiated studies to express cDNA encoding the amino-terminal 1232 amino acids of the MHC (noninserted isoform) using the Baculovirus expression system. Approximately 3.7 kb of cDNA, including 74 nucleotides from the 5' untranslated end, were subcloned into pBlueBac and transfected along with wild-type baculovirus into Sf9 insect cells. The recombinant virus was used to infect Sf9 cells and overexpress a truncated (150 kD) MHC. A similar scheme was used to express the 17 kD MLC from bovine aorta, except that BlueBac-2 was used as transfer vector. Coinfection of Sf9 cells with MHC and MLC led to overexpression of a truncated form of myosin (not containing the 20 kD MLC), which, on partial purification using Sepharose 4B, had the following properties: 1) Immunoblot analysis showed that both the 150 kD MHC and 17 kD MLC were recognized by appropriate antibodies. 2) Most of the partially purified expressed myosin bound to rabbit skeletal actin in an ATP-dependent manner.

Tu-Pos60
CYCLIN-p34^{cdc2} KINASE PHOSPHORYLATES AN ISOFORM OF NONMUSCLE MYOSIN HEAVY CHAIN-B. ((C.A. Kelley, J.H. Yu and R.S. Adelstein)) NHLBI, NIH, Bethesda, MD 20892. (Spon. by M.A. Conti)

The regulation of the cellular reorganization of myosin during mitosis is unknown. Recently, a small amount of mRNA encoding brain and spinal cord myosin heavy chain-B (MHC-B) was found to contain an insert of 30 nucleotides encoding 10 amino acids located near to the ATP binding region. This insert, PESPKPVKHQ, contains a consensus sequence for cyclin-p34^{cdc2} (cdc2) kinase phosphorylation (Takahashi et al., J. B. C. 267: 17864, 1992). A similar inserted sequence was found by Bhatia-Dey et al. (see abstract, this meeting) during the cloning of a cDNA encoding MHC-B from Xenopus XTC cells. This insert retains the putative cdc2 kinase site. Coomassie blue staining and immunoblot analysis of MHCs from XTC cells revealed 2 minor bands which were recognized by antibodies specific for all MHC-B isoforms as well as by antibodies raised against a peptide synthesized based on the Xenopus inserted sequence. In addition, there was a major band that only crossreacted with nonisoform-specific antibodies to MHC. Following immunoprecipitation with MHC-B-specific antibodies, both MHC-B polypeptides served as substrates for cdc2 kinase (from F. Matsumura, Rutgers University). This kinase did not catalyze phosphorylation of the other MHC found in XTC extracts nor the 20 kD myosin light chains.

Tu-Pos61
SECRETION FROM BASOPHILIC RBL-2H3 CELLS IS ASSOCIATED WITH PHOSPHORYLATION OF MYOSIN LIGHT CHAINS BY MYOSIN LIGHT CHAIN KINASE AND PROTEIN KINASE C. ((O.H. Choi, R.S. Adelstein and M.A. Beaven)) NHLBI, NIH, Bethesda, MD 20892

Previously, we have shown that the phosphorylation of myosin light chains (MLCs) and heavy chains by protein kinase C (PKC) is temporally correlated with Ca^{2+}-dependent secretion of granules (Ludowyke et al., *J. Biol. Chem.* 264, 12492, 1989). We now report that whereas MLCs were phosphorylated by the Ca^{2+}/CaM-dependent MLC kinase (MLCK) predominantly at ser-19 in unstimulated cells, stimulation of RBL-2H3 cells with antigen or other stimulants caused increased phosphorylation of MLCs by MLCK at an additional site (thr-18). This phosphorylation by MLCK and the phosphorylation by PKC at ser-1 or ser-2 correlated with the rate of degranulation. Secretion occurred whenever phosphorylation by both enzymes was stimulated by antigen or high concentration of Ca^{2+}-ionophore, A23187 (500 nM) or the combination of low concentration of A23187 (50 nM) and phorbol 12-myristate 13-acetate (PMA, 20 nM). However, PMA which induced phosphorylation of MLCs only by PKC failed to cause secretion of granules. Conversely, selective suppression of phosphorylation by PKC (with Ro31-7549 in antigen-stimulated cells) or by MLCK (with KT5926 in PMA/A23187-stimulated cells) suppressed degranulation. The present results suggest that phosphorylation of MLCs by both PKC and MLCK is necessary for exocytosis in RBL-2H3 cells.

Tu-Pos62
EFFECT OF BACTERIAL TOXINS ON ENDOTHELIAL CELL MYOSIN LIGHT CHAIN PHOSPHORYLATION AND BARRIER FUNCTION.
(J.G.N. Garcia, H.W. Davis, C.E. Patterson and M.A. Goddard)) Department of Medicine, Indiana University School of Medicine, Indianapolis, IN.

Endothelial cell (EC) barrier dysfunction results in part from contraction of the EC. We hypothesize that phosphorylation of myosin light chains (MLC) by myosin light chain kinase, an obligatory step in smooth muscle contraction, is critical to nonmuscle cell contraction. To examine this, we evaluated MLC phosphorylation and contraction of bovine pulmonary artery EC in response to thrombin, pertussis toxin (PT) and cholera toxin (CT). Contraction was assessed both histologically and by EC monolayer permeability to albumin. MLC phosphorylation was determined by urea gel electophoresis and immunoblotting with an MLC-specific antibody. Thrombin-induced (1μM) contraction was maximal at 20 min, as evidenced by a 540% increase in albumin clearance. Maximal MLC phosphorylation occurred by 2 min and then declined. While PT had no effect on basal or thrombin-induced MLC phosphorylation, PT caused a dose-dependent (10 ng/ml to a plateau, 520% increase, at 1μg/ml) increase in albumin transfer across EC and produced an additive increase (900%) in permeability over the maximal thrombin-induced permeability. CT partially blocked thrombin-induced MLC phosphorylation (by ~ 50%) and completely inhibited thrombin-permeability. Downregulation of protein kinase C (PKC) by phorbol myristate acetate (24h, 0.1 μM) attenuated both thrombin-induced MLC phosphorylation and thrombin- and PT-induced albumin clearance (by ~ 50%). These results provide evidence that 1) MLC phosphorylation is involved in thrombin but not PT-induced EC contraction, 2) PKC is partially responsible for the PT- and thrombin-induced events and 3) cAMP (increased by CT) blocks PT- and thrombin-induced EC permeability and thrombin-induced MLC phosphorylation.

Tu-Pos63

EXPRESSION OF A 47 kDa COOH-TERMINAL FRAGMENT OF BRAIN MYOSIN. ((M. Elzinga[1], N. Murakami[1], K. Okajima[1], S.S. Lehrer[2], and W.F. Stafford[2])), [1]New York State Institute for Basic Research, Staten Island, N.Y., and [2]Boston Biomedical Research Institute, Boston, MA. (Spon. J.K. Setlow).

A 47 kDa fragment that corresponds to the COOH-terminal 405 amino acid residues of rabbit non-muscle myosin II B has been expressed and purified. cDNA, generated by PCR using primers based upon the sequence of Kuro-o et al (JBC 266, 3768 [1991]) and mRNA isolated from rabbit brain, was ligated into *Bam* HI and *Sal* I sites in the plasmid pND1-R, and expressed in E. coli. The 405 residues include 361 that are assumed to form α-helical coiled-coils, and 44 that constitute a non-helical "tail piece". The fragment contains two phosphorylation sites, a protein kinase C site near the COOH-end of the α-helical region, and a casein kinase II site within the non-helical region. The fragment exhibits salt-dependent polymerization; analytical ultracentrifugation studies at 20° C show that it is primarily monomeric (2.6 S) at 0.5 M NaCl; at 0.25 M NaCl only about 30% remains as monomer, the remainder forming high molecular weight polymers. Circular dichroism studies confirm that the fragment is primarily α-helical; in 0.5 M NaCl it melts with a single reversible transition at 53°C. At lower salt concentrations, at which the fragments polymerize, the CD melting profile is essentially unchanged, suggesting that the polymers dissociate before the α-helix melting temperature is reached. Results of studies of the effect of phosphorylation upon the physical properties of the fragment will be presented.

Tu-Pos64

PHOSPHORYLATION OF A 47kDa FRAGMENT OF BRAIN MYOSIN BY CASEIN KINASE II AND PROTEIN KINASE C. ((Noriko Murakami and Marshall Elzinga)), New York State Institute for Basic Research in Developmental Disabilities, Staten Island, NY.

The phosphorylation site for casein kinase II is conserved in both nonmuscle and smooth muscle myosin heavy chains, while the site for protein kinase C seems to be conserved for all nonmuscle myosin heavy chains. Because these phosphorylation sites lie near tail end of the nonmuscle and smooth muscle myosins, the region responsible for filament formation, we are examining the role of phosphorylation of the heavy chain in regulation of mammalian myosin filament formation. These myosins contain protein kinase C sites in both their light and heavy chains, and therefore native myosin molecules are not appropriate for such studies. Thus, a 1.2 kb fragment of rabbit brain myosin heavy chain cDNA (Kuro-o et al., 1991, J. Biol. Chem., 266, 3768) coding the COOH-terminal 405 amino acid residues was expressed in E. coli. The purified fragment formed filaments at and below physiological salt concentrations. Addition of 10 mM $MgCl_2$ to the fragment at physiological salt concentrations, conditions generally used for casein kinase II, significantly enhanced the turbidity at 340 nm, indicating that $MgCl_2$ stimulated filament formation. Under these conditions, casein kinase II incorporated one mol of phosphate per mol of the fragment. Protein kinase C also incorporated 1 mol/mol, but high salt, which dissolved the filaments, was required. These results indicate that the phosphorylation site for casein kinase II is exposed on the surface of the filament while the site for protein kinase C lies within the assembly region, sterically hindered within the filament. Phosphorylation by protein kinase C did not inhibit phosphorylation by casein kinase II, and up to 2 mol of phosphate could be incorporated into the fragment. Studies on the effect of phosphorylation by these kinases on the assembly of the fragment are in progress.

Tu-Pos65

EFFECTS OF ATP ON THE CONFORMATION OF MYOSIN II FROM ACANTHAMOEBA CASTELLANII. ((M.J. Redowicz and E.D. Korn)) Laboratory of Cell Biology, NHLBI, NIH, Bethesda, MD 20892.

Acanthamoeba myosin II is a conventional myosin whose actin-activated Mg^{2+}-ATPase and motility activities are regulated by phosphorylation of the C-terminal end of the heavy chains. Our recent studies revealed a strong interaction between the head portion and the tip of the tail. By limited papain proteolysis, we now show an effect of ATP on the conformation of both monomeric and filamentous Acanthamoeba myosin II. Papain splits the myosin heavy chain into 2 major fragments: 73-kDa head and 112-kDa rod. ATP caused the further degradation of the 73-kDa fragment of both monomeric myosins to a 60-kDa derivative. ATP also affected the conformation of the C-terminal rod segment of filamentous phosphorylated myosin II; a 9-kDa C-terminal peptide that contained the phosphorylation sites was produced only in the presence of nucleotide. This cleavage was not observed for dephosphorylated myosin II. The latter result supports the idea of unique communications between the head and tail regions of phosphorylated Acanthamoeba myosin II.

Tu-Pos66

CLONING OF THE cDNA ENCODING THE MYOSIN HEAVY CHAIN B ISOFORM OF XENOPUS NONMUSCLE MYOSIN WITH AN INSERT IN THE HEAD REGION. ((N. Bhatia-Dey, R.S. Adelstein and I.B. Dawid)) NICHD and NHLBI, NIH, Bethesda, MD 20892.

The complete amino acid sequence of Xenopus nonmuscle myosin heavy chain B (MHC-B) has been deduced from overlapping cDNA clones isolated from an XTC cell library. RNA blots of various developmental stages, adult tissues and XTC cells detect a single transcript of 7.5 kb which is expressed ubiquitously at similar levels throughout development. MHC-B mRNA was also detected in ovary, testis, spleen, pancreas, stomach, liver, heart, lung, eye, brain and XTC cells, but not in kidney and skeletal muscle. The mRNA is relatively abundant in heart, lung, spleen and brain, and even more abundant in XTC cells. Protein expression in adult tissues, as visualized by immunoblot analysis, correlates well with mRNA expression. In chickens, a small amount of mRNA encoding the MHC-B isoform was found to contain a 10 amino acid insert at amino acid 211 near to the ATP binding site. This inserted isoform is nervous system-specific (Takahashi et al., J. Biol. Chem. 267: 17,864, 1992). The Xenopus sequence shows a 16 amino acid insertion at the same position; 7 out of 16 residues are identical to the chicken insertion. In contrast to chicken, all tissues and embryonic stages tested contained the inserted form, and no evidence for a non-inserted MHC-B isoform was found in Xenopus.

Tu-Pos67

INTESTINAL BRUSH BORDER MYOSIN I TAIL CONTAINS ACTIN BINDING SITE AND SH3-LIKE REPEATS RELATED TO SEQUENCE IN THE MYOSIN HEAD. ((H. Swanljung-Collins and J.H. Collins.)) Department of Biochemistry, Eastern Virginia Medical School, Norfolk, VA 23501.

The tail of BBMI has previously been shown to contain four calmodulin-binding sites and two lipid-binding domains. We show here that the tail of BBMI contains an actin binding site believed to be a requirement for monomeric myosins to superprecipitate and to crosslink actin. Analysis of the primary structure of the tail reveals similarity to sequence in both gelsolin and alpha-actinin. Gelsolin-like sequence is observed also in the reactive thiol domain and in other highly conserved domains in the head, suggesting that myosin may have formed through duplication of an ancestral actin-like gene like other actin binding proteins. The duplication events appear to have extended throughout the myosin I tail, which was previously thought to not be related to the head. The reactive thiol domain of myosin I is as similar to a segment in actin as is the corresponding sequence in gelsolin. This relatedness to other actin binding proteins and to actin emphasizes the possibility of a common ancestor of the myosin family of motor proteins and a growing group of other actin binding proteins containing multiple actin related segments.

The internal repeat nature of the BBMI carboxyterminal half is more conserved in BBMI than in Acanthamoeba myosins IB and IC and contains four 60-65 residue segments, each 60% homologous to the highly conserved src-homology-domain 3 present in the Acanthamoeba myosins I, but missing in the BBMIs. Dot matrix and Chou-Fasman analysis support our claim that the SH3 domain belongs to the series of internal tail repeats of this type of myosin I.

Tu-Pos68

MYOSIN I IN MAMMALIAN SMOOTH MUSCLE IS REGULATED BY CALDESMON-CALMODULIN. ((S. Chacko, S. S. Jacob and K.Y. Horiuchi) Dept. of Pathobiology, Univ. of Pennsylvania, 3800 Spruce St., Philadelphia, PA

Myosin I, the single headed small myosin, is thought to be ubiquitous to all non-muscle cells. Its role in mediating motility in Acanthamoeba and Dictyostelium has been studied extensively. Myosin I is also shown to be present in intestinal brush border and adrenal cells of vertebrates. In this study, we isolated and characterized myosin I from pig urinary bladder smooth muscle. Myosin I from smooth muscle is a soluble protein with a 117-120 kDa heavy chain and 20 kDa light chain. The Mg-ATPase activity of this myosin is very low (0.002-0.006 μmol pi per mg per min at 30°C). Smooth muscle actin causes a 10-20 fold activation of the ATPase activity both in the presence and absence of Ca^{2+}. Tropomyosin has no effect on the actin-activation. Caldesmon inhibits the actin-activated ATPase activity, and this inhibition is released by Ca^{2+}-Calmondulin. Hence, the single headed myosin I which is thought to play a role in non-muscle cell motility also exists in mammalians smooth muscle cells, and it is Ca^{2+} regulated by calmodulin-caldesmon. Supported by NIH grants DK 39740 & HL 22264.

Tu-Pos69

PHOTOCHEMICAL CLEAVAGE OF ACTIN OCCURRED AT ALMOST CENTER OF THE AMINO ACID SEQUENCE

Yoh OKAMOTO and Takashi SUMITA Department of applied chemistry, Muroran Institute of Technology, Muroran, Hokkaido 050 Japan

Dynein, myosin and adenylate kinase show vanadate dependent cleavage upon irradiation of UV light with 300nm or longer wave length. These photochemical cleavage reaction are quite site specific because of very limited number of vanadate binding sites exist. Actin has been known to undergo exchange and hydrolysis of bound nucleotide. Under those conditions, various conditions of irradiation were examined about the ability of specific cleavage reaction. G-actin has been cleaved at a specific site resulting in appearance of 22kDa and 20kDa fragments. The alignment of the two is determined as this order from the amino terminal end of actin. These two appears to be folded together as before the cleavage but hard to polymerize in the presence of KCl, $MgCl_2$, phalloidin or myosin subfragment one.

Supported by Grant-in-Aid for Scientific Research on Priority Area:"Vascular Endothelium-Smooth Muscle Coupling", from the Ministry of Education, Science and Culture, Japan and by Kuribayashi Science Foundation.

Tu-Pos70

ATOMIC FORCE MICROSCOPY OF COVALENTLY AND ELECTROSTATICALLY IMMOBILIZED F-ACTIN

((David Braunstein, James A. Spudich and *Calvin F. Quate)) Depts of Biochemistry and *Applied Physics Stanford University, Stanford CA 94305

A central problem in the imaging of non-membrane proteins, especially myofibril proteins, in solution, by Atomic Force Microscopy (AFM) has been the need to have the protein tightly adsorbed to a substrate. The present work demonstrates two methods for immobilizing rhodamine-phalloidin stabilized F-actin (Rh-Ph-F-actin) in buffered solution for imaging by AFM. Covalent immobilization was acheived using a cleaved mica surface treated in sucession first with an amino-silane and then glutaraldehyde, providing an amide-carboxyl linkage to the protein surface. Electrostatic immobilization was accomplished on a polished sapphire surface, positively charged at neutral pH. The covalent surfaces bind protein independent of surface charge, but are not as smooth as the polished sapphire, which provides a clean, hard, flat substrate that complements the negative surface charge of F-actin. In both cases, paracrystalline arrays of Rh-Ph-F-actin filaments formed on the surface. The adsorbed filaments display an apparent width of ~100-200 Å, and in the sapphire data, periodic structure can be seen along the filaments, reproducibly, in several images. Even with its limited resolution, AFM should be able to image other myofibril protein assemblies in solution.

Tu-Pos71

NORMAL MODES OF G-ACTIN

Monique M. Tirion*, Daniel Ben Avraham*, & Kenneth Holmes. Max-Planck-Institute for Medical Research, Heidelberg, Germany, * Permanent address: Clarkson University, Physics Department, Potsdam NY 13676.

We undertook a normal mode analysis of the G-actin monomer bound with ADP and Ca^{++}, in order to better understand the internal modes of this protein. The internal coordinates consisted of 1373 single bond torsions, plus an additional 11 torsions to parameterize the motion of the nucleotide and cation with respect to the protein. A generalized eigenvalue problem was solved to yield a complete description of the motion in the 0.1 to 17.0 picosecond time range. The modes were visualized using an interactive graphics routine. The softest, slowest modes include a propeller-like twisting of the large and small domains about the phosphate binding loops; a rolling of subdomain 4 about an α helix axis; and a scissor-type opening and closing of the ADP-binding cleft. The computed temperature factors agree well with experimental ones. A comparable analysis done on G-actin-ATP revealed that the softest modes are highly similar.

Tu-Pos72

F-ACTIN CAN EXIST IN AT LEAST SEVERAL DIFFERENT CONFORMATIONS.

((A. Orlova and E.H. Egelman)) Univ. of Minnesota Medical School, Minneapolis, MN 55455.

A model exists (Holmes *et al., Nature* **347**,44) for the orientation of the G-monomer into the F-filament, but several important questions exist concerning the possibility of conformational changes between G and F and the role of nucleotide hydrolysis. We have shown (Orlova and Egelman, *J. Mol. Biol.* **227**,1043) that the actin subunit exists in two different conformations as a function of ATP hydrolysis and phosphate release. We can now visualize a third conformation of the subunit that results in a filament with a greatly increased flexibility. This conformation can be induced by polymerizing G-Mg^{2+}-ATP with only Mg^{2+}, ensuring that all of the metal-binding sites in actin are occupied by Mg^{2+}, and not Ca^{2+} or K^+, or by using a brominated-ATP (Hegyi *et al., Eur. J. Biochem.* **175**, 271). The flexible actin can also be produced by polymerizing F-Mg^{2+}-ADP from G-Mg^{2+}-ADP (Janmey *et al., Nature* **347**, 95). We measure the same correlation length, about 1.6μ (as opposed to about 6.0μ for "normal" actin), for the flexible actin produced by these different methods, suggesting that this is a well-defined structural state and not the result of denaturation or amorphous aggregation. A 3-D reconstruction of this state shows that it arises from an approximately 18° domain-domain rotation. Such large conformational changes within actin have many implications for muscle and other systems.

Tu-Pos73

ROTATIONAL DYNAMICS IN F-ACTIN STUDIED BY TIME-RESOLVED PHOSPHORESCENCE ANISOTROPY.

((E.Prochniewicz, Q.Zhang, A.Orlova, E.H.Egelman and D.D.Thomas)) University of Minnesota, Minneapolis, MN 55455

Dynamic properties of F-actin were studied using time-resolved phosphorescence anisotropy (TPA). F-actin was labeled at Cys 374 with two phosphorescent dyes: Erythrosin Iodoacetamide (ErIA) and Eosin Iodoacetamide (EoIA). In all samples of labeled actin we observed microsecond decays of the phosphorescence anisotropy, indicating intrafilament rotational motions in F-actin. The rate of anisotropy decay changed in the presence of phalloidin and after exchange of tightly bound ADP into its derivative, BrADP, but the changes were more pronounced for ErIA-labeled than for EoIA-labeled actin. The data were analysed by fitting TPA decays to restricted rotation of monomers in F-actin and torsional movement of the whole filament. These molecular dynamic results were further correlated with structural studies using 3D reconstruction of electron microscope images of negatively stained phosphorescent F-actin and with studies on functional properties of actin, including in vitro motility assay and activation of myosin ATPase. This approach enables us to correlate local structural changes in actin monomers with changes in functional and dynamic properties of the whole filament.

Tu-Pos74

INTERNAL DYNAMICS AND STRUCTURE OF FREE AND MEMBRANE COUPLED ACTIN

((E. Sackmann, J. Käs, H. Strey and G. Isenberg)) Physics Department, Technical University Munich, D-8046 Garching, Germany

The structure and dynamics of transiently and chemically cross-linked actin networks was studied by quasielastic light scattering (QELS), microrheology and single filament flicker spectroscopy. Surprisingly, the dynamic structure factor obeys exactly the same scaling laws as completely flexible Rouse-Zimm chains. Moreover, the frequency, concentration and length dependencies of the viscoelastic parameters obey the same scaling laws as semidilute solutions of high molecular weight synthetic polymers. The persistence length of $L_p \approx 0.3\mu m$ and thus the filament bending stiffness obtained from these power laws is orders of magnitude smaller then the values determined by end-to-end distance measurements. As shown by flicker spectroscopy of single filaments this discrepancy can by explained by a strong decrease of the bending modulus with decreasing (undulation) wavelength of the bending excitation. Other topics presented are the role of the short wavelength excitations for the chain repulsion via undulation forces and the electrostatic coupling of actin networks to partially charged lipid bilayer membranes by taline and hisactophillin.

Tu-Pos75

EFFECTS OF THE TIGHTLY BOUND DIVALENT CATION ON ACTIN TRYPTOPHAN FLUORESCENCE

((L.A. Selden, H.J. Kinosian, J.E. Estes, and L.C. Gershman)) Research and Medical Service, Stratton VA Medical Center, Albany, N.Y. and Departments of Physiology and Medicine, Albany Medical College, Albany, N.Y.

We have investigated the effects of the tightly bound divalent cation on the tryptophan fluorescence characteristics of actin. Experiments using Ca-actin were in good agreement with the earlier work of Kerwar and Lehrer (Biochemistry 11:1211-1217, 1972), and the tryptophan fluorescence of Ca-actin monomer was found to decrease about 10% upon polymerization, as they reported. Mg-ATP-actin monomer, however, exhibits 6-7% higher emission fluorescence intensity than Ca-ATP-actin monomer and, on polymerization, Mg-ATP-actin decreases 23% in fluorescence. This difference between Mg-actin and Ca-actin was not noted by Kerwar and Lehrer, most likely because the very high affinity (and the resultant slow exchange characteristics) of the actin-bound divalent cation was not appreciated at the time. Removal of the divalent cation from the high affinity site results in formation of monomeric divalent-cation-free-actin which exhibits an emission spectrum similar to that of Mg-ATP-actin monomer. It was necessary to remove the cation at 5° C in the presence of excess ATP in order to prevent denaturation of the DCF-actin. Denaturation of actin results in a characteristic shift in the emission spectrum as noted by Kerwar and Lehrer. These changes in fluorescence allow observation of divalent cation exchange and polymer formation using native actin at concentrations as low as 0.2μM. The use of native actin rather than fluorescent-labeled actin eliminates the possibility that the integrity of the actin is compromised by the presence of the fluorescent label. Supported by the Department of Veterans Affairs and NIH Grant GM 32007.

Tu-Pos76

EFFECT OF 18-29 ACTIN PEPTIDE ANTIBODIES ON ACTIN POLYMERIZATION AND NUCLEOTIDE EXCHANGE

S.B.Adams and E.Reisler, Dept. of Chemistry and Biochemistry and Molecular Biology Institute, UCLA, Los Angeles, CA 90024

Previous studies showed that peptide antibodies specific for the 18-29 amino acid sequence on actin inhibited acto-S1(ATP) interactions (Adams and Reisler, Biophys.J. 61:A440, 1992). To examine the structural role of the 18-29 sequence and the effect of antibody on the conformation of actin we examined the nucleotide exchange and the polymerization of actin in the presence of this antibody. Pyrenyl fluorescence showed that IgG (18-29) inhibited $MgCl_2$ polymerization of G-actin by up to 3-fold but did not reduce the polymerization by 0.1M NaCl. Similar reduction of $MgCl_2$ polymerization of actin by IgG (18-29) was also observed when monitoring this process via ε-ATP fluorescence of actin. The presence of the antibody also decreased the rate of nucleotide exchange from G-actin by approximately two-fold. These results suggest that the perturbation of the nucleotide cleft by 18-29 antibodies may be linked to changes in the $MgCl_2$ polymerization of actin.

Tu-Pos77

FLUORESCENCE POLARIZATION STUDY OF ACTIN FILAMENT BUNDLES IN *LISTERIA*-INFECTED CELLS. ((V.Zhukarev, F.T. Ashton, J.M. Sanger, J.W. Sanger, H. Shuman.)) Depts. of Physiology and Cell and Developmental Biology, Univ. Pennsylvania Medical School, Philadelphia, PA

We have used the technique of fluorescence polarization to examine the orientation of the actin filaments that form a column behind *Listeria* bacteria that are moving in host cell cytoplasm. The actin filaments comprising the column are short, and polymerization of additional actin occurs at the bacteria-column interface. A detailed picture of the actin filament organization has not yet been obtained, but would be valuable for understanding the role that the actin filaments play in generating the bacteria motility. Polymerization itself may provide the force to push the bacteria forward, or the actin filaments may need to be aligned so that a myosin motor can interact to move the bacteria. The actin filaments were labeled by the fluorescent probe, rhodamine phalloidin, shown previously (Kinoshita et al., J. Cell Biol. 115: 67-73,1991) to be well aligned along the actin filament axis. The probe was excited with incident polarized light applied parallel (ll) or perpendicular (⊥) to the microscope optical axis. The intensity (I) of polarized fluorescence was measured at each orientation and polarization ratios (P) were calculated: $P_{ll} = (I_{ll\,ll} - I_{ll\,\perp})/(I_{ll\,ll} + I_{ll\,\perp})$ and $P_{\perp} = (I_{\perp\perp} - I_{\perp\,ll})/(I_{\perp\perp} + I_{\perp\,ll})$. With proper orientation of bacteria images $P_{ll}/P_{\perp} = 1.5 - 2.0$ in the region directly behind the bacteria, whereas this ratio is lower in more distal regions of the actin column and in the edges of the tail it is about 1.0. These data indicate that the actin filaments are orientated parallel to the long axis of the column, the most recently polymerized actin filaments are the most highly ordered, and the alignment of filaments is less ordered in the distal regions of the tail and along the lateral edges; conclusions that are supported by electron microscopic data.

Tu-Pos78

NEBULIN IS AN ACTIN-BINDING, LENGTH REGULATING TEMPLATE PROTEIN OF THE THIN FILAMENTS OF SKELETAL MUSCLE: ACTIN-INTERACTION AND CONFORMATION OF A TWO-MODULE HUMAN NEBULIN FRAGMENT. ((M. -J. Chen, C. -L. Shih, & K. Wang)) Clayton Found. Biochem. Inst. Dept. Chem. Biochem. UT Austin Tx. (Spon. by J. Stames)

Nebulin, a family of giant myofibrillar proteins of 600-900 kd, has been proposed as a length-regulating template for the thin filaments of skeletal muscle. Sequence analysis indicated that nebulin contains a large number of highly conserved sequence repeats of 31 to 38 residues (35 on average for each module) which are thought to be building blocks for actin-binding domains along the length of nebulin. We have recently reported that cloned human nebulin fragments containing 6, 7, 8 and 15 modules bind F-actin with high affinity. However, a two-module fragment, ND8, failed to interact with actin under similar conditions (Jin & Wang (1991) *JBC* 266:21215).

We report that highly soluble ND8 preparations purified by an improved protocol do interact with actin. Fluorescence studies of actin polymerization in the presence of ND8 revealed that ND8 reduced the critical concentration and abolished the lag phase of actin polymerization. F-actin cosedimentation assays demonstrated a binding stoichiometry of 2.5 moles of ND8 to one mole of actin. Conformation studies of ND8 by CD, fluorescence, hydrodynamic techniques, and 1-D and 2-D NMR indicated that, contrary to computer sequence prediction, only a maximum of 10% α-helix and 20% β-sheet were detected. Thus, ND8 is not highly structured in aqueous solution.

Our studies indicate that one, or no more than two, nebulin module is required for actin binding. It follows that each nebulin molecule may contain as many as 100-200 actin-binding domains to form a zipper-like nebulin/actin composite filament.

Tu-Pos79

THE VISUALIZATION OF ACTIN FILAMENTS IN SKELETAL MUSCLE FIBRILS WITH FLUORESCENT PHALLOTOXINS ((Danuta Szczesna and Sherwin S. Lehrer)) Boston Biomedical Research Institute, 20 Staniford Street, Boston MA 02114.

Rhodamine-phalloidin was used to visualize actin filaments within myofibrils on the stage of a fluorescence microscope. Initial incubation with excess dye resulted in preferential binding to the ends of actin filaments forming a fluorescent band at the Z-line and a doublet or singlet band in the middle of long and short sarcomeres, respectively. Long time incubation (1-3 hours) resulted in a final pattern of brightly fluorescent Z-bands in the center of uniformly labeled actin I-bands. Measurements of the fluorescence intensities showed that the Z-band contributed 2X the intensity of the I-band. Ghost fibrils showed similar behavior indicating that attached myosin heads did not affect the dye binding. Thus: i) in contrast to isolated actin filaments where short incubation times result in uniform binding, long incubation times are required for uniform binding of dye to actin in fibril, due to the greater rigidity imposed by the sarcomeric structure; ii) the 2X greater actin concentration in the Z-band compared to the I-band confirms recent structural studies (Morris, E.P. et al., J. Cell Biology 111, 2961, 1990; Luther, P.K., J. Cell Biology 113, 1043, 1991); iii) although the small phallotoxin can penetrate the Z-lattice to bind to actin, myosin or tropomyosin are excluded (Szczesna, D. and Lehrer, S.S., Biophys. J. 61, 993, 1992).

Tu-Pos80

ORIENTATION OF ACTIN CORES IN MICROVILLI OF INTESTINAL EPITHELIAL CELLS. ((J. Borejdo, S. Burlacu & J.S. Fordtran)) Baylor Research Institute, Baylor University Medical Center, 3812 Elm St., Dallas, TX 75226

We measured conformation of actin cores in microvilli of epithelial cells from chicken intestine. F-actin was labeled with rhodamine-phalloidin and the orientation of the absorption dipole of rhodamine dye immobilized on the surface of F-actin was measured by polarization of fluorescence. The orientation and the degree of order of fluorophores was the same regardless of whether microvillus formed a part of a brush border or whether it was isolated. Polarization of fluorescence of isolated MV in the absence of nucleotide was consistent with little disorder of fluorophores and with a majority of fluorophores forming an angle Θ=52° with respect to the microvillar axis. The results of 38 experiments in which vertical polarization was measured in the absence of ATP are plotted in the figure (filled circles). The data is plotted in histogram form, i.e. polarization is plotted vs. the percentage of measurements which gave the particular value of polarization. When MV's were activated by ATP, the distribution and the mean of vertical polarization of fluorescence changed, suggesting an increase in disorder and a change in average angle to 54°. The results of 58 experiments in the presence of ATP are plotted as open cirles. The 0.062 difference in the means was statistically highly significant with t=2.39 (P=0.02). These results show that "shaving" of brush borders during preparation of isolated microvilli did not distort structure of actin cores, and suggest that mechanochemical interactions between actin and myosin-I result in transformation of polymer structure of actin in cores. Supported by NIH.

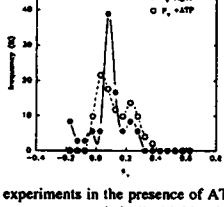

Tu-Pos81

EVIDENCE THAT GELSOLIN SEVERING ACTIVITY IS GREATER WITH Mg-ACTIN THAN WITH Ca-ACTIN.

((L.C. Gershman[2,3,4], L.A. Selden[1], H.J. Kinosian[3], and J.E. Estes[1,3],)) Research[1] and Medical[2] Services, Stratton Dept. of Veterans Affairs Medical Center, Albany, NY 12208, and Departments of Physiology and Cell Biology[3] and Medicine[4], Albany Medical College, Albany, NY 12208.

The divalent cation tightly-bound to actin is most likely Mg^{++} *in vivo*, but is typically Ca^{++} in *in vitro* preparations. Unless care is taken to pre-exchange the divalent cation, polymerization procedures will typically lead to a polymer of heterogeneous composition with respect to the tightly-bound divalent cation. Experiments using homogeneous polymers of Mg-actin and Ca-actin can be performed under identical conditions because the exchange of the tightly bound cation is extremely slow in the polymer. We have prepared homogeneous polymers of Ca-actin and Mg-actin and tested the ability of rat plasma gelsolin to sever both types of polymer. Solutions of both polymers were diluted 100-fold to 50 nM into polymerizing buffer containing various concentrations of gelsolin in the presence and absence of Ca^{2+}. In the presence of Ca^{2+}, a plot of depolymerization rate vs. gelsolin concentration resulted in a straight line with a slope for Mg-actin about twice that for Ca-actin. Mg-actin appears to be less affected by removal of the Ca^{2+} than Ca-actin. The results suggest a difference in conformation between Ca-F-actin and Mg-F-actin and that, in vivo, gelsolin may not require a bound Ca^{2+} for its severing activity. Supported by Dept. of Veterans Affairs and NIH Grant GM-32007.

Tu-Pos82

AFFINITY OF ALPHA-ACTININ FOR ACTIN DETERMINES THE STRUCTURE AND MECHANICAL PROPERTIES OF ACTIN FILAMENT GELS. ((D.H. Wachsstock, W.H. Schwarz, and T.D. Pollard)) Departments of Cell Biology and Anatomy and Chemical Engineering, Baltimore, MD 21205.

Proteins that crosslink actin filaments can either form bundles of parallel filaments or isotropic networks of individual filaments. We have found that mixtures of actin filaments with α-actinin purified from either *Acanthamoeba castellani* or chicken smooth muscle can form bundles or isotropic networks depending on the concentration. Low concentrations of α-actinin with actin form networks indistinguishable in electron micrographs from gels of actin alone. Higher concentrations of α-actinin and actin form bundles. The threshold for bundling depends on the affinity of the α-actinin for actin. The binding of *Acanthamoeba* α-actinin to actin filaments has a K_d of 4.7 μM and a bundling threshold of 0.1 μM; chicken smooth muscle has a K_d of 0.6 μM and a bundling threshold of 1 μM. The physical properties of isotropic networks of crosslinked actin filaments are very different from a gel of bundles: the network behaves like a solid because each actin filament is part of a single structure that encompasses all the filaments. Bundles of filaments behave more like a very viscous fluid because each bundle, while very long and stiff, can slip past other bundles. We have developed a computer model that predicts the bundling threshold based on four variables: the length of the actin filaments, the affinity of the α-actinin for actin, and the concentrations of actin and α-actinin. Supported by NIH Research Grant GM-26338.

Tu-Pos83

A CELLULAR AUTOMATON MODEL OF ACTIN GELATION. ((P.A. Dufort and C.J. Lumsden)) Department of Medicine, University of Toronto, Toronto, Canada, M5S 1A8.

We report a cellular automaton (CA) model of the spatiotemporal behavior of actin at the macromolecular level that simulates the heterogeneous nonequilibrium phenomena suspected to occur *in vivo*. The model incorporates cation and nucleotide binding to actin monomers, actin nucleation and polymerization into filaments, cross-linking with α-actinin, monomer sequestration with profilin, filament severing, capping and nucleation with gelsolin, binding of profilin and gelsolin to membrane-bound phosphatidylinositide biphosphate (PIP_2), and regulation of cross-linking and severing by changing calcium levels. The molecular translation and rotation probabilities required for the CA simulation are derived in terms of molecular size, shape, and cytoplasmic viscosity and temperature. The binding probabilities for adjacent molecules in the lattice are specified in terms of experimentally determined rate constants. An examination of gelation and sol-gel transitions resulting from calcium regulation of α-actinin and gelsolin predicts an inhomogeneous distribution of bound α-actinin and F-actin during conditions of gelation. The simulation results suggest that actin/α-actinin gels may shift from an isotropic to an amorphous phase after shortening of filaments. This may be an important means of regulating the viscoelastic properties of the cell. The close correspondence of the model's predictions with previous experimental and theoretical results suggests that the model can be used to explore the spatial and temporal properties of complex cytoskeletal processes.

MUSCLE ELECTROPHYSIOLOGY

Tu-Pos84

ENHANCEMENT OF CA CURRENT UNDERLIES POTENTIATION, AND ACTIVATION OF K CURRENT DEPRESSION, OF CONTRACTIONS OF THE ARC MUSCLE OF *APLYSIA* BY MODULATORY TRANSMITTERS AND PEPTIDE COTRANSMITTERS. ((V. Brezina, I. Kupfermann and K.R. Weiss)) Dept Physiol & Biophys, Mt Sinai Sch Med, and Ctr Neurobiol & Behav, Columbia U, New York, NY.

Plasticity of feeding movements in *Aplysia* is implemented in part by modulation of contractions of the accessory radula closer (ARC) muscle by peptide cotransmitters of several different families - the small cardioactive peptides (SCPs), myomodulins (MMs) and FMRFamide-related peptides (FRPs) - released from the same two motorneurons whose 'classical' transmitter, ACh, initiates the contractions, and serotonin (5-HT) from separate modulatory neurons. Some of these modulators (the SCPs, 5-HT, MMs) predominantly potentiate, others (the FRPs) depress, and still others (MM_A) at low concentrations potentiate, at higher depress, the contractions. Previous work (*Soc Neurosci Abstr* 18:586) has shown that the potentiating modulators enhance an 'L'-type Ca current in dissociated ARC muscle fibers, those that depress activate a characteristic K current, and those that both potentiate and depress have both effects. We have now obtained more direct evidence that these actions on ion currents indeed underlie the modulation of contractions. Low-micromolar 4-aminopyridine (4-AP) blocks the modulator-activated K current but no other current in the ARC muscle fibers, and completely blocks the depression of contractions by MM_A and the FRPs. An equivalent demonstration in the case of the Ca current is more difficult precisely because the current appears to provide Ca^{2+} necessary for ACh-induced contraction. Block of the current with nifedipine thus blocks contraction as well as its potentiation by 5-HT or SCP. Application of ACh results in contraction only when the ACh-induced depolarization is allowed to reach the activation threshold of the current. It is thus very likely that any enhancement of the current will potentiate contraction. Indeed, contractions due to ACh-independent activation of the current, by depolarizing current injection or high-K^+ solution, are potentiated by 5-HT just like ACh-induced contractions, whereas contractions that bypass its activation, e.g. induced by the Ca^{2+}-ionophore A23187, are not. It thus appears that the enhancement of the 'L'-type Ca current is in large part responsible for the potentiation, and activation of the 4-AP-sensitive K current for the depression, of ARC muscle contractions.

Tu-Pos85

HYDROXIDE AND BUFFER ANION PERMEABILITY OF FROG STRIATED MUSCLE. ((R.A. Venosa, B.A. Kotsias and P. Horowicz)), Univ. of Rochester Med. Ctr., Rochester, NY 14642.

OH^- and buffer anion permeabilities were measured using two methods. In one, membrane potential responses to quick solution changes were recorded in fibers initially equilibrated in isotonic, high K_2SO_4 solutions at pH_O 7.2 buffered with phosphate. In the first solution change Cs^+ replaced K^+. Then pH_O was raised using either 2.5 mM CAPS or CHES. The protonated form of these buffers is a neutral zwitterion. Then total $[buffer]_O$ was changed to 10 mM, keeping pH_O constant. From Vm and constant field equations, the relative permeabilities of OH^- and buffer anions relative to K^+ permeability in K^+-free, Cs^+ containing solutions can be calculated. From reported H^+ permeability calculations show that reducing $[H^+]_O$ can not account for the hyperpolarizations produced by alkaline solutions. In the other method, using pH-sensitive microelectrodes, pH_i changes were recorded when pH_O and $[buffer]_O$ were changed. In this case, external K^+ was kept constant. Using the first method the following average values were obtained at $pH_O = 10 \pm 0.3$: $(P_{OH}/P_K) = 890 \pm 150$; $(P_{CAPS}/P_K) = 12 \pm 2$; $(P_{CHES}/P_K) = 5.3 \pm 0.9$; and $(P_{NO3}/P_K) = 4.7 \pm 0.5$ which was independent of pH_O up to 10.75. At $pH_O = 8.9$, $(P_{Cl}/P_K) = 18 \pm 2$ and at $pH_O = 7.1$, $(P_{HEPES}/P_K) = 20 \pm 2$. Using the second method, the absolute permeabilities of both OH^- and $CAPS^-$ were calculated. For $pH_O = 10 \pm 0.3$, $P_{OH} = 1.6 \pm 0.3 \times 10^{-4}$ cm/sec and $P_{CAPS} = 2.1 \pm 0.7 \times 10^{-6}$ cm/sec. We conclude that OH^- is about 50 times more permeable than Cl^- at alkaline pHs and that anionic forms of commonly used buffers have significant permeabilities. [Support by NIAMS]

Tu-Pos86

A DIHYDROPYRIDINE-SENSITIVE CALCIUM CHANNEL IN THE PLASMA MEMBRANE OF CRUSTACEAN MUSCLE.

((C.Erxleben)) Dept. of Biology, University of Konstanz, D7750 Konstanz. (Spon. by H.-J.Apell)

Although the calcium electrogenesis of crustacean muscle is well established the underlying single channel currents have not yet been studied. In cell-attached patches from the plasma membrane of abdominal extensor muscle fibers of the marine isopod *Idotea baltica*, I have investigated the properties of a Ca^{++} and Ba^{++} permeable channel with a single channel slope conductance of 12 and 20pS respectively. The channel is inactive at the membrane resting potential (about -75mV) but is activated by depolarization with a sensitivity of 8 mV for an e-fold increase in the open probability. Besides its voltage dependence, range of activation, and conductance, it shares several other properties with the L-type Ca^{++} channel of vertebrate muscle and neurons. Channel openings are mostly brief (100-300 μs) but longer openings (1-5 ms) can be observed. The proportion of long openings is greatly promoted by preincubation of the muscle fibres with 10-100μM of the calcium channel agonist, Bay K8644. Channel activity elicited by voltage steps or during maintained depolarization shows characteristic periods with preferred short or long openings or inactivity.

Supported by the DFG, SFB156

Tu-Pos87

A VOLTAGE-DEPENDENT POTASSIUM-SELECTIVE CHANNEL IN THE SARCOLEMMA OF CRUSTACEAN MUSCLE FIBRES.

((T.J.Lea)) Univ.Lab. of Physiology, Parks Road, Oxford, OX1 3PT, U.K.

K^+ channels were recorded from sarcolemmal blebs on enzyme-treated muscle fibres from the crab Carcinus maenas. In inside-out excised patches a commonly observed K^+ channel had a slope conductance of 62 - 122 pS at 0 mV (200 mM KCl in the bath and 0 - 40 mM KCl in the electrode) and a mean open time at 0 mV of about 100 ms (temp. = 20°C). Replacement of bath KCl by NaCl made this channel undetectable. Measurement of the reversal potential with K gluconate in the bath and Na gluconate in the electrode gave a permeability ratio, P(Na)/P(K), of 0.08.

Channel activity was not affected by a reduction of free Ca^{2+} on the sarcoplasmic side from 2 μM to 10 nM by the addition of 1 mM EGTA to the bath solution, nor was it reduced by 5 mM MgATP added to the sarcoplasmic side. The open probability p_o was increased by a change in potential equivalent to depolarisation of the intact muscle fibre; e.g. in a patch with at least 5 identical channels active, Np_o increased from 0.62 at -40 mV to 2.07 at +30 mV. Such a voltage dependency is similar to that of the calculated conductance for the late outward current, I(K2), reported in this crab muscle by Mounier & Vassort (1975, J.Physiol. 251, 589-608).

Tu-Pos88

LEMAKALIM ACTIVATED K_{ATP} CHANNELS IN ISOLATED MYOCYTES OF RABBIT PULMONARY ARTERY OCCUR AT LOW DENSITY AND HAVE A SMALL CONDUCTANCE.

((P.D. LANGTON, *L.H. CLAPP, *A.M. GURNEY & N.B. STANDEN)) Ion Channel group, Department of Physiology, University of Leicester, Leicester LE1 9HN, U.K. *Department of Pharmacology, St Thomas's Hospital, UMDS, Lambeth Palace Road, London SE1 7EH, U.K.

Lemakalim (BRL 38227) hyperpolarizes and relaxes precontracted strips of rabbit pulmonary artery (RPA). These actions are inhibited by glibenclamide and phencyclidine (PCP). Using enzymatically isolated RPA myocytes we have made whole-cell voltage clamp recordings of lemakalim activated current with symmetrical 143 mM K^+ solutions. At -60 mV lemakalim (10μM) activated an inward current of -145 ± 22pA (mean ± S.E.M., n=17), and increased current noise. The response was independent of $[Ca^{2+}]_o$. Lemakalim induced current declined on washout, was well blocked by glibenclamide (10μM) and PCP (30μM), but unaffected by charybdotoxin (100 nM). We have analysed lemakalim-induced or glibenclamide- and PCP-blocked changes in mean current and variance to estimate the unitary current amplitude (*i*) and the number of channels (*N*). Values of mean current and variance from each cell were fitted to an expression relating mean current, variance, *i* and *N*. We estimate *i* to be -1.17 ± 0.08pA (n=16) and *N* to be 360 ± 48 (n=13). Under our conditions *i* corresponds to a slope conductance of 19.5pS. Our estimate for *N* is relatively small and may help to explain why single channels are so rarely observed.

Supported by the MRC, BHF and The Wellcome Trust.

Tu-Pos89

STEADY-STATE WHOLE CELL Ca^{2+} CHANNEL CURRENT AT NEGATIVE POTENTIALS IN ISOLATED MYOCYTES OF RAT BASILAR ARTERY.

((P.D. Langton and N.B. Standen)) Ion Channel Group, Department of Physiology, University of Leicester, Leicester LE1 9HN, U.K.

Ca^{2+} channel currents (10mM Ba^{2+}_o) recorded from isolated rat basilar arterial myocytes either in response to voltage steps or at steady holding potentials were measured using whole cell patch clamp methods. Co^{2+} (2mM) was used to reversibly block inward currents in order to measure and subtract leakage currents. Peak current measured in response to voltage steps from -88mV was -256 ± 39pA (mean ± s.e.m., n=19). Activation curves were constructed by dividing the macroscopic current by previous estimates of the single Ca^{2+} channel amplitude. $N.P_{open}$ measured in this way rose to around 1600. Its dependence on voltage was fit by a Boltzmann function with half activation in the range -8 to -2mV and a steepness factor in the range -6 to -8mV. In 5 cells steady-state Ba^{2+} current, measured as the difference in current in the presence and absence of Co^{2+}, could be detected at voltages as negative as -50mV. Maximum steady-state inward current was recorded around -20mV, current at more positive potentials inactivated rapidly. Mean values for $N.P_{open}$, measured as above, rose from around 1.5 at -48, to 60 at -18mV and could be fit by a Boltzmann function with half activation in the range -5mV and steepness around -6.5mV. Steady-state current in this voltage range may help to support myogenic tone.

Supported by the British Heart Foundation and The Wellcome Trust.

Tu-Pos90

RECOVERY OF THE RESTING MEMBRANE POTENTIAL (Vm) AND INTRACELLULAR SODIUM ($[Na^+]$) FOLLOWING FATIGUING STIMULATION.

((E.M. Balog and R.H. Fitts)) Marquette Univ., Milwaukee, WI 53233.

Decreases in the trans-sarcolemma concentration gradients of Na^+ and K^+ during repeated stimulation of skeletal muscle leads to alterations in the action potential (AP) waveform. In particular, an altered t-tubular AP may contribute to fatigue by reducing SR Ca^{2+} release. We used microelectrodes to assess the role of $[Na^+]i$ in the fatigue in muscle fibers from the semitendinosus of *Rana pipiens*. Measurements were made in resting cells and during recovery from fatiguing stimulation (100 ms trains at 150 Hz, 1/sec for 5 min). This protocol decreased peak tetanic tension (Po) to 10% of its initial value and allowed a fast phase of recovery to 25% of Po by 2 min and a slow phase to 90% of Po by 40 min. Resting Vm and $[Na^+]i$ in 6 fibers were -81.7±2.1 mV and 14.9±1.4 mM. Immediately after stimulation Vm fell to -73.5±2.9 mV, while $[Na^+]i$ rose to 47.1±8.3 mM. Within 10 min Vm recovered to -83.8±1.3 mV and $[Na^+]i$ to 15.7±1.0 mM. We previously showed that the AP overshoot (OS) recovered in less than 5 min. Although a significant correlation existed between $[Na^+]i$ and the OS (r^2=.96), the slower recovery of $[Na^+]i$ suggests that additional factor(s) are involved in the decline of the OS during fatigue. Comparison of the recovery of Po and $[Na^+]i$ suggests that any involvement of Na^+ in fatigue is limited to the fast phase of recovery.